TRANSFER OF PREFORMED IRON-SULFUR CLUSTERS TO CLIENT PROTEINS

by

Andrew J. Melber

A dissertation submitted to the faculty of
The University of Utah
in partial fulfillment of the requirements for the degree of

Doctor of Philosophy

Department of Biochemistry

The University of Utah

May 2017

The University of Utah Graduate School

STATEMENT OF DISSERTATION APPROVAL

The dissertation of **Andrew J. Melber**

has been approved by the following supervisory committee members:

Dennis R. Winge	, Chair	**2/24/2017** Date Approved
Jared P. Rutter	, Member	**2/24/2017** Date Approved
Adam L. Hughes	, Member	**2/24/2017** Date Approved
Jerry Kaplan	, Member	**2/24/2017** Date Approved
Elizabeth A. Liebold	, Member	**2/24/2017** Date Approved
Michael S. Kay	, Member	**2/24/2017** Date Approved

and by **Wesley I. Sundquist & Christopher P. Hill** , Chair/Dean of

the **Department of Biochemistry**

and by David B. Kieda, Dean of The Graduate School.

ABSTRACT

Iron-sulfur (Fe/S) clusters are essential cofactors required to perform unique functions in nitrogen fixation, respiration, metabolite catabolism, ribosome assembly, DNA repair, etc., through their redox-active characteristic, the ability to accept or donate an additional election. Biology has evolved intricate mechanisms to assemble and subsequently transfer the preformed Fe/S clusters to client proteins. Fe/S clusters are found in many of the cell's subcompartments, but all of the clusters' biogenesis begins in the mitochondria.

The mitochondrial iron-sulfur biogenesis pathway (ISC) starts at the ISU complex with the removal of a sulfide from cysteine by a cysteine desulfurase. This sulfide is transferred to a scaffold protein where, with two irons and a reluctant, a [2Fe-2S] cluster is made. This preformed cluster is transferred from the scaffold through a gludaredoxin to the ISA complex. The ISA complex, comprised of three proteins, Isa1, Isa2, and Iba57, receives two [2Fe-2S] clusters that are then condensed into a single [4Fe-4S] cluster. This preformed [4Fe-4S] cluster must then be transferred from the assembly complex to client proteins in a manner that does not expose it to oxidative damage.

The work in this dissertation focused on the biochemical characterization of Nfu1 as the transfer protein for [4Fe-4S] clusters formed by the ISC pathway. Nfu1 was shown to genetically interact with Isa2 and physically interact with all members of the ISA complex. Additionally, physical interactions between Nfu1 and all of the [4Fe-4S] clients

in the yeast, *Saccharomyces cerevisiae*, were identified through proteomic studies. These studies went onto demonstrate the BolA family member Bol3 functions with Nfu1 in the cluster transfer process.

A follow-up study of Nfu1 sought to identify how it recognized client proteins for delivery of a [4Fe-4S] cluster. Using computational approaches identified a five amino acid motif, TIMNM. Sufficiency was demonstrated by creating an interaction between Nfu1 with a heterologous chimeric protein fused with the motif. Necessity was shown in both Sdh2 and aconitase client proteins with mutations to the motif of either client resulting in defects in enzymatic activity and a loss of interaction with Nfu1. Overall, these studies demonstrate that Nfu1 transfers [4Fe-4S] clusters to client proteins that are identified by the TIMNM Nfu1 recognition motif.

TABLE OF CONTENTS

LIST OF FIGURES

CHAPTER 1

INTRODUCTION

1.1 Introduction

Iron-sulfur clusters (Fe/S) are redox-active cofactors that are essential for almost all life forms. The breadth of mechanisms that Fe/S clusters are utilized for illustrates the pertinence of these cofactors in biology. In the nucleus, Fe/S clusters bound to DNA repair enzymes can sense damage by assessing the ability of an electron from a cluster to diffuse along DNA (Arnold et al., 2016). Within the mitochondria, the OXPHOS respiratory complexes utilize Fe/S clusters for the oxidation/reduction transfer of electrons through the respiratory complex (Melber and Winge, 2016). Clusters can perform a catalytic role in an array for nucleotide and amino acid biogenesis pathways throughout the cell. In an altruistic fashion Fe/S clusters can be consumed by enzymes like the radical S-adenosyl-L-methionine (SAM) protein lipoic acid synthase (LIAS), which releases sulfide ions from Fe/S clusters for the generation of lipoate (McLaughlin et al., 2016). The focus of this review will be on the mitochondrial iron-sulfur cluster biogenesis pathway (ISC) that generates [2Fe-2S], [4Fe-4S], and [3Fe-4S] clusters.

1.2 Mitochondrial iron-sulfur clusters

Redox-active cofactors have the ability to donate or accept an electron to facilitate a unique set of chemistries that would otherwise be challenging for biology to perform. Given this redox modularity of Fe/S clusters, it is not surprising that they along with heme and copper atoms are found in abundance within the four OXPHOS respiratory chain complexes to transfer electrons through each complex. Respiratory complex I, NADH:ubiquinone oxidoreductase, contains eight Fe/S clusters, seven of which execute the transfer of electrons (Fiedorczuk et al., 2016; Zhu et al., 2016). It is worth noting that

the commonly used model organism *Saccharomyces cerevisiae* does not have a membrane bound complex I; instead yeast have small soluble NADH:ubiquinone oxidoreductases that do not pump protons and lack redox cofactors (Iwata et al., 2012; Li et al., 1996). Complex II, succinate dehydrogenase (SDH), contains three Fe/S clusters, a [2Fe-2S], a [4Fe-4S], and a [3Fe-4S] cluster, all within the Sdh2 (SdhB) subunit (Sun et al., 2005). Cytochrome bc_1, complex III, contains just a [2Fe-2S] cluster that functions in concert with two heme cofactors (Iwata et al., 1998). Lastly, complex IV, cytochrome oxidase, does not contain any Fe/S clusters, but utilizes heme and copper for electron transfer (Tsukihara et al., 1995).

Fe/S cofactors are not only utilized by the electron transport chain in the mitochondria, many Fe/S clusters act in a catalytic capacity instead. The SAM radical enzyme lipoic acid synthase (LIAS, Lip5 in *S. cerevisiae*) contains two [4Fe-4S] clusters, one of which is consumed during the catalytic cycle to liberate two sulfides used for the generation of a lipoate moiety (McLaughlin et al., 2016). Another mitochondrial radical SAM protein is biotin synthase, Bio2, which requires a [2Fe-2S] cluster that is consumed to provide the sulfurs to biotin and a stable [4Fe-4S] cluster (Berkovitch et al., 2004; Tse Sum Bui et al., 2003). The TCA cycle enzyme aconitase binds a [4Fe-4S] cluster with three thiolate ligands such that the open Fe (II) can coordinate the citrate substrate for isomerization (Robbins and Stout, 1989). In fungi, the [4Fe-4S] hydratases Aco2 and Lys4 preform steps in lysine biosynthesis with a similar mechanism as aconitase (Fazius et al., 2012). Another mitochondrial enzyme that generates amino acids is the dihydroxyacid dehydratase, Ilv3, which requires a [2Fe-2S] cluster for its function in the branch chained amino acid biosynthetic pathway (Muhlenhoff et al., 2011). Glutamate

biosynthesis requires a Fe/S cluster, but it is unresolved whether the yeast glutamate synthase uses a [3Fe-4S] or a [4Fe-4S] cluster (Knaff et al., 1991; Miller and Stadtman, 1972).

Lastly, the mitochondrial ferredoxin (Yah1 in yeast) requires a [2Fe-2S] cluster for its function providing electrons to various biosynthetic processes from NADH by the oxidoreductase, Arh1 (Manzella et al., 1998). Ferredoxin donates electrons to the heme *a* biosynthesis pathways through Cox15, coenzyme Q biogenesis via Coq6, and Fe/S cluster biogenesis via the scaffold ISU complex, which will be discussed in the next section (Barros et al., 2001; Barros et al., 2002; Lange et al., 2000; Ozeir et al., 2011; Pierrel et al., 2010). Given the array of pathways that ferredoxin contributes a reductant to, dysfunctional [2Fe-2S] cluster biogenesis cause exacerbated defects in other mitochondrial biosynthesis pathways.

1.3 Mitochondrial iron-sulfur cluster biogenesis

Three bacterial pathways have independently arisen to generate Fe/S clusters for unique needs of the cell. These pathways are the ISC, SUF, and NIF systems. These systems all function by the same general mechanism: cysteine desulfurases produce sulfide ions, scaffold complexes assemble a *de novo* cluster, and a transfer system traffics the clusters to client proteins (Roche et al., 2013). Eukaryotic mitochondria have adopted the ISC pathway from bacteria and integrated components of the NIF pathway for a single dedicated assembly pathway. The mitochondrial iron-sulfur cluster biogenesis pathway (ISC) not only contributes functional clusters to the mitochondria, but also provides an essential precursor to the cytosolic Fe/S assembly pathway (CIA).

This review will go into great detail about each component of the ISC pathway later, but the general scheme of the pathway is illustrated in Figure 1.1 and briefly described as follows. Within the ISU complex, iron and sulfide ions generated by a cysteine desulfurase enzyme are combined on a scaffold protein to form an initial [2Fe-2S] cluster. The preformed Fe/S cluster is then released from the scaffold by chaperones to a glutaredoxin that mediates delivery to [2Fe-2S] client proteins or to a second complex (ISA complex) in which two [2Fe-2S] clusters are condensed into a single [4Fe-4S] center, which is then transferred to mitochondrial [4Fe-4S] client proteins (Beilschmidt and Puccio, 2014; Rouault, 2015; Stehling et al., 2014). A sulfur-containing adduct requiring the function of the cysteine desulfurase and the scaffolding complex is extruded into the cytoplasm by the ABC transporter Atm1 (Kispal et al., 1999). The identity of this S-compound remains to be elucidated, although several compounds have been proposed (Schaedler et al., 2014; Srinivasan et al., 2014). The cytosolic iron-sulfur cluster biogenesis pathway (CIA) that utilizes this S-compound has been reviewed to a great extent and will not be the focus of this review (Lill et al., 2015; Paul and Lill, 2015). The successful biogenesis of Fe/S clusters is dependent on ferrous iron, sulfur (from cysteine), a ferredoxin reductant, as well as NADH, ATP, and GTP (Pandey et al., 2015).

1.4 [2Fe-2S] cluster assembly by the ISU complex

As mentioned, all cellular Fe/S clusters require the early steps of the ISC pathway within the mitochondria. This starts with the ISU complex. The ISU complex centers on the scaffolding protein Isu1 (a redundant scaffold protein exists in yeast, Isu2) on which

the initial cluster is built. This ISU complex utilizes six different components. The scaffold receives ferrous iron from an unknown source, the sulfide comes from the cysteine desulfurase, Nfs1, and the electrons come from the ferredoxin, Yah1 (Lange et al., 2000; Webert et al., 2014; Yan et al., 2015). The other components that surround the scaffold include the Nfs1 stabilizing proteins Isd11, Acp1, and frataxin, Yfh1 (Schmucker et al., 2011; Shan et al., 2007; Van Vranken et al., 2016; Wiedemann et al., 2006). A caveat to this 'complex' is that each component is likely not stably bound to Isu1 at the same time. This dynamic nature allows for different components to bind directly to the scaffold at the same interface, such as Yah1 and Nfs1 binding to Isu1 at an overlapping interface (Kim et al., 2013). Isu1 has been shown to be in substoichiometric ratios to the Nfs1/Isd11 BN-PAGE complex that was later shown to include Acp1 (Van Vranken et al., 2016; Wiedemann et al., 2006). Contrary to this, several groups have purified a stable Yfh1/Isd11/Nfs1/Isu1 complex (Colin et al., 2013; Schmucker et al., 2011; Tsai and Barondeau, 2010).

The Nfs1 cysteine desulfurase is a pyridoxial phosphate (PLP)-dependent enzyme that liberates sulfane from cysteine releasing alanine and forming a persulfide intermediate on a conserved cysteine of Nfs1 (Kaiser et al., 2000; Mühlenhoff et al., 2004). The persulfide sulfane is transferred to the scaffold Isu1 protein and reduction of sulfane is required before its incorporation as sulfide ions with Fe(II) into the initial [2Fe-2S] cluster (Parent et al., 2015; Smith et al., 2005; Urbina et al., 2001). This reduction is mediated by the mitochondrial ferredoxin, Yah1 (Cai et al., 2017; Lange et al., 2000; Webert et al., 2014).

Nfs1 catalysis is the initial step for the biogenesis of all cellular Fe/S clusters, so

fittingly, evolution has generated several methods of regulation (Smith et al., 2001). One such method of regulation in eukaryotes comes from the LYR protein, Isd11, required for the structural stabilization of Nfs1 (Adam et al., 2006). In addition, Isd11 stimulates persulfide formation on Nfs1 (Adam et al., 2006; Pandey et al., 2012; Wiedemann et al., 2006). Isd11, as with all LYR proteins, is found associated with the acyl carrier protein Acp1 (Huttlin et al., 2015; Van Vranken et al., 2016). Acp1 functions in mitochondrial fatty acid synthesis, yet has additional roles through its association with LYR proteins in the mitochondrial matrix. Fatty acid elongation occurs on a phosphopantheteine cofactor covalently bound to Acp1 and the interaction of Acp1 and two LYR proteins in Complex I reveals the Acp1 acyl chain is embedded within the three helical bundle of the LYR protein (Fiedorczuk et al., 2016; Wu et al., 2016). Many of the other LYR proteins are assembly factors for OXPHOS respiratory complexes (Angerer et al., 2014; Atkinson et al., 2011; Floyd et al., 2016; Na et al., 2014). This provides a potentially interesting regulatory mechanism that links the biogenesis of all cellular Fe/S clusters with the maturation of the respiratory complexes through fatty acid oxidation required to form the lipid that is covalently attached to Acp1.

Another component of the ISU complex that serves to regulate Nfs1 is frataxin. Frataxin was identified as the causative gene of Freidriech's Ataxia in patients and the deletion of the homologue in yeast, Yfh1, was originally described to result in mitochondrial iron accumulation (Babcock et al., 1997; Campuzano et al., 1996). Subsequently, frataxin was postulated to be the iron donor to the Isu1 scaffold in [2Fe-2S] biogenesis because of the protein's iron binding properties (Adamec et al., 2000; Kondapalli et al., 2008; Yoon and Cowan, 2003). However, when mutations were made

to the proposed iron binding ligands of frataxin, only modest defects were observed in Fe/S cluster formation (Correia et al., 2010; Foury et al., 2007). Furthermore, structural studies in bacterial systems have shown that the interaction of the frataxin, CyaY, with the bacteria ISU complex is independent of iron and frataxin oligomerization (an iron-dependent phenomenon) and in fact, the prokaryotic frataxin directly binds with the bacterial desulfurase, IscS, not the scaffold, IscU (Prischi et al., 2010). Lastly, a mutant of the Isu1 scaffold was identified to bypass the functional importance of Yfh1 in yeast (Yoon et al., 2014). Taken together, the iron chaperone role of frataxin has fallen out of favor for other potential roles of frataxin. A new iron donor has yet to be identified.

New potential functions have suggested frataxin to be a regulatory protein for the ISU complex. One proposed method of regulation for frataxin is that it can stimulate binding of the substrate, cysteine, to Nfs1, thereby stimulating cysteine desulfurase activity (Fox et al., 2015; Pandey et al., 2013). An opposing model was reported showing that frataxin stimulates sulfide transfer from Nfs1 to Isu1 (Bridwell-Rabb et al., 2014; Parent et al., 2015). Further studies of these potential mechanisms using mutants that block iron binding and specific protein-protein interactions will hopefully resolve the true function of frataxin for the field.

1.5 Transfer of [2Fe-2S] clusters from the Isu1 scaffold

Once the ISU complex has completed synthesis of an initial [2Fe-2S] cluster, the cluster is released to the glutaredoxin, Grx5, by the DnaJ protein, Jac1, and the Hsp70 chaperone, Ssq1. This cycle is dependent on the constant cycling of ATP on Ssq1 facilitated by the ATP exchange factor Mge1 (Dutkiewicz et al., 2003). Isu1 is separated

from the rest of the complex by the initial binding of Jac1 (Majewska et al., 2013). Grx5/Ssq1 heterotrimer (two Grx5 molecules) binds the Jac1/Isu1 dimer, stimulating ATP hydrolysis, resulting in a structural change to Ssq1 that releases Jac1 and transfers the cluster from Isu1 to Grx5 (Kim et al., 2012; Uzarska et al., 2013). Cluster bound Grx5 consists of a [2Fe-2S] cluster bridged between two Grx5 molecules. Each Grx5 molecule provides one cysteinyl ligand to the bridging [2Fe-2S] cluster, with a second thiolate ligand coming from a Grx5-bound glutathione (Johansson et al., 2011). It is clear that cells lacking Grx5 have defects in cytosolic Fe/S centers and mitochondrial [4Fe-4S] and [2Fe-2S] centers (Muhlenhoff et al., 2003; Rodriguez-Manzaneque et al., 2002; Uzarska et al., 2013). The functional importance of Grx5 is not entirely clear since all of these defects are modest relative to the deletion of upstream components in the ISC pathway that are not viable. Deletion of the downstream Fe/S biogenesis components in the ISA complex results in viable cells that are defective in respiratory growth.

Transfer of [2Fe-2S] clusters from Grx5 to the downstream ISA components has been demonstrated in which two [2Fe-2S] clusters are condensed, forming a single [4Fe-4S] cluster (Banci et al., 2014; Brancaccio et al., 2014; Rodriguez-Manzaneque et al., 2002; Shakamuri et al., 2012). The transfer of a [2Fe-2S] cluster to a eukaryotic mitochondrial [2Fe-2S] target protein has not yet been demonstrated, but [2Fe-2S] transfer from a cytosolic glutaredoxin to cytosolic Fe/S client has been shown with GLRX3 to the client proteins Aft2 and anamorisn (Banci et al., 2015b, Poor et al., 2014).

While evidence supports a role for Grx5 as the predominant [2Fe-2S] transfer agent in the mitochondria, an alternative model was proposed (Maio and Rouault, 2015). This alternative model posits that mitochondrial [2Fe-2S] client proteins bind to the Jac1

and Ssq1 chaperones associated with the ISU complex and clusters are directly transferred to client proteins. The Fe/S-containing subunit (SdhB) of SDH was found to interact with Jac1 and the ISCU scaffold in mammalian cells (Maio et al., 2016; Maio et al., 2014). This 2014 study reported that Glrx5 (mammalian Grx5) was present with the chaperone/ISCU scaffold, but no mention was made of its relevance in cluster transfer. This second model is supported by yeast studies in which the overexpression of Ssq1 can suppress the growth phenotype of Grx5-deficient cells (Rodriguez-Manzaneque et al., 2002). Unfortunately this model has not suggested an alternative function for Grx5 despite Grx5-deficient cells impairment in all mitochondrial and cytosolic Fe/S clusters tested to date.

BolA proteins have been reported to associate with glutaredoxin proteins in prokaryotes and eukaryotes (Li and Outten, 2012). In the eukaryotic cytosol, two glutaredoxins, Grx3 and Grx4, interact with the BolA protein Bol2 (Fra2) in a [2Fe-2S] cluster bridged heterodimeric complex (Kumanovics et al., 2008; Li et al., 2012). Human homologues of this cytosolic glutaredoxin pair have been shown to mediate the *in vitro* transfer of [2Fe-2S] clusters to the client protein anamorisin (Banci et al., 2015a; Frey et al., 2016). Mitochondria contain two BolA proteins, Bol1 and Bol3 (Uzarska et al., 2016). When the mutated mitochondrial BolA3 was identified in human patients with molecular defects in Fe/S centers, it was postulated that the BolA3 might function with Glrx5 (Cameron et al., 2011). However, recent studies revealed that the other mitochondrial BolA protein Bol1 interacted with Grx5 in yeast and in humans (Melber et al., 2016; Uzarska et al., 2016; Willems et al., 2013). Taken all together, it is likely that a Grx5/Bol1 heterodimer bridged by a [2Fe-2S] cluster is a transfer agent to at least some

clients within the mitochondria. How the Grx5/Bol1 and the Grx5/Grx5 dimers interplay with each other and with different fates of the bound [2Fe-2S] cluster (i.e. [2Fe-2S] clients or [4Fe-4S] biogenesis or export to CIA) is yet to be established.

1.6 [4Fe-4S] cluster formation by the ISA complex

Across the cell, [4Fe-4S] clusters are the most commonly used clusters; however, distinct machinery are necessary to generate these clusters in different subcellular compartments. As mentioned, within the mitochondria, conversion of [2Fe-2S] centers into [4Fe-4S] clusters requires the ISA complex in the mitochondrial matrix. In contrast, formation of nuclear and cytoplasmic [4Fe-4S] clusters requires a distinct cytosolic iron sulfur assembly pathway (CIA) that utilizes the substrate exported from the matrix by Atm1 (Kispal et al., 1999). Given that the ISA complex only produces [4Fe-4S] clusters for the mitochondria, cells lacking the ISA complex are only impaired in mitochondrial function, but not in cellular viability as these cells are able to export the sulfur-containing component required for cytoplasmic Fe/S biogenesis. The ISA complex is a hetero-trimeric complex comprised of Isa1, Isa2, and Iba57 (Gelling et al., 2008; Muhlenhoff et al., 2011; Sheftel et al., 2012). Following successful transfer of two [2Fe-2S] clusters by Grx5, one to Isa1 and the other to Isa2, the clusters are condensed to a single [4Fe-4S] cluster (Brancaccio et al., 2014). A remaining challenge in mitochondrial [4Fe-4S] cluster biogenesis is to understand the role of Iba57 in the trimeric complex. Patients of multiple mitochondrial dysfunction syndromes (MMDS) present with functional defects in many mitochondrial Fe/S centers; recently, causative mutations were identified in the genes coding for Iba57 and Isca2 of the ISA complex (Ajit Bolar et al., 2013; Al-Hassnan et al.,

2015; Lossos et al., 2015; Torraco et al., 2017).

1.7 [4Fe-4S] cluster transfer

MMDS patients have also been identified with mutations in the gene for NFU1 (Ahting et al., 2015; Cameron et al., 2011; Invernizzi et al., 2014; Navarro-Sastre et al., 2011; Nizon et al., 2014; Tonduti et al., 2015). Nfu1 has been characterized to bind [4Fe-4S] clusters formed on the ISA complex and to transfer them to a host of client proteins present from yeast to human, including aconitase, Sdh2 (the Fe/S subunit SDH), and lipoic acid synthase (LIAS) (Cai et al., 2016; Melber et al., 2016). While patients present in a similar fashion whether the causative mutation is in genes coding the ISA complex or in the transfer machinery, the transfer machinery is only conditionally important to yeast. This is seen in the mild growth defects of Nfu1-deficient cells and when these cells are grown in anoxic conditions, they do not display defects in Fe/S centers, suggesting that transfer systems are in place to protect preformed clusters from oxidative damage en route to client proteins (Melber et al., 2016; Schilke et al., 1999).

The other gene identified with causative mutations for MMDS was BOLA3, a family member of the BOLA family whose Bol1 family member functions upstream with Grx5 as discussed previously (Baker et al., 2014; Cameron et al., 2011; Haack et al., 2013). Similar to the proposed [2Fe-2S] transfer system of Grx and BolA proteins, Nfu1 functions with Bol3, but the role of Bol3 in late stage cluster transfer with Nfu1 remains unresolved (Melber et al., 2016; Uzarska et al., 2016). Potential functions could include facilitating release of the stable [4Fe-4S] cluster bound to Nfu1 or stabilizing the interaction with client proteins.

Another late step cluster transfer protein is Ind1, which was reported to facilitate [4Fe-4S] cluster transfer to the respiratory complex I, NADH dehydrogenase, which is not present in *S. cerevisiae* (Bych et al., 2008; Sheftel et al., 2009). Since Ind1 has been described as only important for Fe/S delivery to complex I, it is no surprise that patient mutations in Ind1 present differently that of MMDS patients (Calvo et al., 2010; Kevelam et al., 2013). It is not known whether Nfu1 collaborates with Ind1 in the assembly of complex I, but some of the MMDS patients with mutations in the NFU1 gene do present with defects in complex I (Ahting et al., 2015; Cameron et al., 2011; Navarro-Sastre et al., 2011).

1.8 Unresolved questions of mitochondrial Fe/S biogenesis

In recent years, significant advancement in the mitochondrial Fe/S biogenesis pathway has been made; however, many questions remain unanswered. Within the assembly complexes, since the iron donor role of frataxin has been questioned, how the ISU complex receives Fe(II) remains unresolved. Could the mitochondrial iron transporters have a transient interaction with the ISU complex and directly provide Fe(II) ions to the ISU scaffold (Mühlenhoff et al., 2003)? Within the ISA complex, no function has yet to be assigned to Iba57. Brancaccio et al. showed that [4Fe-4S] cluster condensation could occur with just Isa1 and Isa2. This left Iba57 seemingly unimportant for cluster formation, so they suggested Iba57 was recruiting client proteins to the ISA complex. However, this is unlikely given the subsequent characterization of Nfu1. Furthermore, Iba57-deficient cells display a complete loss of function to [4Fe-4S] centers mimicking Isa1 and Isa2-deficient cells, whereas cells lacking the transfer proteins Nfu1

or Grx5 only exhibit partial defects in Fe/S centers. Taken together, this suggests Iba57 functions to facilitate [4Fe-4S] cluster formation with Isa1 and Isa2 in a manner that is not essential *in vitro*.

The controversy surrounding the [2Fe-2S] cluster transfer system needs to be resolved in an unbiased manner directly showing transfer to bona fide [2Fe-2S] cluster clients *in vitro* and *in vivo*. With [2Fe-2S] transfer, the function of Bol1 with Grx5 remains an enigma. Clearly, *in vitro,* a [2Fe-2S] bridged heterodimer of Bol1/Grx5 can exist, however, does this cluster-loaded species exist stably within the matrix, and what purpose does it serve? Additionally, the function of the other mitochondrial BolA protein, Bol3 with Nfu1 in [4Fe-4S] transfer remains in question. Recent *in vitro* studies of the transfer between Nfu1 and client proteins are being expanded to include Bol3 to develop a mechanistic understanding. With further insight to the BolA proteins, we will hopefully understand why the phenotypes of the BolA deletion strains are so mild compared to all other ISC components.

Additionally, entire branches of Fe/S cluster biology potentially still exist awaiting discovery. While Atm1 has been characterized to export an undefined sulfide-containing substrate for the CIA pathway, no additional protein partners have been described to mediate the transition of a [2Fe-2S] cluster to the sulfide compound. While an understanding of the basic biosynthesis for [2Fe-2S] and [4Fe-4S] clusters exists, no biosynthetic machinery has been described for [3Fe-4S] clusters. [3Fe-4S] clusters may potentially arise from oxidative damage to [4Fe-4S] clusters, but whether this mediates [3Fe-4S] cluster formation and transfer remains unclear. Certainly in times of high oxidative stress, the [4Fe-4S] cluster of aconitase (remember it only has three ligands) is

converted by oxidants to a [3Fe-4S] cluster (Flint et al., 1993). Might this be the mechanism by which SdhB creates a [3Fe-4S] cluster? Lastly, given that clusters can be damaged by oxidation, and even in homeostatic conditions the radical SAM Fe/S cluster proteins like LIAS consume a cluster during the enzyme's catalytic cycle, what surveillance mechanisms exist in the matrix to identify damaged clusters and does machinery exist that can fix oxidized clusters (McLaughlin et al., 2016)? Or can known ISC components moonlight to act directly on damaged clusters? This is not a farfetched idea; repair systems do exist in *E. coli* utilizing a cysteine desulfurase from the *isc* operon, IscS (Djaman et al., 2004).

1.9 References

Adam, A.C., Bornhovd, C., Prokisch, H., Neupert, W., and Hell, K. (2006). The Nfs1 interacting protein Isd11 has an essential role in Fe/S cluster biogenesis in mitochondria. EMBO J *25*, 174-183.

Adamec, J., Rusnak, F., Owen, W.G., Naylor, S., Benson, L.M., Gacy, A.M., and Isaya, G. (2000). Iron-dependent self-assembly of recombinant yeast frataxin: implications for Friedreich ataxia. Am J Hum Genet *67*, 549-562.

Ahting, U., Mayr, J.A., Vanlander, A.V., Hardy, S.A., Santra, S., Makowski, C., Alston, C.L., Zimmermann, F.A., Abela, L., Plecko, B.*, et al.* (2015). Clinical, biochemical, and genetic spectrum of seven patients with NFU1 deficiency. Front Genet *6*, 123.

Ajit Bolar, N., Vanlander, A.V., Wilbrecht, C., Van der Aa, N., Smet, J., De Paepe, B., Vandeweyer, G., Kooy, F., Eyskens, F., De Latter, E.*, et al.* (2013). Mutation of the iron-sulfur cluster assembly gene IBA57 causes severe myopathy and encephalopathy. Hum Mol Genet *22*, 2590-2602.

Al-Hassnan, Z.N., Al-Dosary, M., Alfadhel, M., Faqeih, E.A., Alsagob, M., Kenana, R., Almass, R., Al-Harazi, O.S., Al-Hindi, H., Malibari, O.I.*, et al.* (2015). ISCA2 mutation causes infantile neurodegenerative mitochondrial disorder. J Med Genet *52*, 186-194.

Angerer, H., Radermacher, M., Mankowska, M., Steger, M., Zwicker, K., Heide, H., Wittig, I., Brandt, U., and Zickermann, V. (2014). The LYR protein subunit NB4M/NDUFA6 of mitochondrial complex I anchors an acyl carrier protein and is

essential for catalytic activity. Proc Natl Acad Sci U S A *111*, 5207-5212.

Arnold, A.R., Grodick, M.A., and Barton, J.K. (2016). DNA Charge Transport: from Chemical Principles to the Cell. Cell Chem Biol *23*, 183-197.

Atkinson, A., Smith, P., Fox, J.L., Cui, T.Z., Khalimonchuk, O., and Winge, D.R. (2011). The LYR protein Mzm1 functions in the insertion of the Rieske Fe/S protein in yeast mitochondria. Mol Cell Biol *31*, 3988-3996.

Babcock, M., de Silva, D., Oaks, R., Davis-Kaplan, S., Jiralerspong, S., Montermini, L., Pandolfo, M., and Kaplan, J. (1997). Regulation of mitochondrial iron accumulation by Yfh1p, a putative homolog of frataxin. Science *276*, 1709-1712.

Baker, P.R., 2nd, Friederich, M.W., Swanson, M.A., Shaikh, T., Bhattacharya, K., Scharer, G.H., Aicher, J., Creadon-Swindell, G., Geiger, E., MacLean, K.N.*, et al.* (2014). Variant non ketotic hyperglycinemia is caused by mutations in LIAS, BOLA3 and the novel gene GLRX5. Brain *137*, 366-379.

Banci, L., Brancaccio, D., Ciofi-Baffoni, S., Del Conte, R., Gadepalli, R., Mikolajczyk, M., Neri, S., Piccioli, M., and Winkelmann, J. (2014). [2Fe-2S] cluster transfer in iron–sulfur protein biogenesis. Proceedings of the National Academy of Sciences *111*, 6203-6208.

Banci, L., Camponeschi, F., Ciofi-Baffoni, S., and Muzzioli, R. (2015a). Elucidating the Molecular Function of Human BOLA2 in GRX3-Dependent Anamorsin Maturation Pathway. J Am Chem Soc *137*, 16133-16143.

Banci, L., Ciofi-Baffoni, S., Gajda, K., Muzzioli, R., Peruzzini, R., and Winkelmann, J. (2015b). N-terminal domains mediate [2Fe-2S] cluster transfer from glutaredoxin-3 to anamorsin. Nat Chem Biol *11*, 772-778.

Barros, M.H., Carlson, C.G., Glerum, D.M., and Tzagoloff, A. (2001). Involvement of mitochondrial ferredoxin and Cox15p in hydroxylation of heme O. FEBS Lett *492*, 133-138.

Barros, M.H., Nobrega, F.G., and Tzagoloff, A. (2002). Mitochondrial ferredoxin is required for heme A synthesis in Saccharomyces cerevisiae. J Biol Chem *277*, 9997-10002.

Beilschmidt, L.K., and Puccio, H.M. (2014). Mammalian Fe-S cluster biogenesis and its implication in disease. Biochimie *100*, 48-60.

Berkovitch, F., Nicolet, Y., Wan, J.T., Jarrett, J.T., and Drennan, C.L. (2004). Crystal structure of biotin synthase, an S-adenosylmethionine-dependent radical enzyme. Science *303*, 76-79.

Brancaccio, D., Gallo, A., Mikolajczyk, M., Zovo, K., Palumaa, P., Novellino, E., Piccioli, M., Ciofi-Baffoni, S., and Banci, L. (2014). Formation of [4Fe-4S] clusters in the mitochondrial iron-sulfur cluster assembly machinery. J Am Chem Soc *136*, 16240-16250.

Bridwell-Rabb, J., Fox, N.G., Tsai, C.-L., Winn, A.M., and Barondeau, D.P. (2014). Human Frataxin Activates Fe–S Cluster Biosynthesis by Facilitating Sulfur Transfer Chemistry. Biochemistry *53*, 4904-4913.

Bych, K., Kerscher, S., Netz, D.J., Pierik, A.J., Zwicker, K., Huynen, M.A., Lill, R., Brandt, U., and Balk, J. (2008). The iron-sulphur protein Ind1 is required for effective complex I assembly. EMBO J *27*, 1736-1746.

Cai, K., Liu, G., Frederick, R.O., Xiao, R., Montelione, G.T., and Markley, J.L. (2016). Structural/Functional Properties of Human NFU1, an Intermediate [4Fe-4S] Carrier in Human Mitochondrial Iron-Sulfur Cluster Biogenesis. Structure *24*, 2080-2091.

Cai, K., Tonelli, M., Frederick, R.O., and Markley, J.L. (2017). Human Mitochondrial Ferredoxin 1 (FDX1) and Ferredoxin 2 (FDX2) Both Bind Cysteine Desulfurase and Donate Electrons for Iron-Sulfur Cluster Biosynthesis. Biochemistry *56*, 487-499.

Calvo, S.E., Tucker, E.J., Compton, A.G., Kirby, D.M., Crawford, G., Burtt, N.P., Rivas, M., Guiducci, C., Bruno, D.L., Goldberger, O.A.*, et al.* (2010). High-throughput, pooled sequencing identifies mutations in NUBPL and FOXRED1 in human complex I deficiency. Nat Genet *42*, 851-858.

Cameron, J.M., Janer, A., Levandovskiy, V., Mackay, N., Rouault, T.A., Tong, W.-H., Ogilvie, I., Shoubridge, E.A., and Robinson, B.H. (2011). Mutations in iron-sulfur cluster scaffold genes NFU1 and BOLA3 cause a fatal deficiency of multiple respiratory chain and 2-oxoacid dehydrogenase enzymes. Am J Hum Genet *89*, 486-495.

Campuzano, V., Montermini, L., Molto, M.D., Pianese, L., Cossee, M., Cavalcanti, F., Monros, E., Rodius, F., Duclos, F., Monticelli, A.*, et al.* (1996). Friedreich's ataxia: autosomal recessive disease caused by an intronic GAA triplet repeat expansion. Science *271*, 1423-1427.

Colin, F., Martelli, A., Clemancey, M., Latour, J.M., Gambarelli, S., Zeppieri, L., Birck, C., Page, A., Puccio, H., and Ollagnier de Choudens, S. (2013). Mammalian frataxin controls sulfur production and iron entry during de novo Fe4S4 cluster assembly. J Am Chem Soc *135*, 733-740.

Correia, A.R., Wang, T., Craig, E.A., and Gomes, C.M. (2010). Iron-binding activity in yeast frataxin entails a trade off with stability in the alpha1/beta1 acidic ridge region. Biochem J *426*, 197-203.

Djaman, O., Outten, F.W., and Imlay, J.A. (2004). Repair of oxidized iron-sulfur clusters

in Escherichia coli. J Biol Chem *279*, 44590-44599.

Dutkiewicz, R., Schilke, B., Knieszner, H., Walter, W., Craig, E.A., and Marszalek, J. (2003). Ssq1, a mitochondrial Hsp70 involved in iron-sulfur (Fe/S) center biogenesis. Similarities to and differences from its bacterial counterpart. J Biol Chem *278*, 29719-29727.

Fazius, F., Shelest, E., Gebhardt, P., and Brock, M. (2012). The fungal α-aminoadipate pathway for lysine biosynthesis requires two enzymes of the aconitase family for the isomerization of homocitrate to homoisocitrate. Molecular Microbiology *86*, 1508-1530.

Fiedorczuk, K., Letts, J.A., Degliesposti, G., Kaszuba, K., Skehel, M., and Sazanov, L.A. (2016). Atomic structure of the entire mammalian mitochondrial complex I. Nature *538*, 406-410.

Flint, D.H., Tuminello, J.F., and Emptage, M.H. (1993). The inactivation of Fe-S cluster containing hydro-lyases by superoxide. J Biol Chem *268*, 22369-22376.

Floyd, B.J., Wilkerson, E.M., Veling, M.T., Minogue, C.E., Xia, C., Beebe, E.T., Wrobel, R.L., Cho, H., Kremer, L.S., Alston, C.L.*, et al.* (2016). Mitochondrial Protein Interaction Mapping Identifies Regulators of Respiratory Chain Function. Mol Cell *63*, 621-632.

Foury, F., Pastore, A., and Trincal, M. (2007). Acidic residues of yeast frataxin have an essential role in Fe-S cluster assembly. EMBO Rep *8*, 194-199.

Fox, N.G., Das, D., Chakrabarti, M., Lindahl, P.A., and Barondeau, D.P. (2015). Frataxin Accelerates [2Fe-2S] Cluster Formation on the Human Fe–S Assembly Complex. Biochemistry *54*, 3880-3889.

Frey, A.G., Palenchar, D.J., Wildemann, J.D., and Philpott, C.C. (2016). A Glutaredoxin-BolA Complex Serves as an Iron-Sulfur Cluster Chaperone for the Cytosolic Cluster Assembly Machinery. J Biol Chem.

Gelling, C., Dawes, I.W., Richhardt, N., Lill, R., and Muhlenhoff, U. (2008). Mitochondrial Iba57p is required for Fe/S cluster formation on aconitase and activation of radical SAM enzymes. Mol Cell Biol *28*, 1851-1861.

Haack, T.B., Rolinski, B., Haberberger, B., Zimmermann, F., Schum, J., Strecker, V., Graf, E., Athing, U., Hoppen, T., Wittig, I.*, et al.* (2013). Homozygous missense mutation in BOLA3 causes multiple mitochondrial dysfunctions syndrome in two siblings. J Inherit Metab Dis *36*, 55-62.

Huttlin, E.L., Ting, L., Bruckner, R.J., Gebreab, F., Gygi, M.P., Szpyt, J., Tam, S., Zarraga, G., Colby, G., Baltier, K.*, et al.* (2015). The BioPlex Network: A Systematic Exploration of the Human Interactome. Cell *162*, 425-440.

Invernizzi, F., Ardissone, A., Lamantea, E., Garavaglia, B., Zeviani, M., Farina, L., Ghezzi, D., and Moroni, I. (2014). Cavitating leukoencephalopathy with multiple mitochondrial dysfunction syndrome and NFU1 mutations. Front Genet *5*, 412.

Iwata, M., Lee, Y., Yamashita, T., Yagi, T., Iwata, S., Cameron, A.D., and Maher, M.J. (2012). The structure of the yeast NADH dehydrogenase (Ndi1) reveals overlapping binding sites for water- and lipid-soluble substrates. Proc Natl Acad Sci U S A *109*, 15247-15252.

Iwata, S., Lee, J.W., Okada, K., Lee, J.K., Iwata, M., Rasmussen, B., Link, T.A., Ramaswamy, S., and Jap, B.K. (1998). Complete structure of the 11-subunit bovine mitochondrial cytochrome bc1 complex. Science *281*, 64-71.

Johansson, C., Roos, A.K., Montano, S.J., Sengupta, R., Filippakopoulos, P., Guo, K., von Delft, F., Holmgren, A., Oppermann, U., and Kavanagh, K.L. (2011). The crystal structure of human GLRX5: iron-sulfur cluster co-ordination, tetrameric assembly and monomer activity. Biochem J *433*, 303-311.

Kaiser, J.T., Clausen, T., Bourenkow, G.P., Bartunik, H.-D., Steinbacher, S., and Huber, R. (2000). Crystal structure of a NifS-like protein from Thermotoga maritima: implications for iron sulphur cluster assembly1. Journal of Molecular Biology *297*, 451-464.

Kevelam, S.H., Rodenburg, R.J., Wolf, N.I., Ferreira, P., Lunsing, R.J., Nijtmans, L.G., Mitchell, A., Arroyo, H.A., Rating, D., Vanderver, A*., et al.* (2013). NUBPL mutations in patients with complex I deficiency and a distinct MRI pattern. Neurology *80*, 1577-1583.

Kim, J.H., Frederick, R.O., Reinen, N.M., Troupis, A.T., and Markley, J.L. (2013). [2Fe-2S]-ferredoxin binds directly to cysteine desulfurase and supplies an electron for iron-sulfur cluster assembly but is displaced by the scaffold protein or bacterial frataxin. J Am Chem Soc *135*, 8117-8120.

Kim, J.H., Tonelli, M., Frederick, R.O., Chow, D.C., and Markley, J.L. (2012). Specialized Hsp70 chaperone (HscA) binds preferentially to the disordered form, whereas J-protein (HscB) binds preferentially to the structured form of the iron-sulfur cluster scaffold protein (IscU). J Biol Chem *287*, 31406-31413.

Kispal, G., Csere, P., Prohl, C., and Lill, R. (1999). The mitochondrial proteins Atm1p and Nfs1p are essential for biogenesis of cytosolic Fe/S proteins. EMBO J *18*, 3981-3989.

Knaff, D.B., Hirasawa, M., Ameyibor, E., Fu, W., and Johnson, M.K. (1991). Spectroscopic evidence for a [3Fe-4S] cluster in spinach glutamate synthase. J Biol Chem *266*, 15080-15084.

Kondapalli, K.C., Kok, N.M., Dancis, A., and Stemmler, T.L. (2008). Drosophila

frataxin: an iron chaperone during cellular Fe-S cluster bioassembly. Biochemistry *47*, 6917-6927.

Kumanovics, A., Chen, O.S., Li, L., Bagley, D., Adkins, E.M., Lin, H., Dingra, N.N., Outten, C.E., Keller, G., Winge, D.*, et al.* (2008). Identification of FRA1 and FRA2 as Genes Involved in Regulating the Yeast Iron Regulon in Response to Decreased Mitochondrial Iron-Sulfur Cluster Synthesis. J Biol Chem *283*, 10276-10286.

Lange, H., Kaut, A., Kispal, G., and Lill, R. (2000). A mitochondrial ferredoxin is essential for biogenesis of cellular iron-sulfur proteins. Proc Natl Acad Sci USA *97*, 1050-1055.

Li, H., Mapolelo, D.T., Randeniya, S., Johnson, M.K., and Outten, C.E. (2012). Human glutaredoxin 3 forms [2Fe-2S]-bridged complexes with human BolA2. Biochemistry *51*, 1687-1696.

Li, H., and Outten, C.E. (2012). Monothiol CGFS glutaredoxins and BolA-like proteins: [2Fe-2S] binding partners in iron homeostasis. Biochemistry *51*, 4377-4389.

Li, Q., Ritzel, R.G., McLean, L.L., McIntosh, L., Ko, T., Bertrand, H., and Nargang, F.E. (1996). Cloning and analysis of the alternative oxidase gene of Neurospora crassa. Genetics *142*, 129-140.

Lill, R., Dutkiewicz, R., Freibert, S.A., Heidenreich, T., Mascarenhas, J., Netz, D.J., Paul, V.D., Pierik, A.J., Richter, N., Stumpfig, M.*, et al.* (2015). The role of mitochondria and the CIA machinery in the maturation of cytosolic and nuclear iron-sulfur proteins. Eur J Cell Biol *94*, 280-291.

Lossos, A., Stumpfig, C., Stevanin, G., Gaussen, M., Zimmerman, B.E., Mundwiller, E., Asulin, M., Chamma, L., Sheffer, R., Misk, A.*, et al.* (2015). Fe/S protein assembly gene IBA57 mutation causes hereditary spastic paraplegia. Neurology *84*, 659-667.

Maio, N., Ghezzi, D., Verrigni, D., Rizza, T., Bertini, E., Martinelli, D., Zeviani, M., Singh, A., Carrozzo, R., and Rouault, T.A. (2016). Disease-Causing SDHAF1 Mutations Impair Transfer of Fe-S Clusters to SDHB. Cell Metab *23*, 292-302.

Maio, N., and Rouault, T.A. (2015). Iron-sulfur cluster biogenesis in mammalian cells: New insights into the molecular mechanisms of cluster delivery. Biochim Biophys Acta *1853*, 1493-1512.

Maio, N., Singh, A., Uhrigshardt, H., Saxena, N., Tong, W.H., and Rouault, T.A. (2014). Cochaperone binding to LYR motifs confers specificity of iron sulfur cluster delivery. Cell Metab *19*, 445-457.

Majewska, J., Ciesielski, S.J., Schilke, B., Kominek, J., Blenska, A., Delewski, W., Song, J.Y., Marszalek, J., Craig, E.A., and Dutkiewicz, R. (2013). Binding of the chaperone

Jac1 protein and cysteine desulfurase Nfs1 to the iron-sulfur cluster scaffold Isu protein is mutually exclusive. J Biol Chem *288*, 29134-29142.

Manzella, L., Barros, M.H., and Nobrega, F.G. (1998). ARH1 of Saccharomyces cerevisiae: a new essential gene that codes for a protein homologous to the human adrenodoxin reductase. Yeast *14*, 839-846.

McLaughlin, M.I., Lanz, N.D., Goldman, P.J., Lee, K.H., Booker, S.J., and Drennan, C.L. (2016). Crystallographic snapshots of sulfur insertion by lipoyl synthase. Proc Natl Acad Sci U S A *113*, 9446-9450.

Melber, A., Na, U., Vashisht, A., Weiler, B.D., Lill, R., Wohlschlegel, J.A., and Winge, D.R. (2016). Role of Nfu1 and Bol3 in iron-sulfur cluster transfer to mitochondrial clients. eLife *5*, e15991.

Melber, A., and Winge, D.R. (2016). Inner Secrets of the Respirasome. Cell *167*, 1450-1452.

Miller, R.E., and Stadtman, E.R. (1972). Glutamate synthase from Escherichia coli. An iron-sulfide flavoprotein. J Biol Chem *247*, 7407-7419.

Mühlenhoff, U., Balk, J., Richhardt, N., Kaiser, J.T., Sipos, K., Kispal, G., and Lill, R. (2004). Functional Characterization of the Eukaryotic Cysteine Desulfurase Nfs1p from Saccharomyces cerevisiae. Journal of Biological Chemistry *279*, 36906-36915.

Muhlenhoff, U., Gerber, J., Richhardt, N., and Lill, R. (2003). Components involved in assembly and dislocation of iron-sulfur clusters on the scaffold protein Isu1p. EMBO J *22*, 4815-4825.

Muhlenhoff, U., Richter, N., Pines, O., Pierik, A.J., and Lill, R. (2011). Specialized Function of Yeast Isa1 and Isa2 Proteins in the Maturation of Mitochondrial [4Fe-4S] Proteins. J Biol Chem *286*, 41205-41216.

Mühlenhoff, U., Stadler, J.A., Richhardt, N., Seubert, A., Eickhorst, T., Schweyen, R.J., Lill, R., and Wiesenberger, G. (2003). A specific role of the yeast mitochondrial carriers MRS3/4p in mitochondrial iron acquisition under iron-limiting conditions. J Biol Chem *278*, 40612-40620.

Na, U., Yu, W., Cox, J., Bricker, D.K., Brockmann, K., Rutter, J., Thummel, C.S., and Winge, D.R. (2014). The LYR factors SDHAF1 and SDHAF3 mediate maturation of the iron-sulfur subunit of succinate dehydrogenase. Cell Metab *20*, 253-266.

Navarro-Sastre, A., Tort, F., Stehling, O., Uzarska, M.A., Arranz, J.A., Del Toro, M., Labayru, M.T., Landa, J., Font, A., Garcia-Villoria, J.*, et al.* (2011). A fatal mitochondrial disease is associated with defective NFU1 function in the maturation of a subset of mitochondrial Fe-S proteins. Am J Hum Genet *89*, 656-667.

Nizon, M., Boutron, A., Boddaert, N., Slama, A., Delpech, H., Sardet, C., Brassier, A., Habarou, F., Delahodde, A., Correia, I.*, et al.* (2014). Leukoencephalopathy with cysts and hyperglycinemia may result from NFU1 deficiency. Mitochondrion *15*, 59-64.

Ozeir, M., Muhlenhoff, U., Webert, H., Lill, R., Fontecave, M., and Pierrel, F. (2011). Coenzyme Q biosynthesis: Coq6 is required for the C5-hydroxylation reaction and substrate analogs rescue Coq6 deficiency. Chem Biol *18*, 1134-1142.

Pandey, A., Golla, R., Yoon, H., Dancis, A., and Pain, D. (2012). Persulfide formation on mitochondrial cysteine desulfurase: enzyme activation by a eukaryote-specific interacting protein and Fe-S cluster synthesis. Biochem J *448*, 171-187.

Pandey, A., Gordon, D.M., Pain, J., Stemmler, T.L., Dancis, A., and Pain, D. (2013). Frataxin directly stimulates mitochondrial cysteine desulfurase by exposing substrate-binding sites, and a mutant Fe-S cluster scaffold protein with frataxin-bypassing ability acts similarly. J Biol Chem *288*, 36773-36786.

Pandey, A., Pain, J., Ghosh, A.K., Dancis, A., and Pain, D. (2015). Fe-S cluster biogenesis in isolated mammalian mitochondria: coordinated use of persulfide sulfur and iron and requirements for GTP, NADH, and ATP. J Biol Chem *290*, 640-657.

Parent, A., Elduque, X., Cornu, D., Belot, L., Le Caer, J.P., Grandas, A., Toledano, M.B., and D'Autreaux, B. (2015). Mammalian frataxin directly enhances sulfur transfer of NFS1 persulfide to both ISCU and free thiols. Nat Commun *6*, 5686.

Paul, V.D., and Lill, R. (2015). Biogenesis of cytosolic and nuclear iron-sulfur proteins and their role in genome stability. Biochim Biophys Acta *1853*, 1528-1539.

Pierrel, F., Hamelin, O., Douki, T., Kieffer-Jaquinod, S., Muhlenhoff, U., Ozeir, M., Lill, R., and Fontecave, M. (2010). Involvement of mitochondrial ferredoxin and para-aminobenzoic acid in yeast coenzyme Q biosynthesis. Chem Biol *17*, 449-459.

Poor, C.B., Wegner, S.V., Li, H., Dlouhy, A.C., Schuermann, J.P., Sanishvili, R., Hinshaw, J.R., Riggs-Gelasco, P.J., Outten, C.E., and He, C. (2014). Molecular mechanism and structure of the Saccharomyces cerevisiae iron regulator Aft2. Proc Natl Acad Sci U S A *111*, 4043-4048.

Prischi, F., Konarev, P.V., Iannuzzi, C., Pastore, C., Adinolfi, S., Martin, S.R., Svergun, D.I., and Pastore, A. (2010). Structural bases for the interaction of frataxin with the central components of iron-sulphur cluster assembly. Nat Commun *1*, 95.

Robbins, A.H., and Stout, C.D. (1989). Structure of activated aconitase: formation of the [4Fe-4S] cluster in the crystal. Proc Natl Acad Sci U S A *86*, 3639-3643.

Roche, B., Aussel, L., Ezraty, B., Mandin, P., Py, B., and Barras, F. (2013). Iron/sulfur proteins biogenesis in prokaryotes: formation, regulation and diversity. Biochim Biophys

Acta *1827*, 455-469.

Rodriguez-Manzaneque, M.T., Tamarit, J., Belli, G., Ros, J., and Herrero, E. (2002). Grx5 is a mitochondrial glutaredoxin required for the activity of iron/sulfur enzymes. Mol Biol Cell *13*, 1109-1121.

Rouault, T.A. (2015). Mammalian iron-sulphur proteins: novel insights into biogenesis and function. Nat Rev Mol Cell Biol *16*, 45-55.

Schaedler, T.A., Thornton, J.D., Kruse, I., Schwarzlander, M., Meyer, A.J., van Veen, H.W., and Balk, J. (2014). A conserved mitochondrial ATP-binding cassette transporter exports glutathione polysulfide for cytosolic metal cofactor assembly. J Biol Chem *289*, 23264-23274.

Schilke, B., Voisine, C., Beinert, H., and Craig, E. (1999). Evidence for a conserved system for iron metabolism in the mitochondria of Saccharomyces cerevisiae. Proc Natl Acad Sci USA *96*, 10206-10211.

Schmucker, S., Martelli, A., Colin, F., Page, A., Wattenhofer-Donze, M., Reutenauer, L., and Puccio, H. (2011). Mammalian frataxin: an essential function for cellular viability through an interaction with a preformed ISCU/NFS1/ISD11 iron-sulfur assembly complex. PLoS One *6*, e16199.

Shakamuri, P., Zhang, B., and Johnson, M.K. (2012). Monothiol Glutaredoxins Function in Storing and Transporting [Fe2S2] Clusters Assembled on IscU Scaffold Proteins. Journal of the American Chemical Society *134*, 15213-15216.

Shan, Y., Napoli, E., and Cortopassi, G. (2007). Mitochondrial frataxin interacts with ISD11 of the NFS1/ISCU complex and multiple mitochondrial chaperones. Hum Mol Genet *16*, 929-941.

Sheftel, A.D., Stehling, O., Pierik, A.J., Netz, D.J., Kerscher, S., Elsasser, H.P., Wittig, I., Balk, J., Brandt, U., and Lill, R. (2009). Human ind1, an iron-sulfur cluster assembly factor for respiratory complex I. Mol Cell Biol *29*, 6059-6073.

Sheftel, A.D., Wilbrecht, C., Stehling, O., Niggemeyer, B., Elsasser, H.P., Muhlenhoff, U., and Lill, R. (2012). The human mitochondrial ISCA1, ISCA2, and IBA57 proteins are required for [4Fe-4S] protein maturation. Mol Biol Cell *23*, 1157-1166.

Smith, A.D., Agar, J.N., Johnson, K.A., Frazzon, J., Amster, I.J., Dean, D.R., and Johnson, M.K. (2001). Sulfur transfer from IscS to IscU: the first step in iron-sulfur cluster biosynthesis. J Am Chem Soc *123*, 11103-11104.

Smith, A.D., Frazzon, J., Dean, D.R., and Johnson, M.K. (2005). Role of conserved cysteines in mediating sulfur transfer from IscS to IscU. FEBS Lett *579*, 5236-5240.

Srinivasan, V., Pierik, A.J., and Lill, R. (2014). Crystal structures of nucleotide-free and glutathione-bound mitochondrial ABC transporter Atm1. Science *343*, 1137-1140.

Stehling, O., Wilbrecht, C., and Lill, R. (2014). Mitochondrial iron-sulfur protein biogenesis and human disease. Biochimie *100*, 61-77.

Sun, F., Huo, X., Zhai, Y., Wang, A., Xu, J., Su, D., Bartlam, M., and Rao, Z. (2005). Crystal structure of mitochondrial respiratory membrane protein complex II. Cell *121*, 1043-1057.

Tonduti, D., Dorboz, I., Imbard, A., Slama, A., Boutron, A., Pichard, S., Elmaleh, M., Vallee, L., Benoist, J.F., Ogier, H.*, et al.* (2015). New spastic paraplegia phenotype associated to mutation of NFU1. Orphanet J Rare Dis *10*, 13.

Torraco, A., Ardissone, A., Invernizzi, F., Rizza, T., Fiermonte, G., Niceta, M., Zanetti, N., Martinelli, D., Vozza, A., Verrigni, D.*, et al.* (2017). Novel mutations in IBA57 are associated with leukodystrophy and variable clinical phenotypes. J Neurol *264*, 102-111.

Tsai, C.L., and Barondeau, D.P. (2010). Human frataxin is an allosteric switch that activates the Fe-S cluster biosynthetic complex. Biochemistry *49*, 9132-9139.

Tse Sum Bui, B., Benda, R., Schunemann, V., Florentin, D., Trautwein, A.X., and Marquet, A. (2003). Fate of the (2Fe-2S)(2+) cluster of Escherichia coli biotin synthase during reaction: a Mossbauer characterization. Biochemistry *42*, 8791-8798.

Tsukihara, T., Aoyama, H., Yamashita, E., Tomizaki, T., Yamaguchi, H., Shinzawa-Itoh, K., Nakashima, R., Yaono, R., and Yoshikawa, S. (1995). Structures of metal sites of oxidized bovine heart cytochrome c oxidase at 2.8 A. Science *269*, 1069-1074.

Urbina, H.D., Silberg, J.J., Hoff, K.G., and Vickery, L.E. (2001). Transfer of sulfur from IscS to IscU during Fe/S cluster assembly. J Biol Chem *276*, 44521-44526.

Uzarska, M.A., Dutkiewicz, R., Freibert, S.-A., Lill, R., and Mühlenhoff, U. (2013). The mitochondrial Hsp70 chaperone Ssq1 facilitates Fe/S cluster transfer from Isu1 to Grx5 by complex formation. Mol Biol Cell.

Uzarska, M.A., Nasta, V., Weiler, B.D., Spantgar, F., Ciofi-Baffoni, S., Saviello, M.R., Gonnelli, L., Muhlenhoff, U., Banci, L., and Lill, R. (2016). Mitochondrial Bol1 and Bol3 function as assembly factors for specific iron-sulfur proteins. Elife *5*.

Van Vranken, J.G., Jeong, M.Y., Wei, P., Chen, Y.C., Gygi, S.P., Winge, D.R., and Rutter, J. (2016). The mitochondrial acyl carrier protein (ACP) coordinates mitochondrial fatty acid synthesis with iron sulfur cluster biogenesis. Elife *5*.

Webert, H., Freibert, S.A., Gallo, A., Heidenreich, T., Linne, U., Amlacher, S., Hurt, E., Muhlenhoff, U., Banci, L., and Lill, R. (2014). Functional reconstitution of mitochondrial

Fe/S cluster synthesis on Isu1 reveals the involvement of ferredoxin. Nat Commun *5*, 5013.

Wiedemann, N., Urzica, E., Guiard, B., Muller, H., Lohaus, C., Meyer, H.E., Ryan, M.T., Meisinger, C., Muhlenhoff, U., Lill, R.*, et al.* (2006). Essential role of Isd11 in mitochondrial iron-sulfur cluster synthesis on Isu scaffold proteins. EMBO J *25*, 184-195.

Willems, P., Wanschers, B.F., Esseling, J., Szklarczyk, R., Kudla, U., Duarte, I., Forkink, M., Nooteboom, M., Swarts, H., Gloerich, J.*, et al.* (2013). BOLA1 is an aerobic protein that prevents mitochondrial morphology changes induced by glutathione depletion. Antioxid Redox Signal *18*, 129-138.

Wu, M., Gu, J., Guo, R., Huang, Y., and Yang, M. (2016). Structure of Mammalian Respiratory Supercomplex I1III2IV1. Cell *167*, 1598-1609 e1510.

Yan, R., Adinolfi, S., and Pastore, A. (2015). Ferredoxin, in conjunction with NADPH and ferredoxin-NADP reductase, transfers electrons to the IscS/IscU complex to promote iron-sulfur cluster assembly. Biochim Biophys Acta *1854*, 1113-1117.

Yoon, H., Knight, S.A., Pandey, A., Pain, J., Zhang, Y., Pain, D., and Dancis, A. (2014). Frataxin-bypassing Isu1: characterization of the bypass activity in cells and mitochondria. Biochem J *459*, 71-81.

Yoon, T., and Cowan, J.A. (2003). Iron-sulfur cluster biosynthesis. Characterization of frataxin as an iron donor for assembly of [2Fe-2S] clusters in ISU-type proteins. J Am Chem Soc *125*, 6078-6084.

Zhu, J., Vinothkumar, K.R., and Hirst, J. (2016). Structure of mammalian respiratory complex I. Nature *536*, 354-358.

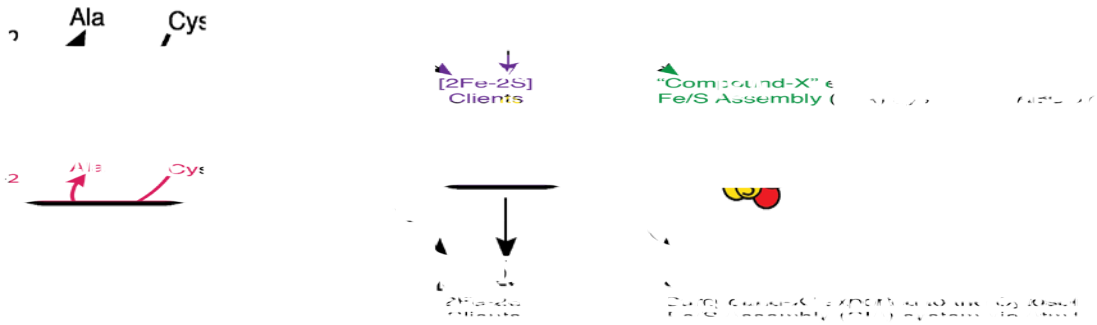

Figure 1.1 General overview of mitochondrial Fe/S cluster biogenesis.
All clusters in the cell require the initial biogenesis by the ISU complex that generates a [2Fe-2S] cluster from iron and cysteine before transferring it through Grx5 to the ISA complex. The ISA complex condenses two [2Fe-2S] clusters to create a single [4Fe-4S] cluster for mitochondrial client proteins. A summary of each component is described in Table 1.1 on the subsequent page.

Table 1.1. List of mitochondrial Fe/S assembly components.
The table includes all known mitochondrial assembly proteins and their function.

	Human	Yeast	Function
ISU Complex	ISCU	Isu1/ Isu2	Scaffold protein for the assembly of the initial [2Fe-2S] cluster
	NFS1	Nfs1	Cysteine desulfurase, provides a sulfide by reducing cysteine to alanine, requires a PLP cofactor
	ISD11	Isd11	Stablizing binding partner of Nfs1 that activates persulfide formation
	ACPM	Acp1	Binds and stablizes Isd11, potentially links Fe/S biogenesis to fatty acid biogensis
	FDX2	Yah1	Ferroredoxin, donates an electron to both Fe/S and heme biosynthesis pathways, contains a [2Fe-2S] cluster
	Frataxin	Yfh1	Stimulates [2Fe-2S] formation on ISCU by activating sulfur transfer from Nfs1 to ISCU
	HSPA9	Ssq1	Hsp70 protein that binds Grx5 during the transfer of the [2Fe-2S] from ISU
	GRPE1	Mge1	Nucleotide exchange factor that cycles ATP on Ssq1 for cluster transfer
	HSC20	Jac1	DNAJ protein that facilitates transfer of the preformed [2Fe-2S] cluster from Isu1 to Grx5
	GLRX5	Grx5	Glutaredoxin that transfers performed [2Fe-2S] clusters to client proteins in the mitochondria
	BOLA1	Bol1	Assists Grx5 in [2Fe-2S] cluster delivery
	ABCB7	Atm1	Inner mitochondrial membrane transport that exports compound x to the cytosolic Fe/S assembly pathway
ISA Complex	ISCA1	Isa1	Binds a single [2Fe-2S] cluster to condense with the cluster from Isa2
	ISCA2	Isa2	Binds a single [2Fe-2S] cluster to condense with the cluster from Isa1
	IBA57	Iba57	Unknown function, but a component of the ISA complex required for [4Fe-4S] biogenesis.
	Nfu1	Nfu1	Transfers [4Fe-4S] clusters from the ISA complex to client proteins to protect clusters from oxidative damage
	BOLA3	Bol3	Assists Nfu1 in [4Fe-4S] transfer, exactly function is unknown

CHAPTER 2

INNER SECRETS OF THE RESPIRASOME

Andrew Melber, Dennis R. Winge

Reprinted with Permission from Cell

Vol. 167, pp.1450-1452, December 1, 2016

Cell

Leading Edge
Previews

Inner Secrets of the Respirasome

Andrew Melber[1] and Dennis R. Winge[1,*]
[1]University of Utah Health Sciences Center, Salt Lake City UT 84132, USA
*Correspondence: dennis.winge@hsc.utah.edu
http://dx.doi.org/10.1016/j.cell.2016.11.025

Structure determination by cryo-electron microscopy has approached atomic resolution and helped solve structures of large membrane-protein complexes that resisted crystallography. The 4.0 Å cryo-EM structure of one of the most intricate enzyme systems, the respirasome, in the mitochondrial inner membrane is reported in this issue of *Cell*.

The 1.7 MDa respirasome complex is a supercomplex consisting of OXPHOS respiratory complexes I (NADH:ubiquinone oxidoreductase), III (cytochrome *c* reductase) and IV (cytochrome *c* oxidase). This polyprotein complex couples electron transfer from the oxidation of NADH to proton pumping across the inner membrane generating the proton gradient used in ATP synthesis. Electron transfer between the three respiratory complexes is mediated by two mobile electron carriers ubiquinone and cytochrome *c* (Figure 1A).

The respirasome, designated as supercomplex SC(I + III_2 + IV), consists of the 44 distinct subunits of Complex I (CI), the 22 subunits of dimeric Complex III (CIII), and one Complex IV (CIV) unit of 14 subunits. This represents only one of a myriad of respiratory supercomplexes. This current porcine heart respirasome structure follows 5.4 Å structures reported this past summer for porcine and ovine heart SC(I + III_2 + IV) complexes (Letts et al., 2016; Gu et al., 2016). In addition, 3.9 and 4.2 Å structures of ovine and bovine Complex I, respectively, were recently reported (Fiedorczuk et al., 2016; Zhu et al., 2016).

The enhanced resolution in the current porcine heart SC(I + III_2 + IV) reported by Wu et al. in this issue of *Cell* leads to a multitude of novel observations. First, whereas crystal structures have been available for bovine CIII and CIV since the late 1990s, the porcine respirasome and ovine CI 3.6 Å and 3.9 Å structures reveal atomic resolution of all 45 subunits of CI (Wu et al., 2016; Fiedorczuk et al., 2016). Second, the previous low resolution ~19–24 Å structures revealed prominent gaps between complexes leading to speculation that additional supercomplex stabilizing factors may be present once higher resolution structures were obtained. In the atomic structures, it is clear that the porcine SC(I + III_2 + IV) lacks any additional stabilizing proteins. Two previously implicated SC stabilizing factors are COX7A2L and HIGD2. Although COX7A2L can exist within SC(I + III_2 + IV), it is now known to primarily facilitate the CIII-CIV interaction (Cogliati et al., 2016; Pérez-Pérez et al., 2016). Different isoforms of COX7A exist including COX7A1, COX7A2, and COX7A2L. The presence of COX7A2 isoform correlates primarily with unassociated monomeric CIV complex, whereas COX7A1-containing CIV species favor dimeric CIV complexes (Cogliati et al., 2016). Replacement of COX7A1 with COX7A2L (SCAFI) permits assembly of the CIII-CIV heterocomplex and SC formation in some tissues (Cogliati et al., 2016). The porcine respirasome clearly lacks the COX7A2L isoform, so additional work is needed to discern the effects of CIV subunit remodeling on respirasome function. The porcine respirasome also lacks HIGD1 or HIGD2 factors implicated in SC stabilization (Chen et al., 2012). The hypoxia-inducible HIGD1a protein has been shown to be a positive regulator of CIV (Hayashi et al., 2015), so one type of CIV remodeling may occur during stress conditions such as hypoxia to enhance respiratory function.

The high-resolution structures reveal numerous cofactors important in CI stability and whose presence opens new questions about regulation (Figure 1B). All eight Fe-S clusters in the peripheral arm of CI are observed as is the FMN moiety in the catalytic NDUFV1 subunit. One question concerns the role of the N1a Fe-S cluster that lies outside the main electron transfer wire to the N2 cluster, the terminal cofactor mediating reduction of ubiquinone. In addition to the Fe-S cofactors, the CI subunit NDUFS6 has a structural Zn(II) (S_3N_1) site. Zn(II) thiolate sites can function as redox switches in that Zn(II) binding is lost by either oxidation or nitrosylation of thiolates from reactive oxygen or nitrogen oxide species. Evidence on whether NDUFS6 is susceptible to nitrosylation is currently lacking, but such a reaction may alter electron transfer through the nearby N6a and N5 Fe-S clusters. A novel cofactor observed is a non-catalytic NADPH bound to NDUFA9 in the peripheral arm of CI and in close juxtaposition to the N2 Fe-S cluster near the ubiquinone site. If NADPH association in NDUFA9 is in dynamic exchange with the matrix milieu, NADPH binding may contribute allosteric regulation of CI. NADPH is critical for maintaining reduced GSH and thioredoxin levels. Thus, CI function may be redox modulated.

An intriguing aspect of the CI structure is that two structural subunits are a repurposed protein, acyl carrrier protein (ACP), which has a critical function in the mitochondrial synthesis of lipoic acid cofactors used in the mitochondrial citric acid cycle. Two ACP molecules, in complex with two distinct leucine/tyrosine/arginine motif (LYRM)-containing subunits, are associated with the peripheral and membrane arms of CI. Deletion of the CI peripheral arm LYRM subunit in *Yarrowia* compromises CI function (Angerer et al., 2014). The ACP-LYRM interaction is mediated in part by the phosphopantetheine cofactor on ACP and the acyl chain appended to it. The decanoyl C10 fatty acid chain on the cofactor is flipped out and embedded within the three-helix

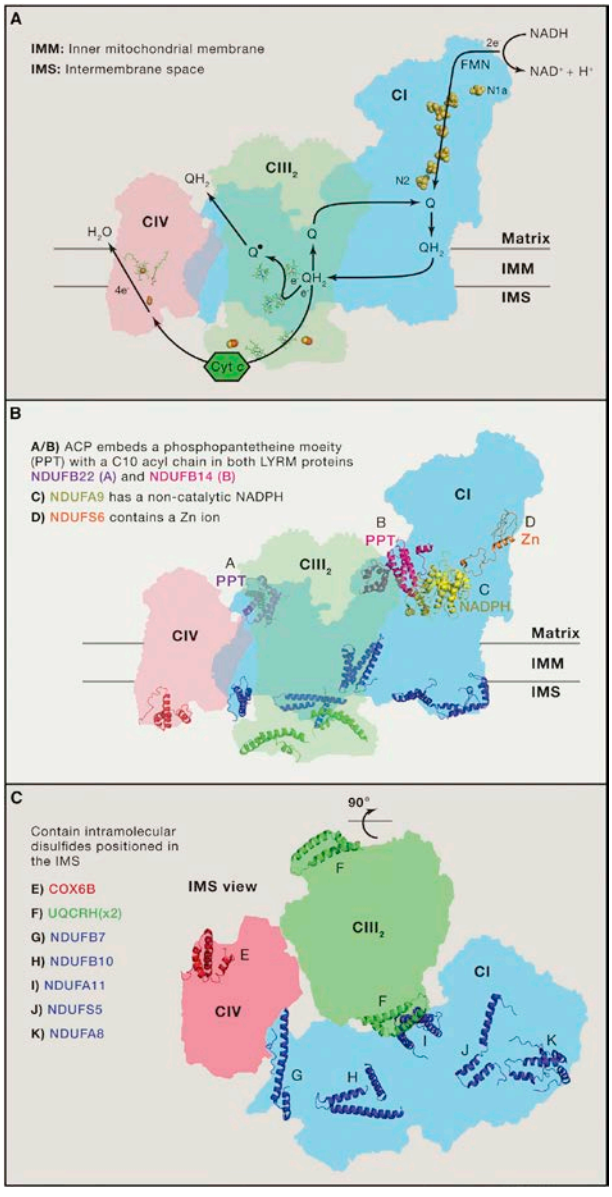

Figure 1. Catalytic and Putative Regulatory Mechanisms of the Respirasome

(A) The (I + III_2 + IV) respirasome couples the oxidation of NADH to reduction of molecular oxygen. CI (outlined in blue) oxidizes NADH and transfers two electrons through its FMN cofactor and seven of its eight Fe-S clusters to reduce ubiquinone (Q) to ubiquinol (QH_2). The dimeric CIII (outlined in green) oxidizes QH_2 and transfers one electron to cytochrome *c* via a heme and a Fe-S cluster and the second electron is used to reduce Q in the Q cycle of proton pumping. CIV (outlined in red) receives four electrons from successive cytochrome *c* transfers and electrons pass through a binuclear copper A center, a heme *a* moiety to a heterobimetallic copper B-heme a_3 center for the 4 electron reduction of molecular oxygen. IMM is the inner mitochondrial membrane, IMS is the intermembrane space and matrix is the space enclosed by the inner membrane.

(B) This side view of the respirasome highlights additional CI cofactors. The ACP protein SDAP-β and the corresponding LYRM protein, NDUFB22 (A, purple/dark purple) and ACP protein SDAP-α and its corresponding LYRM protein, NDUFB14 (B, purple/magenta) are associated by a C:10 acyl chain on the phosphopantetheine (PPT) cofactor of each ACP. These ACP-LYRM dimers provide a potential regulatory link between fatty acid biosynthesis and respiration. A NADPH molecule bound to NDUFA9 (C, yellow) and zinc ion bound to NDUFS6 (D, orange) may act as redox sensors for CI function.

(C) The IMS view of the respirasome shows subunits in all three complexes that contain stabilizing disulfide bonds. Redox changes in these subunits may modulate the respirasome function. The disulfide subunits include COX6B (E, red) in complex CIV, UQCRH (F, green) in CIII, and CI subunits in blue NDUFB7 (G), NDUFB10 (H), NDUFA11 (I), NDUFS5 (J) and NDUFA8 (K).

LYRM conformer. The ACP-acyl-LYRM interaction at the distal end of the membrane arm forms key contacts with CIII to stabilize the respirasome. We have reported recently that ACP with a bound phosphopantetheine is also required for the stability of Nfs1 cysteine desulfurase and its LYRM partner Isd11 (Van Vranken et al., 2016). ACP is implicated in an association with all mitochondrial LYRM proteins, so the CI structures may provide a structural basis for all ACP-LYRM interactions. Taken together, ACP-acyl-LYRM and the required phosphopantetheine reveal a potential regulatory link between mitochondrial fatty acid synthesis and the respirasome function.

The respirasome structure reveals other potential modes of regulation of its function. Numerous OXPHOS complex subunits are known to undergo phosphorylation, and one future challenge is to deduce which phosphorylation sites modulate function. In addition, numerous subunits on the intermembrane space

Cell

exposed side of the respirasome contain disulfide bonds likely introduced by the MIA40 pathway (Figure 1C). Four disulfide bonded twin Cx_9C proteins in CI, and one each in CIII and CIV subunits within the respirasome create a potential regulatory mechanism in which redox changes in the IMS may modulate respirasome activity. In addition, a key CI subunit NDUFA11 that mediates contacts with other CI subunits and CIII, contains a disulfide bond within its transmembrane domain. It has been recently demonstrated that yeast cultured under fermentative conditions experience a more highly reducing IMS and twin Cx_9C proteins, including the CIV COX6B, are reduced and several are retro-translocated out of the mitochondria for proteosomal degradation (Bragoszewski et al., 2015).

For the first time the presence and position of various lipids are evident and lipids can be seen to mediate interaction between subunits and complexes. Lipids are prominent components of these structures, yet it remains to be established whether these lipids are merely structural units or have regulatory roles. Remodeling of cardiolipin via the tafazzin transacylase may exert conformational changes that alter respiratory activity. A novel aspect of the respirasome structure is the identification of at least two conformational states. Movement of the CI matrix arm with respect to CIII forms a tight supercomplex state relative to a second loose state. Conformational dynamics may modulate the activity of the respirasome as well as remodeling of respiratory complexes.

In summary, the atomic level resolution of the respirasome has revealed rich new details that open new challenges for further studies.

REFERENCES

Angerer, H., Radermacher, M., Mańkowska, M., Steger, M., Zwicker, K., Heide, H., Wittig, I., Brandt, U., and Zickermann, V. (2014). Proc. Natl. Acad. Sci. USA *111*, 5207–5212.

Bragoszewski, P., Wasilewski, M., Sakowska, P., Gornicka, A., Böttinger, L., Qiu, J., Wiedemann, N., and Chacinska, A. (2015). Proc. Natl. Acad. Sci. USA *112*, 7713–7718.

Chen, Y.C., Taylor, E.B., Dephoure, N., Heo, J.M., Tonhato, A., Papandreou, I., Nath, N., Denko, N.C., Gygi, S.P., and Rutter, J. (2012). Cell Metab. *15*, 348–360.

Cogliati, S., Calvo, E., Loureiro, M., Guaras, A.M., Nieto-Arellano, R., Garcia-Poyatos, C., Ezkurdia, I., Mercader, N., Vázquez, J., and Enriquez, J.A. (2016). Nature. Published online on October 24, 2016. http://dx.doi.org/10.1038/nature20157.

Fiedorczuk, K., Letts, J.A., Degliesposti, G., Kaszuba, K., Skehel, M., and Sazanov, L.A. (2016). Nature *538*, 406–410.

Gu, J., Wu, M., Guo, R., Yan, K., Lei, J., Gao, N., and Yang, M. (2016). Nature *537*, 639–643.

Hayashi, T., Asano, Y., Shintani, Y., Aoyama, H., Kioka, H., Tsukamoto, O., Hikita, M., Shinzawa-Itoh, K., Takafuji, K., Higo, S., et al. (2015). Proc. Natl. Acad. Sci. USA *112*, 1553–1558.

Letts, J.A., Fiedorczuk, K., and Sazanov, L.A. (2016). Nature *537*, 644–648.

Pérez-Pérez, R., Lobo-Jarne, T., Milenkovic, D., Mourier, A., Bratic, A., García-Bartolomé, A., Fernández-Vizarra, E., Cadenas, S., Delmiro, A., García-Consuegra, I., et al. (2016). Cell Rep. *16*, 2387–2398.

Van Vranken, J.G., Jeong, M.Y., Wei, P., Chen, Y.C., Gygi, S.P., Winge, D.R., and Rutter, J. (2016). eLife *5*, 5.

Wu, M., Gu, J., Guo, R., Huang, Y., and Yang, M. (2016). Cell *167*, this issue, 1598–1609.

Zhu, J., Vinothkumar, K.R., and Hirst, J. (2016). Nature *536*, 354–358.

Retromer Sets a Trap for Endosomal Cargo Sorting

Ludger Johannes[1,*] and Christian Wunder[1]

[1]Institut Curie, PSL Research University, Chemical Biology of Membranes and Therapeutic Delivery unit, INSERM U 1143, CNRS UMR 3666, 26 rue d'Ulm, 75248 Paris Cedex 05, France

*Correspondence: ludger.johannes@curie.fr

http://dx.doi.org/10.1016/j.cell.2016.11.026

Membrane trafficking from endosomes to the *trans*-Golgi network or the plasma membrane is driven by the retromer complex. Through structural analysis of the cargo-bound complex, Lucas et al. describe a mechanism by which endosomal membrane recruitment and cargo recognition are integrated through cooperative interactions between retromer subunits.

Early maturing endosomes serve as central sorting hub in eukaryotic cells from which cargo molecules are directed to three destinations: lysosomes via the late endocytic pathway, the *trans*-Golgi network via the retrograde pathway, and the plasma membrane via the recycling pathway. The retromer complex is an evolutionarily conserved protein assembly (reviewed in Seaman et al., 2013) on early maturing endosomes that recruits cargo for retrograde trafficking and recycling. It functions in a wide variety of physiological processes including nutrient uptake, polarized trafficking, lysosome biogenesis, growth factor receptor signaling, development, autophagy, response to infection, and synaptic transmission. It is not surprising therefore that mutations in retromer proteins are linked to pathologies, including neurodegenerative disorders such as Alzheimer's and Parkinson's disease. New work by Lucas et al. looks at the overall structure of the retromer complex and offers insights into how it recognizes and directs cargo.

CHAPTER 3

ROLE OF NFU1 AND BOL3 IN IRON-SULFUR CLUSTER TRANSFER TO MITOCHONDRIAL CLIENTS

Andrew Melber, Un Na, Ajay Vashisht, Benjamin D Weiler,

Roland Lill, James A Wohlschlegel, Dennis R Winge

Reprinted with Permission from eLife

eLife 2016;5:e15991

eLIFE elifesciences.org

RESEARCH ARTICLE

Role of Nfu1 and Bol3 in iron-sulfur cluster transfer to mitochondrial clients

Andrew Melber[1,2], Un Na[1,2], Ajay Vashisht[3], Benjamin D Weiler[4], Roland Lill[4,5], James A Wohlschlegel[3], Dennis R Winge[1,2]*

[1]Department of Medicine, University of Utah Health Sciences Center, Salt Lake City, United States; [2]Department of Biochemistry, University of Utah Health Sciences Center, Salt Lake City, United States; [3]Department of Biological Chemistry, David Geffen School of Medicine at UCLA, Los Angeles, United States; [4]Institut für Zytobiologie, Philipps-Universität Marburg, Marburg, Germany; [5]LOEWE Zentrum für Synthetische Mikrobiologie SynMikro, Marburg, Germany

Abstract Iron-sulfur (Fe-S) clusters are essential for many cellular processes, ranging from aerobic respiration, metabolite biosynthesis, ribosome assembly and DNA repair. Mutations in *NFU1* and *BOLA3* have been linked to genetic diseases with defects in mitochondrial Fe-S centers. Through genetic studies in yeast, we demonstrate that Nfu1 functions in a late step of [4Fe-4S] cluster biogenesis that is of heightened importance during oxidative metabolism. Proteomic studies revealed Nfu1 physical interacts with components of the ISA [4Fe-4S] assembly complex and client proteins that need [4Fe-4S] clusters to function. Additional studies focused on the mitochondrial BolA proteins, Bol1 and Bol3 (yeast homolog to human BOLA3), revealing that Bol1 functions earlier in Fe-S biogenesis with the monothiol glutaredoxin, Grx5, and Bol3 functions late with Nfu1. Given these observations, we propose that Nfu1, assisted by Bol3, functions to facilitate Fe-S transfer from the biosynthetic apparatus to the client proteins preventing oxidative damage to [4Fe-4S] clusters.
DOI: 10.7554/eLife.15991.001

***For correspondence:** dennis.winge@hsc.utah.edu

Competing interests: The authors declare that no competing interests exist.

Funding: See page 20

Received: 11 March 2016
Accepted: 16 August 2016
Published: 17 August 2016

Reviewing editor: Nikolaus Pfanner, University of Freiburg, Germany

Introduction

A severe syndrome characterized by the dysfunction of multiple mitochondrial enzymes has been described for a series of patients with mutations in four mitochondrial proteins IBA57, ISCA2, NFU1 and BOLA3 (***Seyda et al., 2001***; ***Cameron et al., 2011***; ***Navarro-Sastre et al., 2011***; ***Ferrer-Cortès et al., 2013***; ***Nizon et al., 2014***; ***Baker et al., 2014***; ***Debray et al., 2015***; ***Lossos et al., 2015***; ***Al-Hassnan et al., 2015***). Patients with this Multiple Mitochondria Dysfunctions Syndrome (MMDS) are afflicted with lactic acidosis, nonketotic hyperglycinemia and infantile encephalopathy typically leading to death in their first year of life. The syndrome is associated with an impairment of lipoic acid-dependent 2-oxoacid dehydrogenases arising from defective lipoate synthesis and defects in respiratory complexes I and II in select tissues including muscle and liver. These phenotypes arise from defective iron-sulfur (Fe-S) cluster assembly within the mitochondria. The deficiency in protein lipoylation is due to impaired activity of lipoic acid synthetase, which requires two [4Fe-4S] cluster cofactors (***Hiltunen et al., 2010***). The hyperglycinemic phenotype arises from failed lipoylation of the glycine cleavage enzyme. Whereas IBA57 and ISCA2 are known components of the ISA complex, along with ISCA1, which functions in the formation of [4Fe-4S] clusters within mitochondria (***Mühlenhoff et al., 2011***; ***Gelling et al., 2008***; ***Sheftel et al., 2012***), the functions of NFU1 and BOLA3 in Fe-S cluster assembly remain an enigma.

Yeast cells lacking Nfu1 are partially compromised in mitochondrial [4Fe-4S] cluster formation, but the defect is not as pronounced as in cells lacking components of the ISA complex (Isa1, Isa2 and

eLife digest Proteins perform almost all of the tasks necessary for cells to survive. Some of these proteins need to contain collections of iron and sulfur ions known as iron-sulfur clusters to work properly. The iron-sulfur clusters are first assembled from individual ions and then attached to the correct target proteins. In humans, yeast and other eukaryotic cells, the first step of this process happens in compartments called mitochondria and makes a cluster that contains two of each ion, known as [2Fe-2S] clusters. These [2Fe-2S] clusters can either be directly incorporated into target proteins, or they may be used to make larger iron-sulfur clusters – such as [4Fe-4S] clusters – in the mitochondria or the main compartment of the cell (the cytoplasm).

Defects that affect the assembly of proteins with iron-sulfur clusters are associated with severe diseases that affect metabolism, the nervous system and the blood. Mitochondria contain at least 17 proteins involved in making iron-sulfur proteins, but there may be others that have not yet been identified. For example, a study on patients with a rare human genetic disease suggested that proteins called BOLA3 and NFU1 might also play a role in this process.

Melber et al. used genetics to study how [4Fe-4S] clusters are assembled in the mitochondria of yeast cells. The experiments show that the yeast equivalents of NFU1 and BOLA3 (known as Nfu1 and Bol3) act to incorporate completed [4Fe-4s] clusters into their target proteins. This process is particularly important when iron-sulfur clusters are in high demand, such as when a cell needs to produce a lot of energy. Melber et al. also showed that a protein called Bol1 – which is closely related to Bol3 – is needed in an earlier stage of iron-sulfur cluster assembly.

The next steps following on from this work will be to look more closely at how Nfu1 and Bol3 deliver iron-sulfur clusters to the right target proteins. A future challenge will be to find out how other types of iron-sulfur clusters are transferred to their target proteins.

DOI: 10.7554/eLife.15991.002

Iba57) (***Navarro-Sastre et al., 2011***; ***Schilke et al., 1999***). As in patient cells with mutations in NFU1, yeast *nfu1*Δ cells have diminished protein lipoylation levels (***Navarro-Sastre et al., 2011***). Humans and yeast have two mitochondrial BolA proteins termed BolA1 (Bol1 in yeast) and BolA3 (Bol3 in yeast) (***Cameron et al., 2011***; ***Willems et al., 2013***), but little is known concerning their physiological function. The similarities of phenotypes in patients with MMDS mutations in NFU1 and BOLA3 suggest that BOLA3 may likewise function in mitochondrial Fe-S biogenesis (***Cameron et al., 2011***).

Fe-S cluster synthesis within the mitochondria occurs on a scaffold complex and preformed clusters are subsequently transferred to recipient proteins (***Lill et al., 2012***). The initial cluster formed is a [2Fe-2S] cluster assembled on the ISU scaffold complex consisting of five proteins, Nfs1, Isd11, Yfh1, Yah1 and Isu1 (or Isu2; yeast nomenclature) (***Lill et al., 2012***; ***Schmucker et al., 2011***; ***Tsai and Barondeau, 2010***; ***Lange et al., 2000***; ***Webert et al., 2014***). The sulfide ions are provided by the Nfs1 cysteine desulfurase, along with its effector proteins Isd11 and Yfh1 (***Tsai and Barondeau, 2010***; ***Lill and Mühlenhoff, 2008***; ***Gerber et al., 2003***; ***Biederbick et al., 2006***; ***Bridwell-Rabb et al., 2014***; ***Parent et al., 2015***; ***Fox et al., 2015***). Assembled [2Fe-2S] clusters on Isu1 are transferred to the monothiol glutaredoxin Grx5 through the action of the Ssq1 ATPase and the DnaJ protein Jac1 (***Ciesielski et al., 2012***; ***Majewska et al., 2013***; ***Uzarska et al., 2013***). Two [2Fe-2S] clusters transferred by Grx5 are condensed into a [4Fe-4S] cluster on the downstream ISA complex (Isa1, Isa2 and Iba57) prior to transfer to client proteins (***Mühlenhoff et al., 2011***; ***Gelling et al., 2008***; ***Sheftel et al., 2012***; ***Brancaccio et al., 2014***).

Nfu1 has been implicated to function as a late Fe-S maturation factor in bacteria and fungi (***Navarro-Sastre et al., 2011***; ***Bandyopadhyay et al., 2008***; ***Py et al., 2012***), an alternate scaffold protein for cluster synthesis (***Cameron et al., 2011***; ***Tong et al., 2003***) or as a persulfide reductase associated with the sulfide transfer (***Liu et al., 2009***). The lack of NfuA in *Escherichia coli* and *Azotobacter vinelandii* is associated with decreased viability under stress conditions (***Bandyopadhyay et al., 2008***; ***Py et al., 2012***; ***Angelini et al., 2008***). Nfu proteins from most species are multidomain proteins. *E. coli* NfuA and human Nfu1 are two domain proteins with the C-terminal domain containing the functionally important CxxC motif that is known to bind a [4Fe-4S] cluster at a homodimer interface (***Bandyopadhyay et al., 2008***; ***Tong et al., 2003***; ***Angelini et al.,***

2008; Gao et al., 2013). The N-terminal domains differ between the *E. coli* and human proteins and lack a related CxxC motif. Recombinant expression and purification of *Azotobacter* NfuA or human Nfu1 did not result in Fe-S cluster bound to the purified protein, but in vitro Fe-S reconstitution studies followed by Mössbauer spectral studies demonstrated the presence of a [4Fe-4S] cluster (Bandyopadhyay et al., 2008; Py et al., 2012; Tong et al., 2003; Angelini et al., 2008). *Synechocystis* NifU was reported to bind a [2Fe-2S] cluster (Yabe et al., 2004; Nishio and Nakai, 2000), but Mössbauer spectral studies were not done to validate the assignment. The ability of Nfu1 to bind a [4Fe-4S] cluster supported the suggestions that Nfu1 was either an alternative scaffold protein involved in Fe-S cluster formation or involved in a late cluster transfer step. The ability of bacterial NfuA to transfer its cluster to apo-aconitase in vitro is consistent with a role in a late step of cluster transfer (Bandyopadhyay et al., 2008; Angelini et al., 2008).

BolA proteins are also known to coordinate Fe-S clusters in conjunction with monothiol glutaredoxins (Li and Outten, 2012). One of the three BolA proteins in *Arabidopsis thaliana* BolA1 was shown to bind a [2Fe-2S] cluster in a complex with glutaredoxin (Grx) (Roret et al., 2014). The cluster associated with the BolA:Grx complex is coordinated by two thiolate ligands, one from Grx and the other from an associated glutathione, and two histidine ligands from BolA1. Likewise, the cytosolic BolA2 proteins of yeast and humans coordinate [2Fe-2S] clusters at the heterodimer interface with monothiol glutaredoxins (Li and Outten, 2012; Li et al., 2012). Little is known about the physiological function of mitochondrial BolA proteins, designated Bol1 and Bol3. BolA proteins are found only in aerobic species (Willems et al., 2013). Depletion of the mitochondrial BolA1 in HeLa cells caused an oxidative shift in the mitochondrial thiol/disulfide redox ratio (Willems et al., 2013).

We set out to define the functional steps of Nfu1 and two mitochondrial BolA proteins in yeast. We report that Nfu1 and Bol3 function at a late step in the transfer of Fe-S clusters from the ISA complex to mitochondrial client proteins as a protective measure for [4Fe-4S] clusters from oxidative stress damage. In contrast to Bol3, the related mitochondrial Bol1 shows an interaction with Grx5 but not with the ISA complex or [4Fe-4S] client proteins.

Results

Nfu1 is associated with mitochondrial [4Fe-4S] cluster formation

S. cerevisiae cells lacking the mitochondrial Nfu1 protein (*nfu1*Δ cells) are markedly impaired in growth on synthetic complete medium with acetate as a carbon source (Figure 1A). However, the mutant cells display only a slight growth impairment on glycerol/lactate medium, suggesting a partial respiratory growth defect that is exacerbated with acetate as the carbon source. It was previously reported that *nfu1*Δ cells exhibit specific but partial defects in the formation of [4Fe-4S] clusters analogous to phenotypes seen in patients with mitochondrial dysfunction syndrome (Navarro-Sastre et al., 2011; Schilke et al., 1999). We confirmed the defects in [4Fe-4S] client enzymes reported for *nfu1*Δ cells showing that aconitase and succinate dehydrogenase (SDH) activities are markedly impaired, yet residual activity persists (Figure 1B). Aconitase activity is markedly attenuated in *nfu1*Δ yeast cells, whereas its activity is not significantly depleted in human *nfu1* patients (Cameron et al., 2011; Navarro-Sastre et al., 2011). No defect was observed in the yeast mutant in respiratory complex III, cytochrome bc_1, which requires a [2Fe-2S] cluster in its Rieske Rip1 subunit or in cytochrome oxidase that requires a [2Fe-2S] cluster in Yah1 for heme *a* formation (Figure 1B).

Consistent with the known defects of *nfu1*Δ yeast cells and human *nfu1* patients, lipoic acid (LA) conjugates on pyruvate dehydrogenase (PDH) and oxoglutarate dehydrogenase (KDH) were attenuated in *nfu1*Δ cells (Figure 1C) (Navarro-Sastre et al., 2011). As mentioned, lipoic acid formation is dependent on the [4Fe-4S] lipoic acid synthase Lip5 (Hiltunen et al., 2010). Steady-state protein analysis by SDS-PAGE showed diminished Sdh2 levels, the Fe-S subunit of SDH. Sdh2 contains three distinct Fe-S clusters ([2Fe-2S], [4Fe-4S], and [3Fe-4S] clusters), which transfer electrons from the catalytic Sdh1 subunit to ubiquinone. In the absence of Fe-S cluster insertion, Sdh2 stability is compromised (Kim et al., 2012) (Figure 1C) In contrast, the aconitase protein stability is not dependent on the presence of its [4Fe-4S] cluster (Gelling et al., 2008).

Two enzymes involved in yeast lysine biosynthesis Aco2 and Lys4 contain [4Fe-4S] clusters (Fazius et al., 2012). Whereas yeast lacking the ISA complex are auxotrophic for lysine and accumulate homocitrate as a metabolic intermediate, *nfu1*Δ cells propagate normally in medium lacking lysine

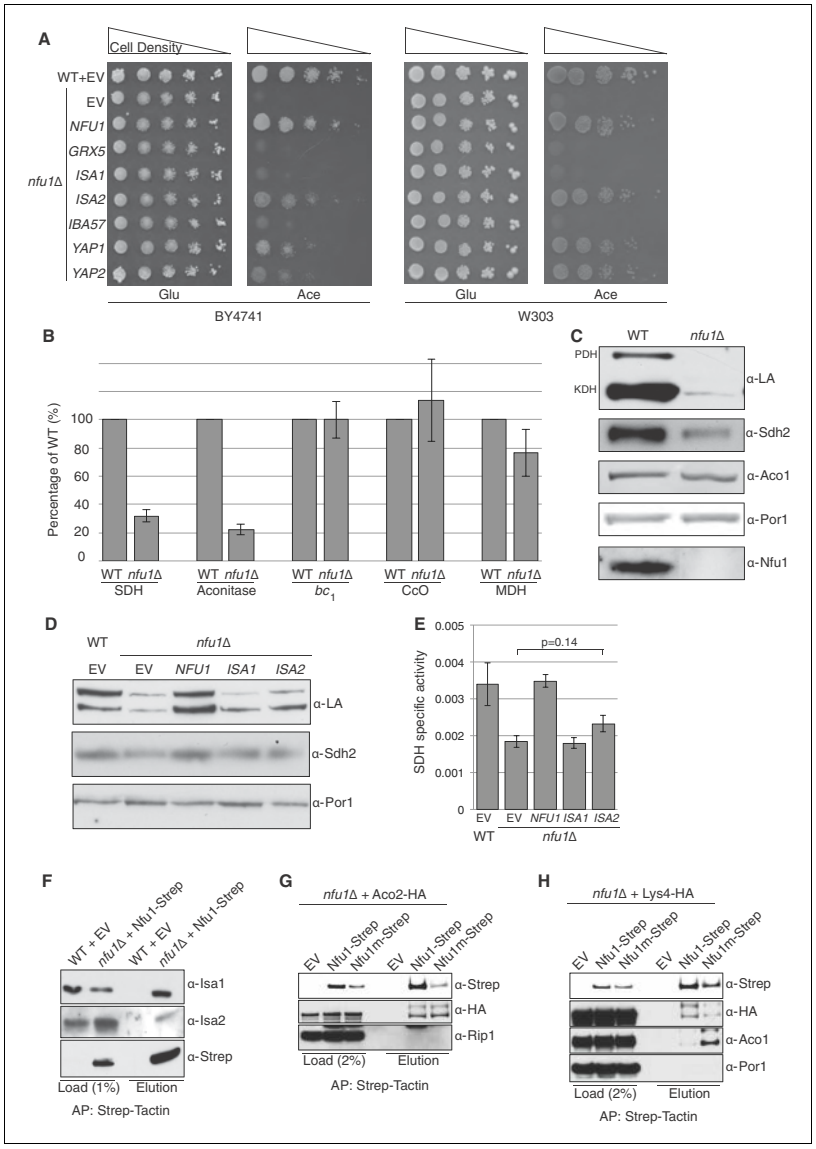

Figure 1. Nfu1 functions with both the ISA [4Fe-4S] assembly complex and [4Fe-4S] client proteins. Cells lacking Nfu1 exhibit defects in [4Fe-4S] cluster enzymes in mitochondria. (**A**) Respiratory growth defects revealed by yeast drop-test. Cells harboring empty vectors (EV) or high-copy plasmids expressing designated genes were pre-cultured in liquid synthetic complete (SC) glucose media lacking uracil. Serially diluted cells (10-fold) were spotted on SC media plates at 30°C. Grx5 is a monothiol glutaredoxin involved in mitochondrial Fe-S biogenesis. Isa1, Isa2 and Iba57 are subunits of

Figure 1 continued on next page

Figure 1 continued

the ISA scaffold complex required for [4Fe-4S] cluster synthesis. Yap1 is a transcription factor that induces expression of anti-oxidant genes. Glu is 2% glucose and Ace is 2% acetate. (**B**) The relative activity of aconitase, SDH, cytochrome bc_1, cytochrome *c* oxidase (CcO), and malate dehydrogenase (MDH) were measured in isolated mitochondria from cells cultured in SC media with 2% raffinose. Data are shown as mean ± SE (n = 3) (CcO, n = 4). (**C**) Steady-state protein levels measured by SDS-PAGE followed by immunoblotting in isolated mitochondria. Anti-LA antibody is an antibody specific to lipoic acid (LA) that is conjugated to proteins. PDH is pyruvate dehydrogenase and KDH is α-ketoglutarate dehydrogenase. Sdh2 is the Fe-S cluster subunit of SDH. Aco1 is mitochondrial aconitase. Por1 is a mitochondrial loading control. (**D**) Restoration of LA moieties on PDH and KDH shown by SDS-PAGE followed by immunoblotting in isolated mitochondria from *nfu1*Δ cells over-expressing *ISA1* and *ISA2*. (**E**) Enzymatic activity of SDH in mitochondria isolated from *nfu1*Δ cells over-expressing *ISA1* and *ISA2*. Data are shown as mean ± SE (n = 3). (**F**) Strep-tag affinity purification of Nfu1-Strep revealed the Nfu1 interaction with Isa1 and Isa2. Mitochondria were solubilized with 0.1% n-dodecyl maltoside (DDM). Clarified lysates were incubated with Strep-Tactin superflow beads for 16 hr. After washing, proteins were eluted with 2.5 mM desthiobiotin, and then analyzed by immunoblotting. (**G**) Strep-tag affinity purification of Nfu1-Strep in the presence of ectopically expressed Aco2-HA. Nfu1m-Strep is the G/T>H mutant described in ***Figure 4***. (**H**) Strep-tag affinity purification of Nfu1-Strep in the presence of ectopically expressed Lys4-HA. Lys4 and Aco2 are both nuclear DNA-encoded mitochondrial proteins that require a [4Fe-4S] cluster for each function in the lysine biosynthetic pathway in yeast. Nfu1m-Strep is the G/T>H mutant described in ***Figure 4***.

DOI: 10.7554/eLife.15991.003

and do not accumulate homocitrate as shown by GC-MS metabolomic studies (data not shown). Thus, sufficient [4Fe-4S] cluster synthesis and distribution occurs in *nfu1*Δ cells for lysine synthesis.

The growth defect of *nfu1*Δ yeast cells on acetate medium was severe, creating an opportunity to conduct screening for genetic suppressors of the respiratory defect. In a screen using transformants with a high-copy yeast DNA library, we isolated respiratory competent vector-borne clones of *nfu1*Δ BY4741 cells containing *NFU1, ISA2*, and the *YAP2* transcriptional activator. Each gene was recloned into yeast vectors and *nfu1*Δ transformants of both BY4741 and W303 genetic backgrounds were analyzed for growth on acetate medium for respiratory function. Although Isa2 is a component of the mitochondrial ISA heterotrimeric complex comprised of Isa1, Isa2 and Iba57, overexpression of Isa2 was the only ISA component capable of partially restoring respiratory growth of *nfu1*Δ cells on acetate medium (***Figure 1A***). *ISA2* transformants of *nfu1*Δ cells showed a partial restoration lipoylation of KDH and SDH activity suggesting that the respiratory capacity of the mutant cells was partially restored by elevated Isa2 levels (p value ~0.14) (***Figure 1D and E***). Thus, the respiratory function of Nfu1 can be partially replaced by super-physiological levels of the Isa2 component of the ISA complex.

Nfu1 binds the ISA complex and [4Fe-4S] client proteins

An association of Nfu1 with the mitochondrial ISA complex was suggested by the observed suppression of the respiratory defect of *nfu1*Δ cells by *ISA2* overexpression along with defects in [4Fe-4S] mitochondrial enzymes. We tested if Nfu1 physically interacts with the ISA complex by co-immunoprecipitation studies using a functional C-terminal Strep tagged chimera of Nfu1. Affinity purification of Nfu1-Strep with Strep-Tactin beads showed co-purification of Isa1 and Isa2 (***Figure 1F***). In addition to the interaction with Isa1 and Isa2, Nfu1 associated with three [4Fe-4S] client proteins Aco1, Aco2 and Lys4, but not the [2Fe-2S] client protein Rip1 (***Figure 1G and H***).

Nfu1 is necessary for protecting Fe-S clusters from oxidative damage

The partial respiratory function of *nfu1*Δ cells was also restored by overexpression of Yap2 or its paralogue Yap1 (***Figure 1A***). Yap1 and Yap2 are transcriptional activators that induce the expression of a battery of antioxidant genes, including thioredoxin, thioredoxin reductase and glutathione reductase, in response to oxidative stress (***Fernandes et al., 1997***). To confirm that the suppression of *nfu1*Δ cells by the YAP transcription factors was specifically due to a recovery of the [4Fe-4S] centers, we analyzed mitochondria from the transformants to test for restoration of lipoic acid conjugates of PDH and KDH and observed a clear restoration of LA-associated PDH (***Figure 2A***). The identification of *YAP1* and *YAP2* as high copy suppressors of *nfu1*Δ cells suggested a role for Nfu1 during oxidative stress. Consistent with this postulate, the respiratory growth of *nfu1*Δ cells was partially restored with the addition of the antioxidants, GSH and N-acetyl cysteine (NAC) to the growth medium (***Figure 2B***). These results support a role for Nfu1 during oxidative metabolism.

Since Nfu1 is important under oxidative conditions, we tested whether Nfu1 is dispensable during anoxic growth. WT and *nfu1*Δ cells were cultured to mid-log growth in normoxic or anoxic

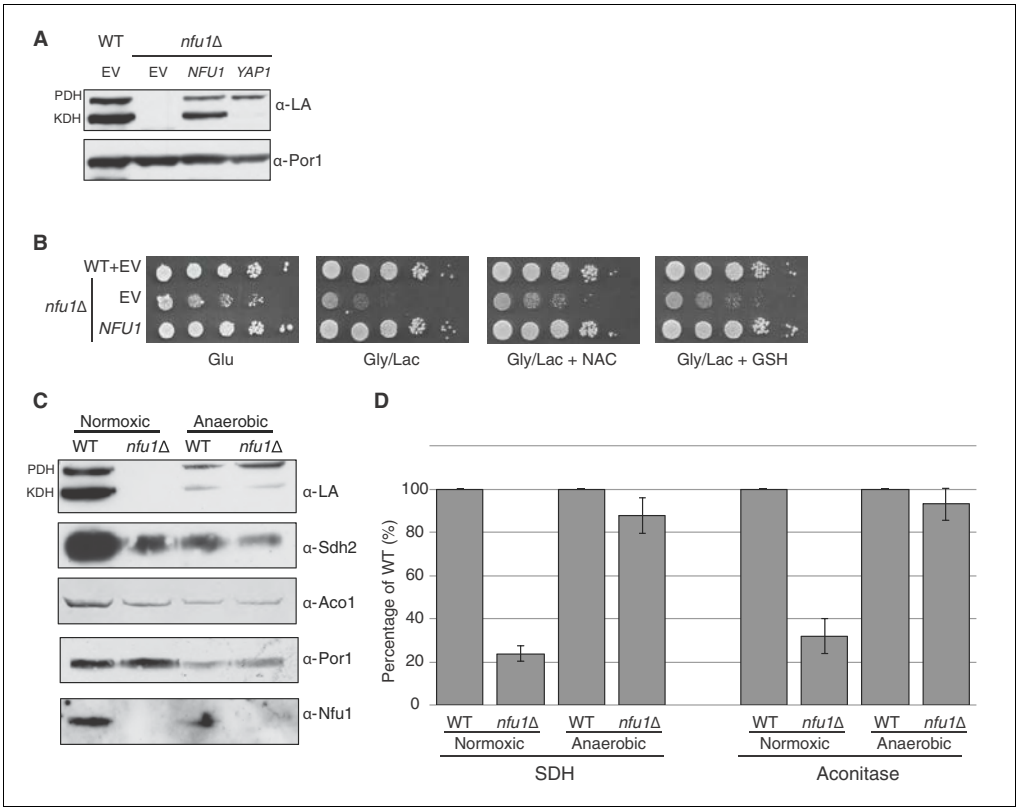

Figure 2. Nfu1 has a heighted importance during times of oxidative stress and is expendable in anoxic conditions. Defects in cells lacking Nfu1 are pronounced under oxidative stress conditions. (**A**) Steady-state levels of proteins in isolated mitochondria from *nfu1*Δ cells harboring high-copy *NFU1* plasmids or *YAP1* plasmids. (**B**) Yeast drop-test with 5 mM n-acetyl cysteine (NAC) and 2 mM glutathione (GSH). Gly/Lac is SC medium with 2% glycerol and 2% lactate as carbon sources. (**C**) Steady-state levels of proteins in isolated mitochondria from cells cultured under normoxic conditions or anaerobic conditions. (**D**) Relative activity of SDH and aconitase in mitochondria from panel **C**. Data are shown as mean ± SE (n = 3).
DOI: 10.7554/eLife.15991.004

conditions. Mitochondria isolated from the cells were analyzed by steady-state protein analysis and enzymatic function of various [4Fe-4S] cluster enzymes. As previously described normoxic *nfu1*Δ cells exhibited the expected marked attenuation in SDH and aconitase activities and reduced lipoic acid adducts; however, the anoxic cells did not exhibit a significant difference between WT and *nfu1*Δ cells (***Figure 2C and D***). It should be noted that anoxic WT cells showed a marked reduction in mitochondrial enzymatic activities and steady-state protein levels compared to normoxic WT cells (~30% of normoxia), yet anoxic *nfu1*Δ cells did not show a marked further attenuation in SDH and lipoic acid conjugates. Thus, the cells are more dependent on Nfu1 during oxidative metabolism.

The NfuC domain of Nfu1 harbors a CxxC motif required for function

Nfu1 consists of two domains in addition to the N-terminal mitochondrial targeting sequence (MTS) based on sequence homologies (***Figure 3A***). The N-terminal domain (NfuN, residues 22–126) is only

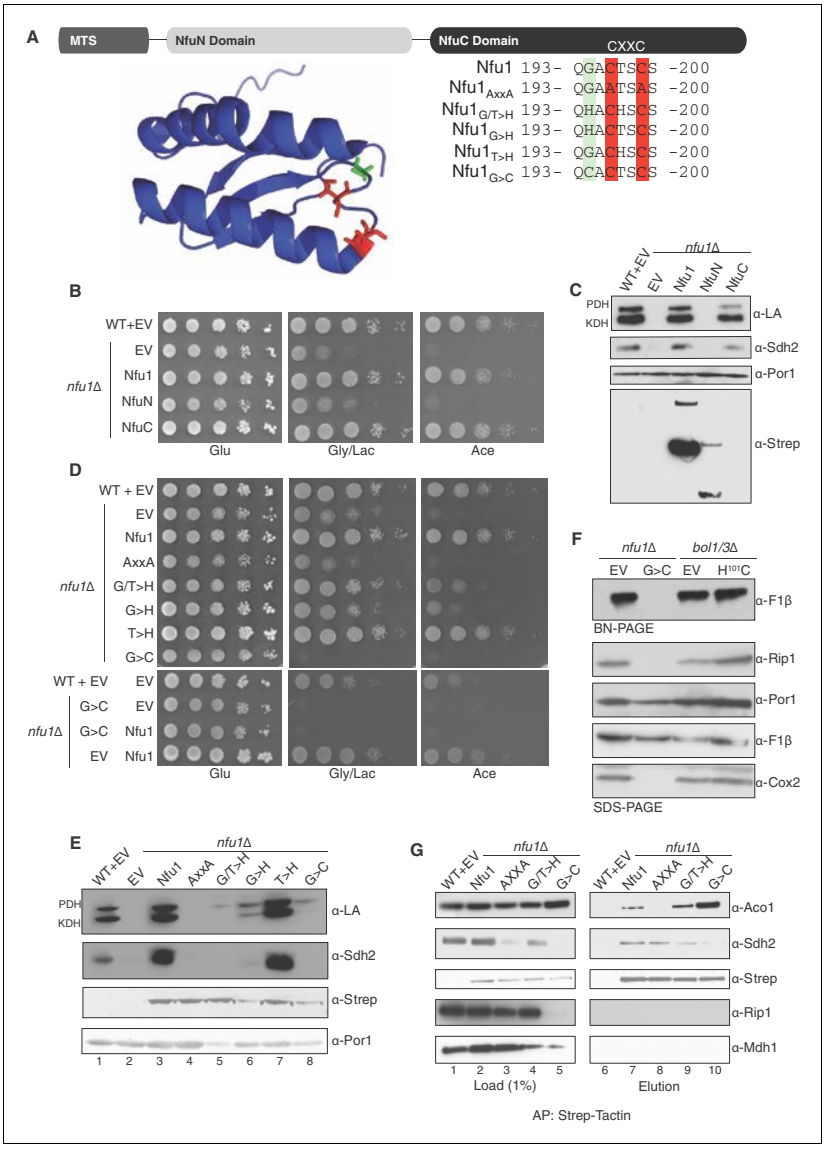

Figure 3. The CxxC motif of C-terminal domain of Nfu1 is essential for function. The CxxC motif is critical for Nfu1 function. (**A**) A schematic representation of Nfu1 domains. MTS, the mitochondrial targeting sequence; NfuN, the N-terminal domain of Nfu1; NfuC, the C-terminal domain harboring the highly conserved CxxC motif. The human NfuC tertiary structure (PDB: 2M5O) and primary sequences showing the CxxC motif (red) and adjacent amino acids indicated in partial sequences (green). (**B**) The respiratory growth defect of *nfu1Δ* cells was rescued with NfuC. Nfu1, NfuN, and

Figure 3 continued on next page

Figure 3 continued

NfuC were all fused with a C-terminal Strep-tag and expressed exogenously using low-copy plasmids. (**C**) Restoration of Nfu1 target proteins by NfuC expression in *nfu1*Δ cells. (**D**) Respiratory growths of *nfu1*Δ cells that express Nfu1 sequence variants were tested. All variants were fused with a Strep-tag and expressed on low-copy plasmids. (**E**) Steady-state levels of LA-conjugated proteins and Sdh2 in *nfu1*Δ cells that express Nfu1 variants. (**F**) BN-PAGE and SDS-PAGE analysis of [4Fe-4S] cluster independent enzymes in the dominant negative backgrounds *nfu1*Δ + G>C and *bol1/3*Δ + $H^{101}C$. (**G**) Strep-tag purification of Nfu1 sequence variants as described in ***Figure 3B*** immunoblotting for [4Fe-4S] cluster client proteins Aco1 and Sdh2.

DOI: 10.7554/eLife.15991.005

The following figure supplements are available for figure 3:

Figure supplement 1. Yeast growth tests evaluating respiratory growth (Gly/Lac) of *nfu1*Δ + G>C cells following treatment with 5'-Fluoroorotic acid (5-FOA) to show cells have not lost their mitochondrial DNA (rho^-).

DOI: 10.7554/eLife.15991.006

Figure supplement 2. Affinity purification using Strep-Tactin to immobilize Strep tagged Nfu1 and the Nfu1 AxxA variant expressed ectopically in the BY4743 background with a single copy of Lys4 chromosomally tagged with GFP.

DOI: 10.7554/eLife.15991.007

conserved within eukaryote species, while the C-terminal NifU-like domain (NfuC, residues 143–256) is widely conserved in all species and contains the important the Fe-S binding CxxC motif (***Figure 3A***). To test the functional importance of the two domains, both domains were separately expressed in *nfu1*Δ cells with the endogenous MTS of Nfu1 (1–21) to ensure proper delivery to the mitochondrial matrix.

Cells containing only the Nfu1 NfuC domain were capable of respiratory growth on either glycerol/lactate or acetate medium (***Figure 3B***), whereas cells harboring only the Nfu1N domain failed to propagate. Additionally, cells with the NfuC, but not the NfuN, domain showed normal Sdh2 and lipoic acid levels. Although the NfuN domain failed to restore Nfu1 function, the fragment was well expressed in cells, unlike the functional C-terminal domain that was markedly attenuated in protein stability (***Figure 3C***). The functionality of the NfuC domain suggests that only minimal levels of Nfu1 are important for function. The NfuN domain exhibited a putative dimeric species, analogous to the intact Nfu1 on the denaturing gels.

To further address the functional importance of the NfuC domain, we generated a series of amino acid substitutions within and near the conserved CxxC motif to the full-length Nfu1 protein (***Figure 3A***). One Nfu1 variant generated had the two cysteinyl residues in the CxxC motif (highlighted in red in ***Figure 3A***) replaced with alanines. Cells harboring Nfu1 with the two CxxC cysteinyl residues replaced by alanines exhibited a respiratory growth defect analogous to *nfu1*Δ cells suggesting a loss-of-function phenotype (***Figure 3D and E***). The critical role of the CxxC motif cysteines was previously shown in the *E. coli* NfuA (***Angelini et al., 2008***).

A conserved glycine just upstream of the CxxC motif is commonly mutated to a cysteine in patients with MMDS (***Navarro-Sastre et al., 2011***; ***Nizon et al., 2014***). We generated amino acid substitution of this Gly to Cys or His residues and replaced the conserved threonine between the two Cys residues by a His. Each mutant of Nfu1 was expressed in *nfu1*Δ cells and tested for function. The most striking substitution was the G>C mutant that mimics the MMDS1 patient allele, which displayed a severe synthetic sick phenotype on glycerol/lactate medium (***Figure 3D***). SDH biogenesis was markedly decreased and in addition Rip1 levels were low suggesting a block in bc_1 biogenesis (***Figures 3E and G***, lane 5). This dominant negative phenotype was reversed when cells were plated on medium containing 5-fluoroorotic acid (5-FOA) to shed the *URA3*-containing plasmid harboring the $G^{194}C$ Nfu1 mutant (***Figure 3—figure supplement 1***). Thus, the synthetic phenotype did not arise from mtDNA loss or any other irreversible pleiotropic defects. In addition, co-expression of a wild-type Nfu1 with the $G^{194}C$ Nfu1 mutant failed to restore respiratory growth, demonstrating the dominant negative nature of this mutant (***Figure 3D***, bottom panel).

Although *nfu1*Δ cells with the $G^{194}C$ mutant retained its mtDNA, mitochondrial translation was likely impaired due to attenuated levels of the assembled F_1F_0 ATPase on BN-PAGE and Cox2 steady-state levels (***Figure 3F***). Although the assembled F_1F_0 ATPase complex is markedly diminished, the steady-state levels of Atp2 in the F_1 sector are normal. Cells impaired in lipoic acid formation are deficient in tRNA processing by RNase P leading to attenuation in mitochondrial translation (***Schonauer et al., 2008***; ***Hiltunen et al., 2009***). Diminished mitochondrial translation of the bc_1 cytochrome *b* subunit would account for the reduced Rip1 levels observed (***Figure 3F and G***). In

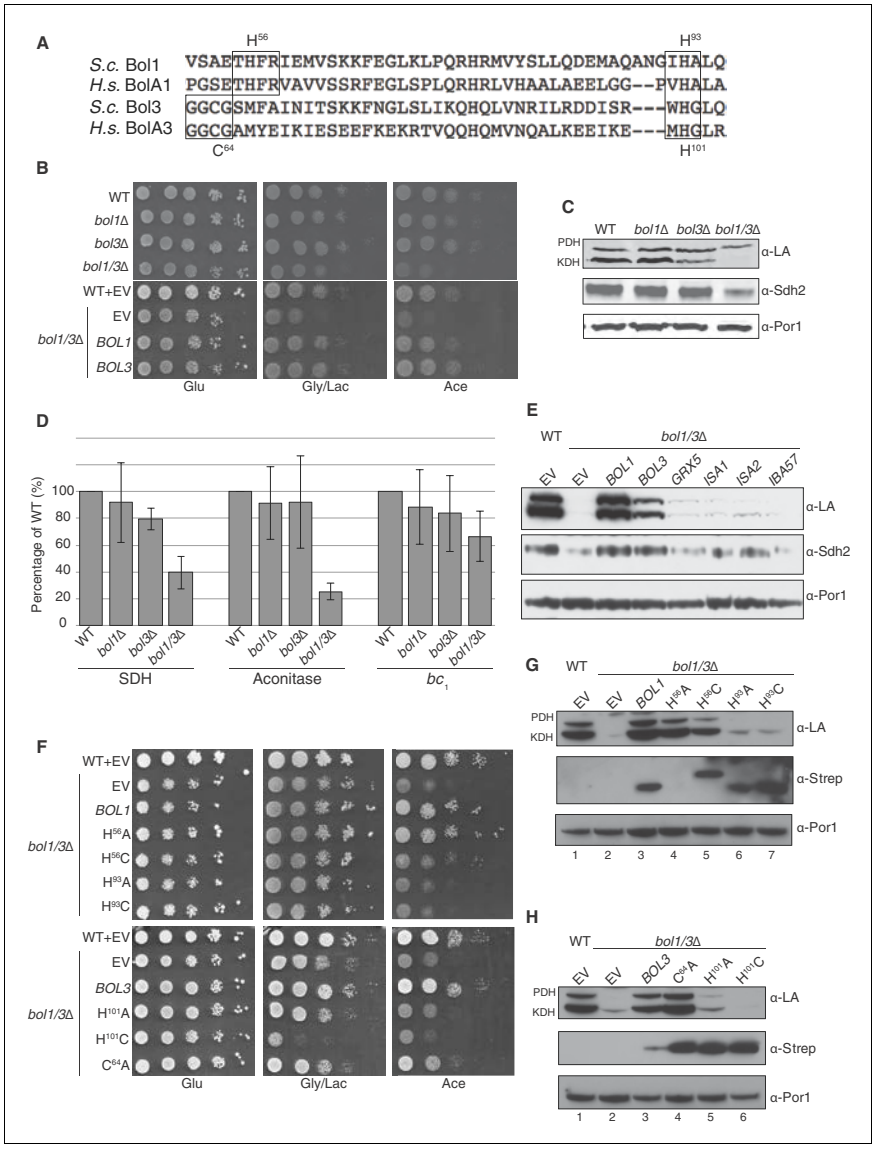

Figure 4. The Mitochondrial Bol1 and Bol3 proteins function in Fe-S biogenesis. Bol1 and Bol3 play roles in Fe-S cluster biogenesis in mitochondria (**A**) Partial sequences of yeast and human mitochondrial BolA proteins. Boxed are conserved motifs with proposed ISC ligands that were mutated in this work. (**B**) Respiratory growth defects of *bol1Δ* cells, *bol3Δ* cells and *bol1Δbol3Δ* double mutants and complementation by plasmid-borne *BOL1* or *BOL3*. (**C**) Steady-state levels of LA-conjugated proteins and Sdh2 in cells lacking Bol1 and/or Bol3. (**D**) Relative activity of SDH, cytochrome bc_1

Figure 4 continued on next page

Figure 4 continued

complex and aconitase were measured. Data are shown as mean ± SE (n=3). (**E**) Observation of LA moieties on PDH and KDH and Sdh2 steady-state levels by SDS-PAGE followed by immunoblotting in isolated mitochondria from *bol1*/3Δ cells over-expressing the indicated Fe-S cluster gene. (**F**) Respiratory function of Bol1 and Bol3 sequence variants in conserved residues were examined by yeast drop-test. All Bol1 variants were fused with a C-terminal Strep-tag and expressed on low-copy plasmids. All Bol3 variants were fused with a N-terminal Strep-tag between the MTS and the remainder of the protein and expressed on low-copy plasmids. (**G** and **H**) Steady-state levels of LA-conjugated proteins in cells lacking Bol1 and Bol3 with Bol1 variants (**G**) and Bol3 variants (**H**) exogenously expressed.

DOI: 10.7554/eLife.15991.008

The following figure supplement is available for figure 4:

Figure supplement 1. Yeast growth tests evaluating the viability of cells expressing mitochondrial Bol1 and Bol3 N-terminal ligands mutated to lysine in the *bol1*/3Δ background.

DOI: 10.7554/eLife.15991.009

contrast to cells harboring the Nfu1 $G^{194}C$ patient mutation, *nfu1*Δ cells have normal F_1F_0 ATPase levels on BN-PAGE and Cox2 steady-state levels suggesting that mitochondrial translation is normal without Nfu1.

We tested whether the dominant negative effect arises from changes in interactions between Nfu1 and client proteins. We performed affinity purification of Nfu1-Strep on Strep-Tactin beads for the WT and mutant alleles. The loss-of-function AxxANfu1mutant failed to show a detectable interaction with Aco1 (***Figure 3G***, lane 8) and was impaired in its interaction with Lys4 (***Figure 3—figure supplement 2***). In contrast, the $G^{194}C$ Nfu1mutant exhibited an enhanced interaction with Aco1 (***Figure 3G***, lane 10). An interaction with Sdh2 is unclear, since Sdh2 levels are markedly depleted in $G^{194}C$ Nfu1 cells. These data show the functional importance of the NfuC domain and its CxxC motif.

The two mitochondrial BolA proteins function in Fe-S protein biogenesis

MMDS2 patients have been reported to have mutations in the mitochondrial BOLA3 protein (***Seyda et al., 2001***; ***Cameron et al., 2011***; ***Baker et al., 2014***). The clinical phenotypes of patients with mutations in *NFU1* or *BOLA3* were similar with neurological regression, infantile encephalopathy and hyperglycinemia (***Cameron et al., 2011***; ***Navarro-Sastre et al., 2011***). In addition, biochemical defects in protein lipolyation and succinate dehydrogenase were observed.

Due to the clinical and biochemical similarities in mutant NFU1 or BOLA3 patients, we tested the function of the yeast BOLA3 homolog, Bol3, and the related Bol1 protein (***Figure 4A***). In human cells, BOLA1 and BOLA3 are known to be mitochondrial proteins (***Willems et al., 2013***). We confirmed that Bol1 and Bol3 are likewise localized within the mitochondria of yeast cells (data not shown). Yeast devoid of either Bol1 or Bol3 lacks a clear respiratory phenotype, but a double *bol1*Δ*bol3*Δ null strain displayed a growth defect on acetate medium and to a lesser extent on glycerol/lactate medium (***Figure 4B***). Mitochondria isolated from single mutants and the double null mutant were used for biochemical characterization studies. As with *nfu1*Δ cells, protein lipoylation was partially impaired in KDH in the *bol3*Δ null, but the defect in KDH lipoylation was enhanced in the *bol1*Δ*bol3*Δ null strain (***Figure 4C***). SDH and aconitase activities were depressed in the double null strain, but not significantly changed in the individual single mutants (***Figure 4D***). The attenuation of aconitase activity in both *bol1*Δ*bol3*Δ null and *nfu1*Δ cells is in contrast to BOLA3 and NFU1 patient mutant cells. A modest attenuation was seen in bc_1 activity in the *bol1*Δ*bol3*Δ null strain, but this was not observed in *nfu1*Δ cells.

Since the respiratory growth defect of *nfu1*Δ cells was partially suppressed by overexpression of *ISA2*, we tested whether overexpression of a series of late mitochondrial Fe-S cluster assembly genes would likewise rescue the respiratory defect of *bol1*Δ*bol3*Δ cells. No growth restoration was observed on acetate or glycerol/lactate media, and only minimal lipoylation of PDH and KDH was observed in cells harboring elevated levels of Grx5, Isa1, and Isa2 (***Figure 4E***).

BolA proteins are implicated in binding Fe-S clusters. Whereas Nfu1 is known to bind a [4Fe-4S] cluster at the homodimer interface, BolA proteins have been shown to bind [2Fe-2S] clusters in association with glutaredoxins as heterodimers (***Li and Outten, 2012***; ***Roret et al., 2014***; ***Li et al., 2012***). We evaluated the roles of potential Fe-S cluster ligands in Bol1 and Bol3. Bol1 has conserved His56 and His93 residues (***Figure 4A***), which in the case of *Arabidopsis thaliana* BolA1 the

corresponding His residues are apparent ligands to a [2Fe-2S] cluster in association with a monothiol glutaredoxin (**Roret et al., 2014**). Bol3 has conserved Cys64 and His101 residues in corresponding loops to that of Bol1 and are expected to serve as ligands for a Fe-S cluster. We replaced the conserved histidine residues with alanines or cysteines and tested phenotypic effects. We observed that the C-terminal His in each BolA protein was important for the respiratory growth of cells (**Figure 4F, G and H**). Whereas the $H^{101}A$ Bol3 mutant was non-functional, the variant containing a $H^{101}C$ substitution exhibited a synthetic sick phenotype in that the respiratory growth on glycerol/lactate medium was more impaired relative to the starting *bol1Δbol3Δ* null strain (**Figure 4F and H** lane 6). The Bol3 $C^{64}A$ mutant was only a partial loss-of-function allele. In contrast, the Bol1 $H^{93}A$ or $H^{93}C$ mutants exhibited similar loss-of-function phenotypes without any observed dominant negative effects. The upstream Bol1 $H^{56}A$ mutant retains function, but the $H^{56}C$ allele was a partial loss of function mutant (**Figure 4F and G**, lane 5).

Since substitutions in the upstream conserved His56 in Bol1 and Cys64 in Bol3 failed to yield a significant phenotype, they may not contribute to a candidate FeS cluster binding. To confirm this prediction, we converting the His56 in Bol1 and Cys64 in Bol3 to lysine residues to create electrostatic repulsion to a candidate FeS cluster Fe atom. Bol1 $H^{56}K$ and Bol3 $C^{64}K$ mutants did not exhibit an enhanced phenotype (**Figure 4—figure supplement 1**) ruling out that they are important FeS cluster ligands. Together, these data show a functional importance of Bol1 and Bol3 in mitochondrial Fe-S cluster biogenesis and highlights the need for the C-terminal conserved His in each protein for physiological function. Bol1 and Bol3, like Nfu1, are not essential for mitochondrial Fe-S protein biogenesis, as a bypass exists enabling limited respiratory growth on glycerol/lactate medium.

Nfu1 and Bol3 physically interact with [4Fe-4S] client mitochondrial proteins

To glean further insights into the function of Nfu1, Bol1 and Bol3 in mitochondrial Fe-S cluster biogenesis, we performed proteomic analyses on affinity purified Nfu1, Bol1 and Bol3 proteins with each expressed as Strep fusions. Purification of each protein was accomplished on Strep-Tactin resin and protein eluates were analyzed by mass spectrometry. Multiple independent proteomic analyses were conducted on WT proteins as well as mutant proteins of each (G/T>H Nfu1, $H^{93}C$ Bol1 and $H^{101}C$ Bol3) (**Figure 5A and B**; **Figure 5—source data 1**). Of the mutant proteins, BolA3 $H^{101}C$ was synthetic sick in the *bol1Δbol3Δ* null strain (**Figure 4F**); Nfu1 G/T>H mimicked the severe dominant negative mutant, $G^{194}C$ found in patients, however the substitutions were less detrimental to growth (**Figure 3D**); and the Bol1 $H^{93}C$ variant was a loss-of-function mutant without a dominant negative characteristic (**Figure 4F**). Inspection of datasets of protein interactors revealed a common set of [4Fe-4S] client proteins associating with both Nfu1 and Bol3. These include Aco1, Aco2, Lys4, Sdh2, Lip5 and Bio2. For all client proteins except Sdh2, the observed total spectral count that was markedly higher for clients purified with mutant Nfu1 and Bol3 variants (**Figure 5A** and **Figure 5—source data 1**). Additionally, the mutant forms of Bol3 and Nfu1 both co-purified with the ISA complex component, Isa2 (**Figure 5B** and **Figure 5—source data 1**). The physical interactions of Nfu1 with the clients, Aco1, Lys4, Aco2 and Sdh2, and with the ISA complex are consistent with the results shown by affinity purification experiments followed by SDS-PAGE and immunoblotting (**Figure 1F,G and H**). Two Bol3 pulldown studies revealed limited levels of copurified Nfu1, although we never observed Bol3 in the pulldown of Nfu1 (**Figure 5—source data 1**).

Unlike Bol3, Bol1 purification did not lead to appreciable co-purification of [4Fe-4S] client proteins, but Grx5 was isolated as a reproducible interactor with WT but not the loss-of-function $H^{93}C$ Bol1 mutant (**Figure 5B**). Grx5 was a significantly less abundant interactor with Bol3 or Nfu1. Human BOLA1 was previously shown to associate with Grx5 in HEK293 cells (**Willems et al., 2013**).

We conducted in vitro experiments to verify the observed selective interaction of Bol1 with Grx5 using human orthologs. Solution binding analyses were conducted using microscale thermophoresis, which assesses molecular diffusion in a microscopic temperature gradient. Due to their higher stability, we used the human proteins. Apo-GLRX5 or the holo-GLRX5 dimer containing the bridging [2Fe-2S] cluster were incubated with either recombinant human BOLA1 or BOLA3 proteins for assessment binding (**Figure 5C** and **Figure 5—figure supplement 1**). Holo-GLRX5 associated with BOLA1 with a 50-fold greater affinity than with BOLA3, while similar affinities of apo-GLRX5 were observed for the two human BOLA proteins. As a control, no significant interaction of the BOLA proteins with the human [2Fe-2S] ferredoxin FDX2 was observed. Together, these results indicate a strong preference

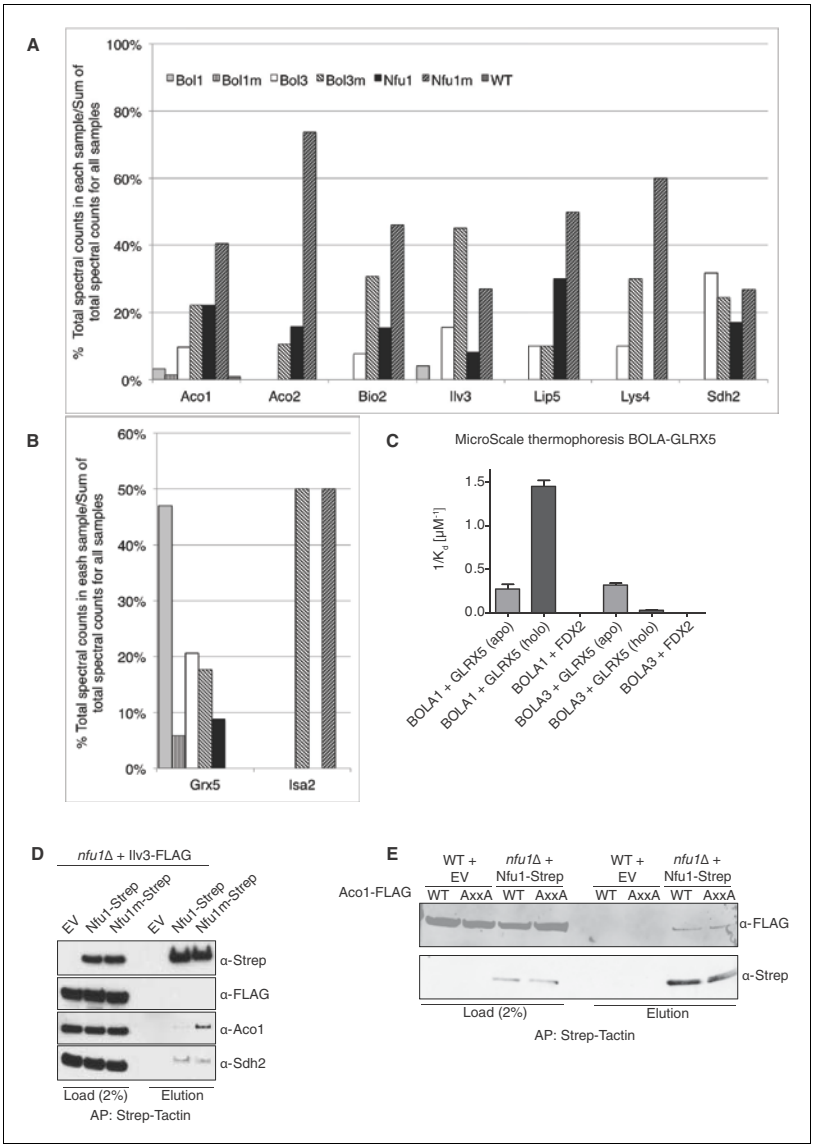

Figure 5. Proteomic analysis of Nfu1, Bol1 and Bol3 establishes function within mitochondrial Fe-S for Bol1 and Bol3. (**A** and **B**) Percentages of spectral counts identified by MS proteomics. Percentages were calculated by the number of spectral counts identified for a denoted protein in an individual Strep-tagged protein divided by the total number of spectral counts for that protein identified from all seven samples. Strep-tagged proteins were expressed from low-copy plasmids in corresponding single deletion mutants. Samples were Strep-affinity purified as in ***Figure 3***. Bol1m is the H93C

Figure 5 continued on next page

Figure 5 continued

variant. Bol3m is the $H^{101}C$ variant. Nfu1m is the G/T>H variant. WT is wild-type BY4741 expressing an empty vector. All were fused with a C-terminal Strep-tag. WT is BY4741 wild type harboring a low-copy empty plasmid. (**C**) Human GLRX5 or NFU1 were used in apo- and holo- form and mixed at increasing concentrations with 200 nM fluorescently labelled BOLA1 or BOLA3. Microscale thermophoresis were performed and dissociation constants (K_d) were determined. Error bars indicate the SD (n=3). (**D**) Strep-tag affinity purification of Nfu1-Strep in the presence of ectopically expressed Ilv3-FLAG. (**E**) Affinity purification using Strep-Tactin agarose beads to purify Nfu1-Strep from an *nfu1*Δ background expressing either WT Aco1 or Aco1 AxxA mutant.

DOI: 10.7554/eLife.15991.010

The following source data and figure supplements are available for figure 5:

Source data 1. (Table 1) Spectral counts, unique peptides, and coverage of mitochondrial Fe-S client proteins, bait proteins, and Fe-S assembly machinery identified by MS proteomics.

DOI: 10.7554/eLife.15991.011

Figure supplement 1. Interaction studies of human BOLA proteins with GLRX5.

DOI: 10.7554/eLife.15991.012

Figure supplement 2. Ilv3 activity assay using wild-type and *nfu1*Δ purified mitochondria along with wild-type overexpressing Ilv3 as a control.

DOI: 10.7554/eLife.15991.013

of BOLA1 for the holoform of GLRX5. We predict, based on the yeast Bol1 $H^{93}C$ mutant, that BOLA1:GLRX5 interaction is mediated by a [2Fe-2S] cluster.

The Nfu1 and Bol3 proteomics experiments did not identify any novel mitochondrial [4Fe-4S] cluster client proteins. Interestingly, the [2Fe-2S] enzyme dihydroxyacid dehydratase (Ilv3) was recovered in multiple independent mass spectrometry analyses in Nfu1 and Bol3 samples. However, we were unable to verify that interaction when using a FLAG-tagged Ilv3 chimera in the Nfu1-Strep affinity capture (***Figure 5D***). Furthermore, enzymatic activity of Ilv3 was not altered in *nfu1*Δ cells (***Figure 5—figure supplement 2***). Thus, Nfu1 does not appear to be important for the function of the [2Fe-2S] Ilv3 enzyme.

We sought to address whether the binding of Nfu1 to a client protein was mediated through a bridging [4Fe-4S] cluster. Aco1 binds its [4Fe-4S] cluster through a conserved CxxC motif and one distant Cys residue in the primary sequence. We generated a double AxxA mutant and tested its ability to associate with Nfu1-Strep. No difference in binding was observed between WT and the AxxA Aco1 proteins with Nfu1 (***Figure 5E***).

Nfu1 and Bol3 function together in [4Fe-4S] cluster transfer from the ISA complex to apo-client proteins

The distinct overlap of [4Fe-4S] client protein interactors between Bol3 and Nfu1 suggested a potential overlap or partnership in the function of the two proteins in late step [4Fe-4S] cluster transfer. We tested whether a genetic linkage exists between the proteins by evaluating whether a synthetic phenotype exists in cells lacking Bol1, Bol3 and Nfu1. The triple deletion cell (*bol1*Δ*bol3*Δ*nfu1*Δ, designated *b*ΔΔ*nfu1*Δ) exhibited a strong synergistic growth defect on glycerol/lactate medium (***Figure 6A***). While the defects are too severe to see the synergism by protein lipolyation and Sdh2 steady-state levels, the enzymatic activities of SDH and aconitase do reflect a synergistic effect (***Figure 6B and C***). In addition, the level of assembled F1F0 ATPase was markedly reduced in the triple mutant (***Figure 6D***). The severity of the phenotype and the impairment in F1F0 ATPase in the triple mutant likely arises from reduced mitochondrial translation likely through RNaseP, similar to the dominant negative Nfu1 G>C mutant discussed above (***Figure 3F***). The growth defect of the triple mutant can be partially rescued by re-expression of *BOL1* or *NFU1*, but not by *BOL3* (***Figure 6E***). This may suggest that Bol3 requires Nfu1 for its function.

Affinity purification of Nfu1-Strep expressed in the *bol1*Δ*bol3*Δ*nfu1*Δ triple null mutant was carried out to test the effect of loss of the two BolA proteins on the interaction of Nfu1 with [4Fe-4S] client proteins. As can be seen in ***Figure 6F*** there was enhanced co-purification of Aco1 in the absence of Bol1 and Bol3. Likewise, a similarly enhanced interaction between client proteins and Nfu1 was apparent in cells lacking a functional ISA complex in *isa2*Δ cells (***Figure 6G***). These data are consistent with a role of Nfu1 in [4Fe-4S] cluster transfer from the ISA complex to client proteins.

Given the strong genetic interaction between the mitochondrial BOLA genes and *NFU1*, we attempted to substantiate the linkage. The proteomic results suggested an association of Bol1 and

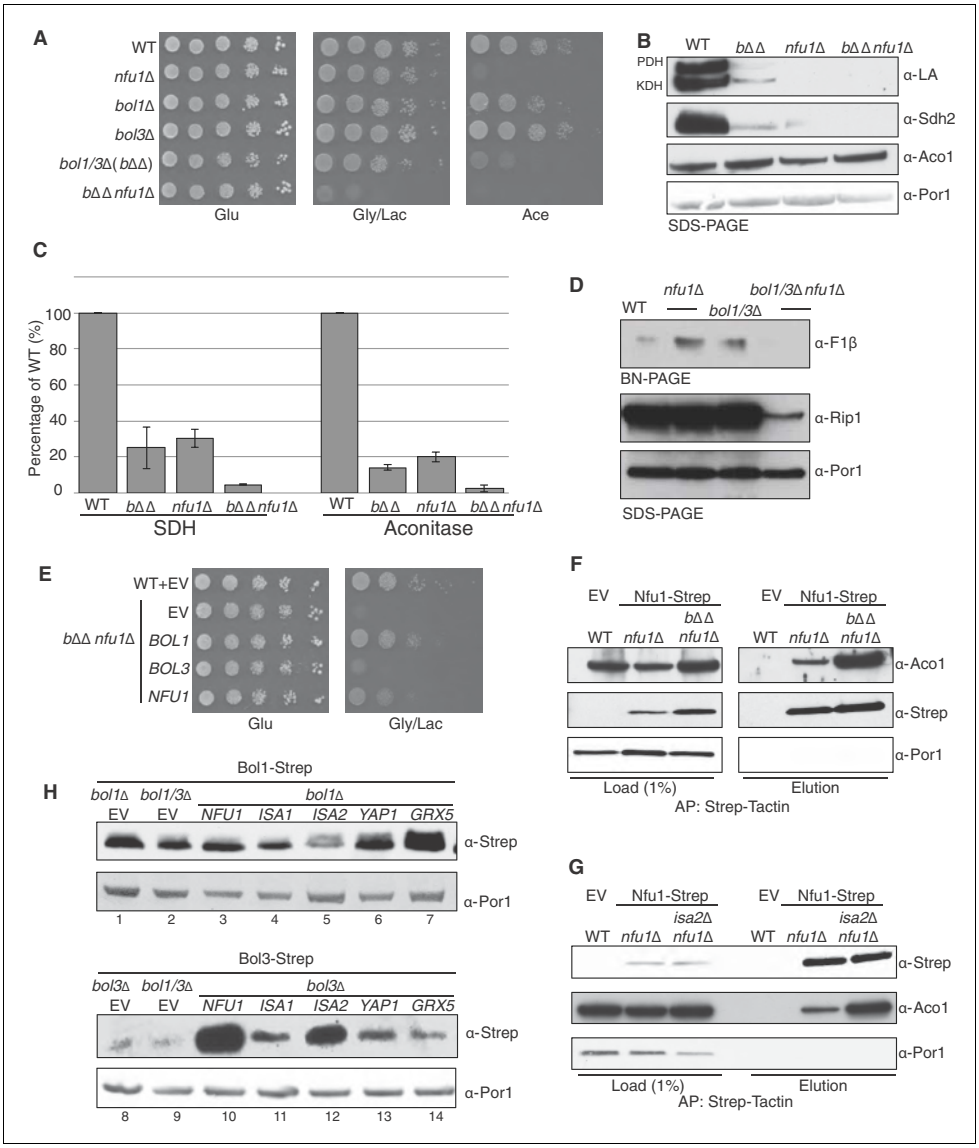

Figure 6. Nfu1 and Bol3 function together in [4Fe-4S] delivery. (**A**) Exacerbated respiratory growth defects of *bol1Δbol3Δnfu1Δ* triple mutants (designated *bΔΔnfu1Δ*) compared to *nfu1Δ* single mutants and *bol1Δbol3Δ* double mutants on non-fermentable carbon sources. (**B**) Steady-state levels of LA-conjugated proteins and Sdh2 in the absence of Bol1, Bol3 or Nfu1. (**C**) Relative activity of SDH and aconitase in the absence of Bol1, Bol3 or Nfu1. Data are shown as mean ± SE (n=3) (**D**) BN-PAGE and SDS-PAGE analysis of [4Fe-4S] cluster independent enzymes in the *bΔΔnfu1Δ* triple

Figure 6 continued on next page

Figure 6 continued

deletion mutant background. F1β is a subunit of ATP synthase. (**E**) Respiratory growth of *bΔΔnfu1Δ* triple mutants harboring plasmid-borne *BOL1, BOL3* and *NFU1*, respectively. (**F**) Strep-tag purification of Nfu1-Strep in the absence of Bol1 and Bol3. (**G**) Strep-tag purification of Nfu1-Strep in the absence of Isa2. (**H**) Steady-state levels of Bol1-Strep (upper panel) and Bol3-Strep (bottom panel) in response to overexpression of genes as indicated.

DOI: 10.7554/eLife.15991.014

The following figure supplement is available for figure 6:

Figure supplement 1. SDS-PAGE followed by immunoblotting to evaluate the different steady state levels of Nfu1-Strep, Bol1-Strep, and Bol3-Strep while being expressed under the same heterologous *MET25* promoter and *CYC1* terminator.

DOI: 10.7554/eLife.15991.015

Grx5, whereas Bol3 was associated with Nfu1 function. Mitochondrial BolA proteins are low abundance molecules (***Figure 6—figure supplement 1***) making co-immunoprecipitation studies challenging. Because of this, we tested whether increasing the levels of candidate interacting proteins would alter the abundance of Bol1 or Bol3. As can be seen in ***Figure 6H***, the steady-state levels of Bol3, but not Bol1, were dramatically increased in cells with elevated levels of Nfu1. Additionally, *ISA1* and *ISA2* overexpression resulted in a modest increase in Bol3, but not Bol1, protein levels. In contrast, Grx5 overexpression led to a marked enhancement in Bol1 levels without altering Bol3 (***Figure 6H***). In these studies Strep-chimeras of Bol1 and Bol3 were expressed from heterologous promoters, so the changes in protein levels are likely occurring through post-transcriptional stabilization. These stabilization experiments corroborate the genetic and proteomic experiments, all of which suggest that Bol3 (BOLA3) functions with Nfu1 in [4Fe-4S] cluster transfer to client proteins and Bol1 functions with Grx5 for a yet to be determined purpose.

Nfu1 exists as a steady-state homodimer lacking Bol3

Mitochondrial lysates were subjected to gel filtration studies to assess the extent of interaction between Nfu1 and Bol3. Mitochondrial lysates prepared from either Nfu1-Strep or Bol3-Strep cells were separately chromatographed and fractions were assayed for Nfu1 or Bol3. The bulk of Nfu1 eluted in fractions corresponding to a globular mass of ~47 kDa, consistent with a homo-dimeric complex (***Figure 7A***). Nfu2 from *Arabidopsis* is a dimeric species both as an apo-protein and with a [4Fe-4S] cluster (***Gao et al., 2013***). In contrast, Bol3 eluted predominantly in fractions corresponding to a globular mass of 13 kDa consistent with a monomeric protein. No significant co-elution was observed between Nfu1 and Bol3, indicating that any Nfu1/Bol3 interaction is transient in nature. An additional set of chromatographic studies were done with mitochondrial lysates containing Nfu1-Strep in which lysates were treated with either 0.1 mM DTT or 2 mM dithionite to assess whether the apparent Nfu1 dimer was a disulfide-linked homo-dimer or a Fe-S cluster bridged complex (***Figure 7B***). The abundance of Nfu1 in fraction 13 assessed by immunoblotting indicated that the elution properties of Nfu1 were unaffected by preincubation with DTT (followed by alkylation of cysteines by Iodoacetamide), whereas treatment with dithionite attenuated the apparent dimeric complex abundance. Fe-S clusters are susceptible of disassembly with dithionite treatment, suggesting that a significant fraction of steady-state Nfu1 in WT yeast mitochondria may be Fe-S loaded. In support of this conclusion is the observation that the Nfu1 AxxA mutant fractionates predominantly as a monomer.

If Nfu1 exists in a FeS-loaded conformer, the question arose whether [4Fe-4S]-Nfu1 serves as a reservoir of [4Fe-4S] clusters for client proteins. We specifically focused on Lip5 that catalyzes formation of lipoic acid. In its catalytic cycle, one of its [4Fe-4S] clusters is consumed to provide two sulfur atoms needed to generate lipoic acid (***Cicchillo and Booker, 2005***; ***Cicchillo et al., 2004***). Thus, [4Fe-4S] cluster regeneration is needed to support Lip5 catalysis and lipoic acid levels. To address a role of Nfu1 in cluster regeneration in Lip5, we utilized cells containing a chromosomal *NFS1* under the control of *GAL1* promoter enabling glucose-mediated repression of Nfs1 expression. The GAL-*NFS1* strain was transformed with an empty vector or a vector containing either *NFU1* under the control of the regulatable *MET25* promoter, *BOL3* or *ACO1*. If Nfu1 were a reservoir of [4Fe-4S] clusters, we predicted that elevated levels of holo-Nfu1 would enable sufficient [4Fe-4S] cluster transfer to Lip5 to support lipoic acid formation in cells depleted of Nfs1. Cells pre-cultured in galactose were shifted to glucose-containing medium to repress *NFS1* expression and mitochondrial lysates were collected 8 hr later (***Figure 7C***). The lipoic acid level in pyruvate dehydrogenase was

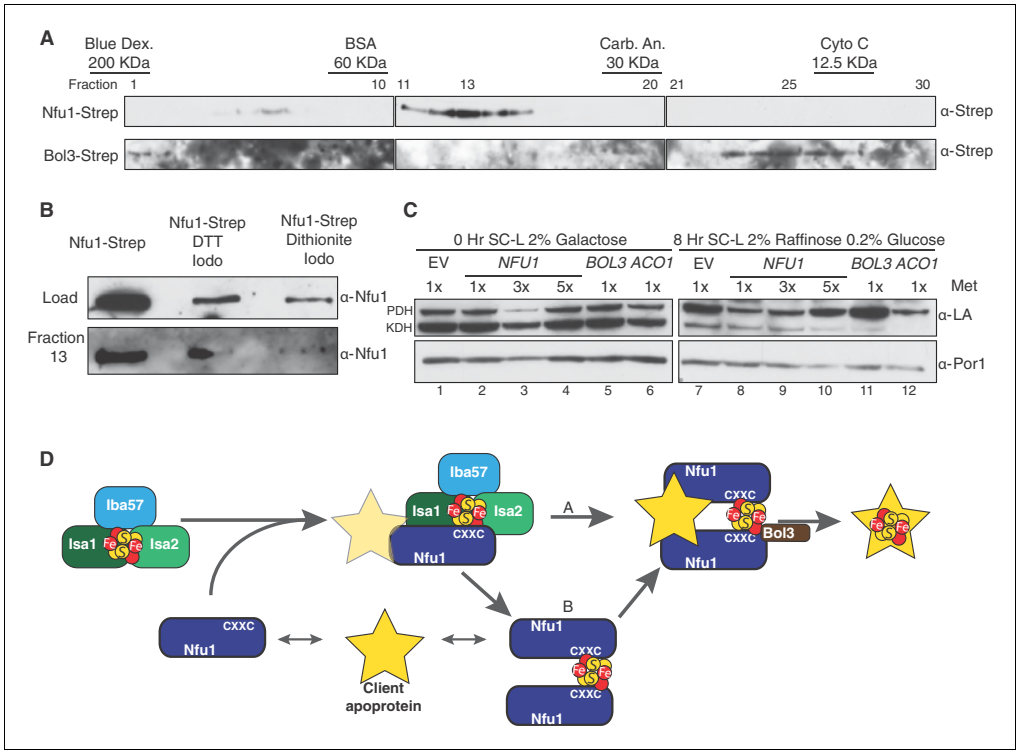

Figure 7. Nfu1 exists as a dimer bridged by a Fe-S cluster. (**A**) Immunoblotting of fractions from *nfu1*Δ + Nfu1-Strep or *bol3*Δ + Bol3-Strep lysates separated by size exclusion chromatography. Molecular weight standards [bovine serum albumin (BSA), carbonic anhydrase (CA) and cytochrome c] are displayed above the corresponding fractions were used to create a standard curve to calculate apparent molecular weights. Fraction 13 has an apparent molecular weight of 47.6 KDa and Fraction 26 has an apparent molecular weight of 13.2 kDa. (**B**) Immunoblotting of fraction 13 from *nfu1*Δ + Nfu1-Strep lysates pretreated with nothing, 100 mM DTT followed by 200 mM iodoacetamide, or 2 mM dithionite followed by 200 mM iodoacetamide were separated by size exclusion chromatography. (**C**) GAL-*NFS1* shutdown was induced over 8 hr with over-expression of *NFU1*, *BOL3*, and *ACO1* and LA levels were observed by immunoblotting. Nfu1 protein levels were reduced with increasing amounts of methionine by utilizing a *MET25* promoter is repressed with excess methionine (1x = 0.6 mM methionine). (**D**) A working model of late stage mitochondrial iron-sulfur cluster biogenesis and delivery. Two potential pathways of cluster transfer are shown in **A** and **B**.

DOI: 10.7554/eLife.15991.016

reduced, rather than maintained, in cells expressing elevated levels of Nfu1 (low 1x methionine cultures) (***Figure 7C***, lane 8, top band), but unaffected in cells overexpressing Bol3 (lane 11). Overexpression of the aconitase mimicked the reduced lipoic acid levels seen with elevated Nfu1 (lane 12). These results do not support a reservoir function of [4Fe-4S]-Nfu1 and suggest that elevated levels of a [4Fe-4S] protein, e.g. [4Fe-4S] Nfu1, may negatively impair routing [4Fe-4S] transfer to Lip5 for lipoic acid formation.

Discussion

A role of Nfu1 in Fe-S cluster biogenesis has long been implicated (***Jacobson et al., 1989***; ***Schilke et al., 1999***); however, its molecular mechanism has not been definitely established. Patients

harboring mutations in NFU1, as well as BOLA3, exhibit biochemical abnormalities in a set of [4Fe-4S] enzymes leading to speculation that Nfu1, and BolA3, function as a late Fe-S maturation factor (**Navarro-Sastre et al., 2011**; **Py et al., 2012**) or that Nfu1 is an alternate Fe-S cluster synthesis scaffold protein used for a subset of specific Fe-S client proteins (**Cameron et al., 2011**; **Tong et al., 2003**). The phenotypic similarity between Nfu1 and BolA3 mutations suggests the two proteins function in a common step of the Fe-S protein maturation pathway.

We demonstrate in studies using yeast as a model system that the yeast orthologs of human NFU1 and BOLA3 function in a late step of transfer of [4Fe-4S] clusters to specific client proteins. Yeast lacking Nfu1 are partially deficient in the [4Fe-4S] enzymes aconitase, succinate dehydrogenase and lipoic acid synthase. The defect in lipoic acid synthase is highlighted by the pronounced defect in protein lipoylation in mitochondria. The defect in yeast lacking Bol3 is modest, but is exacerbated in cells lacking both mitochondrial Bol3 and Bol1. The double null cells show related partial defects in [4Fe-4S] enzymes aconitase, succinate dehydrogenase and lipoic acid synthase, although the defects are not as pronounced as in *nfu1*Δ cells. Yeast lacking all three proteins Nfu1, Bol1 and Bol3 show an exaggerated phenotype approaching the defect seen in cells lacking the ISA complex required for [4Fe-4S] cluster synthesis. Clearly, *nfu1*Δ cells do not exhibit any defects in enzymes dependent on [2Fe-2S] centers, suggesting that Nfu1 functions in the [4Fe-4S] cluster transfer pathway.

Our systematic approach to identify endogenous binding partners of Nfu1, Bol1 and Bol3 revealed the step in Fe-S cluster biogenesis in which they function. Affinity purification of Nful1 coupled with mass spectrometry led to the identification of [4Fe-4S] client proteins as physically associating proteins of Nfu1. It is of interest that the $G^{194}C$ Nfu1 variant exhibiting a partial dominant negative effect showed enhanced interaction with the same client proteins. This yeast mutant mimics the known $G^{208}C$ patient mutation in human NFU1 that causes MMSD. Recombinant Nfu1 has been shown to bind a [4Fe-4S] cluster and ^{55}Fe in vivo labeling studies showed a strong increase in ^{55}Fe binding by the patient mimic $G^{194}C$ Nfu1 yeast variant (**Navarro-Sastre et al., 2011**). Moreover, it is also noteworthy that Gly194 is in juxtaposition to the CxxC motif, which has been shown to bind Fe-S clusters. Therefore, it is plausible that the dominant negative effect of the $G^{194}C$ Nfu1 variant may result from the inefficient release of [4Fe-4S] clusters from the Nfu1 variant to client proteins.

The dramatic phenotype of cells harboring $G^{194}C$ Nfu1 is likely due to secondary effects of impaired lipoic acid formation. As mentioned, yeast lacking enzymes involved in octanoic acid formation or lipoic acid synthase are deficient in tRNA processing by RNase P leading to attenuation in mitochondrial translation (**Schonauer et al., 2008**; **Hiltunen et al., 2009**). Consistent with impaired RNase P function, $G^{194}C$ Nfu1 cells are markedly attenuated in levels of the F_1F_0 ATPase and Cox2 steady-state levels. In contrast, the RNase P function is normal in either *nfu1*Δ cells or *bol1*Δ*bol3*Δ cells based on normal F_1F_0 ATPase assembled complexes.

The physical interactions of Nfu1 with Isa1 and Isa2 corroborate our model that Nfu1 functions in [4Fe-4S] cluster transfer to client proteins. Interestingly, we isolated Isa2 as a suppressor of the respiratory defect of *nfu1*Δ cells. Whereas the condensation of two [2Fe-2S] to form a single [4Fe-4S] cluster requires the participation of Isa1, Isa2 and Iba57, Isa2 is capable of forming homo-dimers that may exert a limited transfer function as proposed for Nfu1.

The same [4Fe-4S] client proteins were pulled down in affinity purification of Bol3, but not Bol1, compared to proteins interacting with Nfu1. In the case of Bol3, the dominant negative $H^{101}C$ Bol3 variant also showed enhanced interactions with [4Fe-4S] client proteins. The dominant negative phenotype of the $H^{101}C$ Bol3 mutant (putative Fe-S ligand) but only loss of function phenotype for the $H^{101}A$ mutant is consistent with a model that Bol3 His101 participates in Fe-S cluster transfer.

The partial deficiency of [4Fe-4S] enzyme activities in *nfu1*Δ cells suggests that the function of Nfu1 may be conditionally important in [4Fe-4S] cluster transfer and that a bypass mechanism exists in yeast. We demonstrate that Nfu1 in yeast has a heightened importance in cells undergoing oxidative metabolism as opposed to anoxic metabolism. In addition, *nfu1*Δ cell growth defect is partially suppressed with supplemental GSH in the growth medium. Identification of the Yap1 and Yap2, transcription factors that are important for oxidative stress tolerance, as high copy suppressors emphasized the importance of Nfu1 during oxidative metabolism.

One curiosity is that human patients with mutations in NFU1 or BOLA3 lack defects in mitochondrial aconitase, whereas the yeast mutants, *nfu1*Δ and the double *bol1*Δ *bol3*Δ, exhibit a partial aconitase defect. There are two implications of this result. First, Nfu1 may exhibit different client

selectivity in the actual transfer of [4Fe-4S] clusters. Although Nfu1 binds many [4Fe-4S] client proteins, it may facilitate cluster transfer to select clients and this may differ between human and yeast cells as in the case of aconitase. This postulate is supported by the observed role for Nfu1 in Aco1 and Lip5 activation, but not the function of Aco2 and Lys4. Second, since the partial respiratory function persists in *nfu1*Δ cells, Nfu1 may facilitate cluster transfer in oxidative growth conditions and this may differ between yeast and human cells.

One dramatic phenotype in human and yeast Nfu1 mutant cells is impaired protein lipoylation. Yeast and human cells require lipoylation on E2 subunits of pyruvate dehydrogenase, 2-oxoglutarate dehydrogenase and the glycine cleavage enzyme complex. In addition, the human branched chain 2-oxoacid dehydrogenase requires lipoylation for function. Lip5 catalyzing formation of the lipoate coenzyme binds two [4Fe-4S] clusters, one of which serves as the sulfur donor for lipoic acid formation in a radical S-adenosylmethionine dependent reaction (***Cicchillo and Booker, 2005***; ***Cicchillo et al., 2004***). Two sulfide ions from this auxiliary cluster are used for formation of lipoate resulting in disassembly of the cluster. Each catalytic cycle of the enzyme requires repair or replacement of the auxiliary cluster (***Cronan, 2014***). Nfu1 may have a specialized role in cluster repair in lipoic acid synthase or alternatively provides a [4Fe-4S] replacement.

For most [4Fe-4S] client proteins, Nfu1 appears to have evolved to shield its [4Fe-4S] cluster from endogenous oxidants during the cluster transfer step. Oxidants are generated by 2-oxoacid dehydrogenases (***Boutigny et al., 2013***), so Nfu1-mediated cluster transfer may be critical to ensure intact [4Fe-4S] insertion. Nfu1 may also serve as a chaperone of apo-client protein, preventing their aggregation in the absence of a bound Fe-S cluster. Additional studies are necessary to define these candidate roles.

Bol3, but not Bol1, was found to associate with [4Fe-4S] client proteins, whereas Bol1 reproducibly associated with Grx5 both in in vivo and in vitro studies. BolA:glutaredoxin complexes reported to date only bind [2Fe-2S] clusters (***Li and Outten, 2012***). Thus, Bol1 is anticipated to function with Grx5 in a [2Fe-2S] cluster step, whereas Bol3 is likely to function, independent of Grx5, in a Nfu1-mediated [4Fe-4S] cluster step. These studies suggest that Bol1 and Bol3 have specialized functions within the same pathway, such that cells lacking both Bol1 and Bol3 have a synthetic defect.

In summary, the present work suggests that Nfu1 has a significant role in a late step transfer of [4Fe-4S] clusters to select client proteins. Nfu1 binds the client proteins independent of the ISA complex and its association with the ISA complex may serve to recruit apo-clients to the ISA complex where [4Fe-4S] clusters are formed (***Figure 7D***). Some [4Fe-4S] client proteins may get their [4Fe-4S] cluster directly from the ISA complex, whereas others may derive their clusters after prior transfer of a [4Fe-4S] cluster to Nfu1. In these cases Nfu1 facilitates the process as an adapter protein in oxidatively growing cells. Additional work is required to discern the client selectivity in [4Fe-4S] cluster transfer by Nfu1. This model of eukaryotic Nfu1 function resembles the role of the *E. coli* Nfu1 ortholog NfuA, which binds a subset of Fe-S apo-client proteins and facilitates cluster transfer especially under oxidative stress conditions (***Py et al., 2012***; ***Angelini et al., 2008***; ***Boutigny et al., 2013***). Likewise, the *Azobacter* NfuA is reported to be critical under oxidative growth conditions (***Bandyopadhyay et al., 2008***). In the case of *E. coli*, NfuA cluster transfer is likely mediated directly by NfuA (***Py et al., 2012***). Bol3 likely functions with Nfu1 in cluster transfer, but its mechanism remains nebulous. Clearly, interaction studies separate Bol1 and Bol3 into two distinct classes, with Bol3 working with Nfu1 in [4Fe-4S] client binding and Bol1 working with Grx5, which has one known function upstream of the ISA complex (***Uzarska et al., 2013***; ***Kim et al., 2010***; ***Banci et al., 2014***). However, cells lacking both mitochondrial BolA proteins show a synthetic defect. The Bol3 protein may facilitate [4Fe-4S] cluster dissociation from either the ISA complex or Nfu1 in [4Fe-4S] cluster transfer. Additional work will be required to discern their mechanisms.

Materials and methods

Yeast strains and plasmids

BY4741 strains were used unless indicated otherwise. Deletion strains were generated by homologous recombination and confirmed by PCR analyses of loci as described earlier (***Longtine et al., 1998***). Plasmids used in this study were constructed using general subcloning techniques. For mutagenesis or adding epitope tags, Phusion DNA Polymerases (Thermo Fisher Scientific, Waltham, MA)

were used. All plasmid-borne genes were expressed under the *MET25* promoter and the *CYC1* terminator unless indicated otherwise.

Strep-tag affinity purification

Affinity purifications of Strep-tagged proteins were conducted using Strep-Tactin superflow beads (Qiagen, Germany) following the manufacturer's instruction with slight changes. Briefly, isolated mitochondria were solubilized with 0.1% n-dodecyl maltoside (DDM) in the lysis buffer, 50 mM NaH_2PO_4 (pH 8.0), 300 mM NaCl and 1x protease inhibitor (cOmplete mini, Roche, Switzerland), for 30 min on ice. After clarification of solubilized mitochondria by high-speed centrifugation, the supernatants were incubated with Strep-Tactin superflow beads for 16 hr at 4˚C. The beads were washed five times with the lysis buffer. Strep-tagged proteins bound to the beads were eluted with 2.5 mM dethiobiotin in the lysis buffer, which were subjected to mass spectrometry analyses or immunoblotting.

Enzymatic activity assay

Activity assays for aconitase, succinate dehydrogenase (SDH), cytochrome bc_1 complex and cytochrome *c* oxidase were performed as described previously (***Atkinson et al., 2011***; ***Na et al., 2014***). Aconitase activity was determined by measuring the initial rate of conversion of 100 mM *cis*-aconitate to isocitrate in 50 mM Tris (pH 7.4) at 240 nm. Soluble fractions of mitochondria were obtained by repetitive freeze-thaw. SDH activity was measured by quinone-mediated reduction of dichlorophenolindophenol (DCPIP) upon succinate oxidation at 600 nm. For cytochrome bc_1 complex activity, the reduction rate of cytochrome *c* was measured upon the oxidation of reduced decylubiquinol at 550 nm. Cytochrome *c* oxidase activity was determined by measuring the initial rate of oxidation of cytochrome *c* oxidation (***Pierrel et al., 2007***). Dihydroxy acid dehydratase (Ilv3) catalytic activity was assayed using an end point assay measuring 2,4-dinitophenylhydrazine (DNPH) as a proton acceptor as described previously (***Limberg et al., 1995***). Purified mitochondria (30 µg) were lysed by sonication in assay buffer (20 mM KPO_4 and 10 mM $MgCl_2$), spun at 20,000 ×g for 15 min, before incubation with 100 mM dihydroxyisovalerate for 10 min in a total volume of 1 ml. The reaction was quenched with 100 µl of 50% TCA. Next 200 µl of DNPH (saturated in 2 N HCl) was added for 15 min when 500 µl of 2.5N NaOH was added to quench the reaction. The absorbance was measured at 540nm by a UV-VIS spectrophotometer.

Mass spectrometry analysis

The purified Strep-tagged protein complexes were reduced, alkylated and digested as described (***Kaiser and Wohlschlegel, 2005***; ***Wohlschlegel, 2009***). The digested peptide mixture was desalted using C18-packed pipette tips (Thermo Fisher Scientific) and fractionated online using a 75 µM inner diameter fritted fused silica capillary column with a 5 µM pulled electrospray tip and packed in-house with 15 cm of Luna C18 (2) 3 µM reversed phase particles. The gradient was delivered via an easy-nLC 1000 ultra high-pressure liquid chromatography (UHPLC) system (Thermo Fisher Scientific). MS/MS spectra were collected on a Q-Exactive mass spectrometer (Thermo Fisher Scientific) (***Kelstrup et al., 2012***; ***Michalski et al., 2011***). Data analysis was carried out using the ProLuCID and DTASelect2 implemented in the Integrated Proteomics Pipeline - IP2 (Integrated Proteomics Applications, Inc., San Diego, CA) (***Cociorva et al., 2007***; ***Tabb et al., 2002***; ***Xu et al., 2006***). Protein and peptide identifications were filtered using DTASelect and required at least two unique peptides per protein with a peptide-level false positive rate of 5% as estimated by a decoy database strategy (***Elias and Gygi, 2007***). Normalized spectral abundance factor (NSAF) values were calculated as described (***Florens et al., 2006***) and multiplied by a factor of 10^5 for readability.

Size exclusion chromatography

Purified mitochondria (1.5 mg) were lysed by sonication in 50 mM $NaPO_4$ 150 mM NaCl (pH 7.0) buffer. Lysates were precleared and filtered prior being applied to a HiLoad Superdex 75 PG 16/600 column (GE Healthcare Life Sciences, United Kingdom) with a flow rate of 1 mL/Min. Fractions of 1.33 mL were collected, TCA precipitated and analyzed by immunoblotting.

Affinity measurements using microscale thermophoresis (MST)

For MicroScale Thermophoresis the proteins were fluorescently labeled using the Monolith NT Protein Labeling Kit RED with NT-647 dye as recommended by the supplier (NanoTemper Technologies, Germany). The fluorescently labelled protein (200 nM) was titrated with serial dilutions of unlabeled protein (from 200 µM to 6.1 nM) in buffer containing 50 mM KP_i, pH 7.4, 150 mM NaCl, 5% glycerol, 0.05 mg/mL BSA, and 0.05% Tween20. Thermophoresis assays were performed using Monolith NT.115 at 21˚C (LED power – between 40% and 60%, IR laser power 75%) in standard capillaries under anaerobic conditions. At least three independent experiments were recorded at 680 nm. The thermophoresis data were processed by Nano Temper Analysis 1.2.009 and GraphPad Prism5 software to estimate the K_d values.

Chemical reconstitution of Fe-S clusters

Chemical reconstitution was done in a COY (Grass Lake, MI) anaerobic chamber using freshly dissolved stock solutions. Protein solutions were reduced with 5 mM DTT for 2–3 hr on ice in reconstitution buffer (50 mM Tris-HCl, pH 8.0, 150 mM NaCl, 5% glycerol). Reconstitution was started at room temperature by the addition of a 2-3-fold excess of ferric ammonium citrate by inverting the tube. After 5 min a 2-3-fold excess of lithium sulfide was added slowly. Reconstituted proteins were desalted after 2 hr incubation on a PD-10 column equilibrated with reconstitution buffer. Incorporation of the Fe/S clusters into apoproteins was monitored by UV-Vis (V-550, Jasco Inc., Easton, MD) and CD spectroscopy (J-815, Jasco Inc).

Miscellaneous procedures

Yeast mitochondria isolation was performed using the method of Glick and Pon (***Glick and Pon, 1995***). Standard procedures were performed for SDS-PAGE and immunoblotting. Anti-Sdh2 was from the previous study (***Kim et al., 2012***). BN-PAGE was performed as described previously with mitochondrial lysates in 1% digitonin solution (***Schilke et al., 1999***). Anti-Strep was purchased from Qiagen. Antibodies against LA-conjugated proteins were from Calbiochem (San Diego, CA). Anti-Myc and anti-HA were from Santa Cruz Biotechnology (Dallas, TX). Anti-Por1 was purchased from Molecular Probes and anti-FLAG was from Sigma-Aldrich.(St. Louis, MO) Protein concentration was determined by the Bradford assay.

Acknowledgements

We thank James Cox and the University of Utah Metabolomics Core facility for the metabolomic analyses. We acknowledge support of funds in conjunction with grant P30 CA042014 awarded to Huntsman Cancer Institute. AM was supported by training grant T32 DK007115 from the National Institutes of Health. This research was supported by grants RO1 GM110755 and R01 GM112763 from the National Institutes of Health awarded to DRW and JAW, respectively. RL acknowledges generous financial support from Deutsche Forschungsgemeinschaft (SPP 1710 and SPP 1927), and the LOEWE program of state Hessen.

Additional information

Funding

Funder	Grant reference number	Author
National Institutes of Health	T32 DK007115	Andrew Melber
Deutsche Forschungsgemeinschaft	SPP 1710	Roland Lill
Deutsche Forschungsgemeinschaft	Spp 1927	Roland Lill
National Institutes of Health	R01 GM112763	James A Wohlschlegel
National Institutes of Health	RO1 GM110755	Dennis R Winge
National Institutes of Health	P30 CA042014	Dennis R Winge

LOEWE Zentrum für Synthetische Mikrobiologie SynMikro	Roland Lill

The funders had no role in study design, data collection and interpretation, or the decision to submit the work for publication.

Author contributions

AM, Conception and design, Acquisition of data, Analysis and interpretation of data, Drafting or revising the article, Contributed unpublished essential data or reagents; UN, Acquisition of data, Analysis and interpretation of data, Drafting or revising the article; AV, BDW, Acquisition of data, Analysis and interpretation of data; RL, JAW, Analysis and interpretation of data; DRW, Conception and design, Analysis and interpretation of data, Drafting or revising the article

Author ORCIDs

Roland Lill, http://orcid.org/0000-0002-8345-6518
Dennis R Winge, http://orcid.org/0000-0003-1160-1189

References

Al-Hassnan ZN, Al-Dosary M, Alfadhel M, Faqeih EA, Alsagob M, Kenana R, Almass R, Al-Harazi OS, Al-Hindi H, Malibari OI, Almutari FB, Tulbah S, Alhadeq F, Al-Sheddi T, Alamro R, AlAsmari A, Almuntashri M, Alshaalan H, Al-Mohanna FA, Colak D, et al. 2015. ISCA2 mutation causes infantile neurodegenerative mitochondrial disorder. *Journal of Medical Genetics* **52**:186–194. doi: 10.1136/jmedgenet-2014-102592

Angelini S, Gerez C, Ollagnier-de Choudens S, Sanakis Y, Fontecave M, Barras F, Py B. 2008. NfuA, a new factor required for maturing Fe/S proteins in Escherichia coli under oxidative stress and iron starvation conditions. *Journal of Biological Chemistry* **283**:14084–14091. doi: 10.1074/jbc.M709405200

Atkinson A, Smith P, Fox JL, Cui TZ, Khalimonchuk O, Winge DR. 2011. The LYR protein Mzm1 functions in the insertion of the Rieske Fe/S protein in yeast mitochondria. *Molecular and Cellular Biology* **31**:3988–3996. doi: 10.1128/MCB.05673-11

Baker PR, Friederich MW, Swanson MA, Shaikh T, Bhattacharya K, Scharer GH, Aicher J, Creadon-Swindell G, Geiger E, MacLean KN, Lee WT, Deshpande C, Freckmann ML, Shih LY, Wasserstein M, Rasmussen MB, Lund AM, Procopis P, Cameron JM, Robinson BH, et al. 2014. Variant non ketotic hyperglycinemia is caused by mutations in LIAS, BOLA3 and the novel gene GLRX5. *Brain* **137**:366–379. doi: 10.1093/brain/awt328

Banci L, Brancaccio D, Ciofi-Baffoni S, Del Conte R, Gadepalli R, Mikolajczyk M, Neri S, Piccioli M, Winkelmann J. 2014. [2Fe-2S] cluster transfer in iron-sulfur protein biogenesis. *PNAS* **111**:6203–6208. doi: 10.1073/pnas.1400102111

Bandyopadhyay S, Naik SG, O'Carroll IP, Huynh BH, Dean DR, Johnson MK, Dos Santos PC. 2008. A proposed role for the Azotobacter vinelandii NfuA protein as an intermediate iron-sulfur cluster carrier. *Journal of Biological Chemistry* **283**:14092–14099. doi: 10.1074/jbc.M709161200

Biederbick A, Stehling O, Rösser R, Niggemeyer B, Nakai Y, Elsässer HP, Lill R. 2006. Role of human mitochondrial Nfs1 in cytosolic iron-sulfur protein biogenesis and iron regulation. *Molecular and Cellular Biology* **26**:5675–5687. doi: 10.1128/MCB.00112-06

Boutigny S, Saini A, Baidoo EE, Yeung N, Keasling JD, Butland G. 2013. Physical and functional interactions of a monothiol glutaredoxin and an iron sulfur cluster carrier protein with the sulfur-donating radical S-adenosyl-L-methionine enzyme MiaB. *Journal of Biological Chemistry* **288**:14200–14211. doi: 10.1074/jbc.M113.460360

Brancaccio D, Gallo A, Mikolajczyk M, Zovo K, Palumaa P, Novellino E, Piccioli M, Ciofi-Baffoni S, Banci L. 2014. Formation of [4Fe-4S] clusters in the mitochondrial iron-sulfur cluster assembly machinery. *Journal of the American Chemical Society* **136**:16240–16250. doi: 10.1021/ja507822j

Bridwell-Rabb J, Fox NG, Tsai CL, Winn AM, Barondeau DP. 2014. Human frataxin activates Fe-S cluster biosynthesis by facilitating sulfur transfer chemistry. *Biochemistry* **53**:4904–4913. doi: 10.1021/bi500532e

Cameron JM, Janer A, Levandovskiy V, Mackay N, Rouault TA, Tong WH, Ogilvie I, Shoubridge EA, Robinson BH. 2011. Mutations in iron-sulfur cluster scaffold genes NFU1 and BOLA3 cause a fatal deficiency of multiple respiratory chain and 2-oxoacid dehydrogenase enzymes. *The American Journal of Human Genetics* **89**:486–495. doi: 10.1016/j.ajhg.2011.08.011

Cicchillo RM, Lee KH, Baleanu-Gogonea C, Nesbitt NM, Krebs C, Booker SJ. 2004. Escherichia coli lipoyl synthase binds two distinct [4Fe-4S] clusters per polypeptide. *Biochemistry* **43**:11770–11781. doi: 10.1021/bi0488505

Cicchillo RM, Booker SJ. 2005. Mechanistic investigations of lipoic acid biosynthesis in Escherichia coli: both sulfur atoms in lipoic acid are contributed by the same lipoyl synthase polypeptide. *Journal of the American Chemical Society* **127**:2860–2861. doi: 10.1021/ja042428u

Ciesielski SJ, Schilke BA, Osipiuk J, Bigelow L, Mulligan R, Majewska J, Joachimiak A, Marszalek J, Craig EA, Dutkiewicz R. 2012. Interaction of J-protein co-chaperone Jac1 with Fe-S scaffold Isu is indispensable in vivo and conserved in evolution. *Journal of Molecular Biology* **417**:1–12. doi: 10.1016/j.jmb.2012.01.022

Cociorva D, Tabb D L, Yates JR. 2007. Validation of tandem mass spectrometry database search results using DTASelect. *Current Protocols in Bioinformatics* **Chapter 13:Unit 13.4**:13.4.1–13.4.14. doi: 10.1002/0471250953.bi1304s16

Cronan JE. 2014. The structure of lipoyl synthase, a remarkable enzyme that performs the last step of an extraordinary biosynthetic pathway. *Biochemical Journal* **464**:e1–3. doi: 10.1042/BJ20141061

Debray FG, Stümpfig C, Vanlander AV, Dideberg V, Josse C, Caberg JH, Boemer F, Bours V, Stevens R, Seneca S, Smet J, Lill R, van Coster R. 2015. Mutation of the iron-sulfur cluster assembly gene IBA57 causes fatal infantile leukodystrophy. *Journal of Inherited Metabolic Disease* **38**:1147–1153. doi: 10.1007/s10545-015-9857-1

Elias JE, Gygi SP. 2007. Target-decoy search strategy for increased confidence in large-scale protein identifications by mass spectrometry. *Nature Methods* **4**:207–214. doi: 10.1038/nmeth1019

Fazius F, Shelest E, Gebhardt P, Brock M. 2012. The fungal α-aminoadipate pathway for lysine biosynthesis requires two enzymes of the aconitase family for the isomerization of homocitrate to homoisocitrate. *Molecular Microbiology* **86**:1508–1530. doi: 10.1111/mmi.12076

Fernandes L, Rodrigues-Pousada C, Struhl K. 1997. Yap, a novel family of eight bZIP proteins in *Saccharomyces cerevisiae* with distinct biological functions. *Molecular and Cellular Biology* **17**:6982–6993. doi: 10.1128/MCB.17.12.6982

Ferrer-Cortès X, Font A, Bujan N, Navarro-Sastre A, Matalonga L, Arranz JA, Riudor E, del Toro M, Garcia-Cazorla A, Campistol J, Briones P, Ribes A, Tort F. 2013. Protein expression profiles in patients carrying NFU1 mutations. Contribution to the pathophysiology of the disease. *Journal of Inherited Metabolic Disease* **36**:841–847. doi: 10.1007/s10545-012-9565-z

Florens L, Carozza MJ, Swanson SK, Fournier M, Coleman MK, Workman JL, Washburn MP. 2006. Analyzing chromatin remodeling complexes using shotgun proteomics and normalized spectral abundance factors. *Methods* **40**:303–311. doi: 10.1016/j.ymeth.2006.07.028

Fox NG, Das D, Chakrabarti M, Lindahl PA, Barondeau DP. 2015. Frataxin accelerates [2Fe-2S] cluster formation on the human Fe-S assembly complex. *Biochemistry* **54**:3880–3889. doi: 10.1021/bi5014497

Gao H, Subramanian S, Couturier J, Naik SG, Kim SK, Leustek T, Knaff DB, Wu HC, Vignols F, Huynh BH, Rouhier N, Johnson MK. 2013. Arabidopsis thaliana Nfu2 accommodates [2Fe-2S] or [4Fe-4S] clusters and is competent for in vitro maturation of chloroplast [2Fe-2S] and [4Fe-4S] cluster-containing proteins. *Biochemistry* **52**:6633–6645. doi: 10.1021/bi4007622

Gelling C, Dawes IW, Richhardt N, Lill R, Mühlenhoff U. 2008. Mitochondrial Iba57p is required for Fe/S cluster formation on aconitase and activation of radical SAM enzymes. *Molecular and Cellular Biology* **28**:1851–1861. doi: 10.1128/MCB.01963-07

Gerber J, Mühlenhoff U, Lill R. 2003. An interaction between frataxin and Isu1/Nfs1 that is crucial for Fe/S cluster synthesis on Isu1. *EMBO Reports* **4**:906–911. doi: 10.1038/sj.embor.embor918

Glick BS, Pon LA. 1995. Isolation of highly purified mitochondria from *Saccharomyces cerevisiae*. *Methods in Enzymology* **260**:213–223 . doi: 10.1016/0076-6879(95)60139-2

Hiltunen JK, Schonauer MS, Autio KJ, Mittelmeier TM, Kastaniotis AJ, Dieckmann CL. 2009. Mitochondrial fatty acid synthesis type II: more than just fatty acids. *Journal of Biological Chemistry* **284**:9011–9015. doi: 10.1074/jbc.R800068200

Hiltunen JK, Autio KJ, Schonauer MS, Kursu VAS, Dieckmann CL, Kastaniotis AJ. 2010. Mitochondrial fatty acid synthesis and respiration. *Biochimica Et Biophysica Acta (BBA)* **1797**:1195–1202. doi: 10.1016/j.bbabio.2010.03.006

Jacobson MR, Cash VL, Weiss MC, Laird NF, Newton WE, Dean DR. 1989. Biochemical and genetic analysis of the nifUSVWZM cluster from Azotobacter vinelandii. *MGG Molecular & General Genetics* **219**:49–57. doi: 10.1007/BF00261156

Kaiser P, Wohlschlegel J. 2005. Identification of ubiquitination sites and determination of ubiquitin-chain architectures by mass spectrometry. *Methods in Enzymology* **399**:266–277. doi: 10.1016/S0076-6879(05)99018-6

Kelstrup CD, Young C, Lavallee R, Nielsen ML, Olsen JV. 2012. Optimized fast and sensitive acquisition methods for shotgun proteomics on a quadrupole orbitrap mass spectrometer. *Journal of Proteome Research* **11**:3487–3497. doi: 10.1021/pr3000249

Kim KD, Chung WH, Kim HJ, Lee KC, Roe JH. 2010. Monothiol glutaredoxin Grx5 interacts with Fe-S scaffold proteins Isa1 and Isa2 and supports Fe-S assembly and DNA integrity in mitochondria of fission yeast. *Biochemical and Biophysical Research Communications* **392**:467–472. doi: 10.1016/j.bbrc.2010.01.051

Kim HJ, Jeong MY, Na U, Winge DR. 2012. Flavinylation and assembly of succinate dehydrogenase are dependent on the C-terminal tail of the flavoprotein subunit. *Journal of Biological Chemistry* **287**:40670–40679. doi: 10.1074/jbc.M112.405704

Lange H, Kaut A, Kispal G, Lill R. 2000. A mitochondrial ferredoxin is essential for biogenesis of cellular iron-sulfur proteins. *PNAS* **97**:1050–1055. doi: 10.1073/pnas.97.3.1050

Li H, Outten CE. 2012. Monothiol CGFS glutaredoxins and BolA-like proteins: [2Fe-2S] binding partners in iron homeostasis. *Biochemistry* **51**:4377–4389. doi: 10.1021/bi300393z

Li H, Mapolelo DT, Randeniya S, Johnson MK, Outten CE. 2012. Human glutaredoxin 3 forms [2Fe-2S]-bridged complexes with human BolA2. *Biochemistry* **51**:1687–1696. doi: 10.1021/bi2019089

Lill R, Mühlenhoff U. 2008. Maturation of iron-sulfur proteins in eukaryotes: mechanisms, connected processes, and diseases. *Annual Review of Biochemistry* **77**:669–700. doi: 10.1146/annurev.biochem.76.052705.162653

Lill R, Hoffmann B, Molik S, Pierik AJ, Rietzschel N, Stehling O, Uzarska MA, Webert H, Wilbrecht C, Mühlenhoff U. 2012. The role of mitochondria in cellular iron–sulfur protein biogenesis and iron metabolism. *Biochimica Et Biophysica Acta (BBA)* **1823**:1491–1508. doi: 10.1016/j.bbamcr.2012.05.009

Limberg G, Klaffke W, Thiem J. 1995. Conversion of aldonic acids to their corresponding 2-keto-3-deoxy-analogs by the non-carbohydrate enzyme dihydroxy acid dehydratase (DHAD). *Bioorganic & Medicinal Chemistry* **3**: 487–494. doi: 10.1016/0968-0896(95)00072-O

Liu Y, Qi W, Cowan JA. 2009. Iron-sulfur cluster biosynthesis: functional characterization of the N- and C-terminal domains of human NFU. *Biochemistry* **48**:973–980. doi: 10.1021/bi801645z

Longtine MS, McKenzie A, Demarini DJ, Shah NG, Wach A, Brachat A, Philippsen P, Pringle JR. 1998. Additional modules for versatile and economical PCR-based gene deletion and modification in *Saccharomyces cerevisiae. Yeast* **14**:953–961. doi: 10.1002/(SICI)1097-0061(199807)14:10<953::AID-YEA293>3.0.CO;2-U

Lossos A, Stümpfig C, Stevanin G, Gaussen M, Zimmerman BE, Mundwiller E, Asulin M, Chamma L, Sheffer R, Misk A, Dotan S, Gomori JM, Ponger P, Brice A, Lerer I, Meiner V, Lill R. 2015. Fe/S protein assembly gene IBA57 mutation causes hereditary spastic paraplegia. *Neurology* **84**:659–667. doi: 10.1212/WNL.0000000000001270

Majewska J, Ciesielski SJ, Schilke B, Kominek J, Blenska A, Delewski W, Song JY, Marszalek J, Craig EA, Dutkiewicz R. 2013. Binding of the chaperone Jac1 protein and cysteine desulfurase Nfs1 to the iron-sulfur cluster scaffold Isu protein is mutually exclusive. *Journal of Biological Chemistry* **288**:29134–29142. doi: 10.1074/jbc.M113.503524

Michalski A, Damoc E, Hauschild JP, Lange O, Wieghaus A, Makarov A, Nagaraj N, Cox J, Mann M, Horning S. 2011. Mass spectrometry-based proteomics using Q Exactive, a high-performance benchtop quadrupole Orbitrap mass spectrometer. *Molecular & Cellular Proteomics* **10**:M111.011015. doi: 10.1074/mcp.M111.011015

Mühlenhoff U, Richter N, Pines O, Pierik AJ, Lill R. 2011. Specialized function of yeast Isa1 and Isa2 proteins in the maturation of mitochondrial [4Fe-4S] proteins. *Journal of Biological Chemistry* **286**:41205–41216. doi: 10.1074/jbc.M111.296152

Na U, Yu W, Cox J, Bricker DK, Brockmann K, Rutter J, Thummel CS, Winge DR. 2014. The LYR factors SDHAF1 and SDHAF3 mediate maturation of the iron-sulfur subunit of succinate dehydrogenase. *Cell Metabolism* **20**: 253–266. doi: 10.1016/j.cmet.2014.05.014

Navarro-Sastre A, Tort F, Stehling O, Uzarska MA, Arranz JA, Del Toro M, Labayru MT, Landa J, Font A, Garcia-Villoria J, Merinero B, Ugarte M, Gutierrez-Solana LG, Campistol J, Garcia-Cazorla A, Vaquerizo J, Riudor E, Briones P, Elpeleg O, Ribes A, et al. 2011. A fatal mitochondrial disease is associated with defective NFU1 function in the maturation of a subset of mitochondrial Fe-S proteins. *The American Journal of Human Genetics* **89**:656–667. doi: 10.1016/j.ajhg.2011.10.005

Nishio K, Nakai M. 2000. Transfer of iron-sulfur cluster from NifU to apoferredoxin. *Journal of Biological Chemistry* **275**:22615–22618. doi: 10.1074/jbc.C000279200

Nizon M, Boutron A, Boddaert N, Slama A, Delpech H, Sardet C, Brassier A, Habarou F, Delahodde A, Correia I, Ottolenghi C, de Lonlay P. 2014. Leukoencephalopathy with cysts and hyperglycinemia may result from NFU1 deficiency. *Mitochondrion* **15**:59–64. doi: 10.1016/j.mito.2014.01.003

Parent A, Elduque X, Cornu D, Belot L, Le Caer JP, Grandas A, Toledano MB, D'Autréaux B. 2015. Mammalian frataxin directly enhances sulfur transfer of NFS1 persulfide to both ISCU and free thiols. *Nature Communications* **6**:5686. doi: 10.1038/ncomms6686

Pierrel F, Bestwick ML, Cobine PA, Khalimonchuk O, Cricco JA, Winge DR. 2007. Coa1 links the Mss51 post-translational function to Cox1 cofactor insertion in cytochrome c oxidase assembly. *The EMBO Journal* **26**: 4335–4346. doi: 10.1038/sj.emboj.7601861

Py B, Gerez C, Angelini S, Planel R, Vinella D, Loiseau L, Talla E, Brochier-Armanet C, Garcia Serres R, Latour JM, Ollagnier-de Choudens S, Fontecave M, Barras F. 2012. Molecular organization, biochemical function, cellular role and evolution of NfuA, an atypical Fe-S carrier. *Molecular Microbiology* **86**:155–171. doi: 10.1111/j.1365-2958.2012.08181.x

Roret T, Tsan P, Couturier J, Zhang B, Johnson MK, Rouhier N, Didierjean C. 2014. Structural and spectroscopic insights into BolA-glutaredoxin complexes. *Journal of Biological Chemistry* **289**:24588–24598. doi: 10.1074/jbc.M114.572701

Schilke B, Voisine C, Beinert H, Craig E. 1999. Evidence for a conserved system for iron metabolism in the mitochondria of *Saccharomyces cerevisiae. PNAS* **96**:10206–10211. doi: 10.1073/pnas.96.18.10206

Schmucker S, Martelli A, Colin F, Page A, Wattenhofer-Donzé M, Reutenauer L, Puccio H. 2011. Mammalian frataxin: an essential function for cellular viability through an interaction with a preformed ISCU/NFS1/ISD11 iron-sulfur assembly complex. *PLoS One* **6**:e16199. doi: 10.1371/journal.pone.0016199

Schonauer MS, Kastaniotis AJ, Hiltunen JK, Dieckmann CL. 2008. Intersection of RNA processing and the type II fatty acid synthesis pathway in yeast mitochondria. *Molecular and Cellular Biology* **28**:6646–6657. doi: 10.1128/MCB.01162-08

Seyda A, Newbold RF, Hudson TJ, Verner A, MacKay N, Winter S, Feigenbaum A, Malaney S, Gonzalez-Halphen D, Cuthbert AP, Robinson BH. 2001. A novel syndrome affecting multiple mitochondrial functions, located by microcell-mediated transfer to chromosome 2p14-2p13. *The American Journal of Human Genetics* **68**:386–396. doi: 10.1086/318196

Sheftel AD, Wilbrecht C, Stehling O, Niggemeyer B, Elsässer HP, Mühlenhoff U, Lill R. 2012. The human mitochondrial ISCA1, ISCA2, and IBA57 proteins are required for [4Fe-4S] protein maturation. *Molecular Biology of the Cell* **23**:1157–1166. doi: 10.1091/mbc.E11-09-0772

Tabb DL, McDonald WH, Yates JR. 2002. DTASelect and Contrast: tools for assembling and comparing protein identifications from shotgun proteomics. *Journal of Proteome Research* **1**:21–26. doi: 10.1021/pr015504q

Tong W-H, Jameson GNL, Huynh BH, Rouault TA. 2003. Subcellular compartmentalization of human Nfu, an iron-sulfur cluster scaffold protein, and its ability to assemble a [4Fe-4S] cluster. *PNAS* **100**:9762–9767. doi: 10.1073/pnas.1732541100

Tsai CL, Barondeau DP. 2010. Human frataxin is an allosteric switch that activates the Fe-S cluster biosynthetic complex. *Biochemistry* **49**:9132–9139. doi: 10.1021/bi1013062

Uzarska MA, Dutkiewicz R, Freibert SA, Lill R, Mühlenhoff U. 2013. The mitochondrial Hsp70 chaperone Ssq1 facilitates Fe/S cluster transfer from Isu1 to Grx5 by complex formation. *Molecular Biology of the Cell* **24**:1830–1841. doi: 10.1091/mbc.E12-09-0644

Webert H, Freibert SA, Gallo A, Heidenreich T, Linne U, Amlacher S, Hurt E, Mühlenhoff U, Banci L, Lill R. 2014. Functional reconstitution of mitochondrial Fe/S cluster synthesis on Isu1 reveals the involvement of ferredoxin. *Nature Communications* **5**:5013. doi: 10.1038/ncomms6013

Willems P, Wanschers BF, Esseling J, Szklarczyk R, Kudla U, Duarte I, Forkink M, Nooteboom M, Swarts H, Gloerich J, Nijtmans L, Koopman W, Huynen MA. 2013. BOLA1 is an aerobic protein that prevents mitochondrial morphology changes induced by glutathione depletion. *Antioxidants & Redox Signaling* **18**:129–138. doi: 10.1089/ars.2011.4253

Wittig I, Braun HP, Schägger H. 2006. Blue native PAGE. *Nature Protocols* **1**:418–428. doi: 10.1038/nprot.2006.62

Wohlschlegel JA. 2009. Identification of SUMO-conjugated proteins and their SUMO attachment sites using proteomic mass spectrometry. *Methods in Molecular Biology* **497**:33–49. doi: 10.1007/978-1-59745-566-4_3

Xu T, Venable JD, Park SK, Cociorva D, Lu B, Liao L, Wohlschlegel J, Hewel J, Yates JR. 2006. ProLuCID, a fast and sensitive tandem mass spectra-based protein identification program. *Molecular & Cellular Proteomics* **5**:S174.

Yabe T, Morimoto K, Kikuchi S, Nishio K, Terashima I, Nakai M. 2004. The arabidopsis chloroplastic NifU-like protein CnfU, which can act as an iron-sulfur cluster scaffold protein, is required for biogenesis of ferredoxin and photosystem I. *The Plant Cell Online* **16**:993–1007. doi: 10.1105/tpc.020511

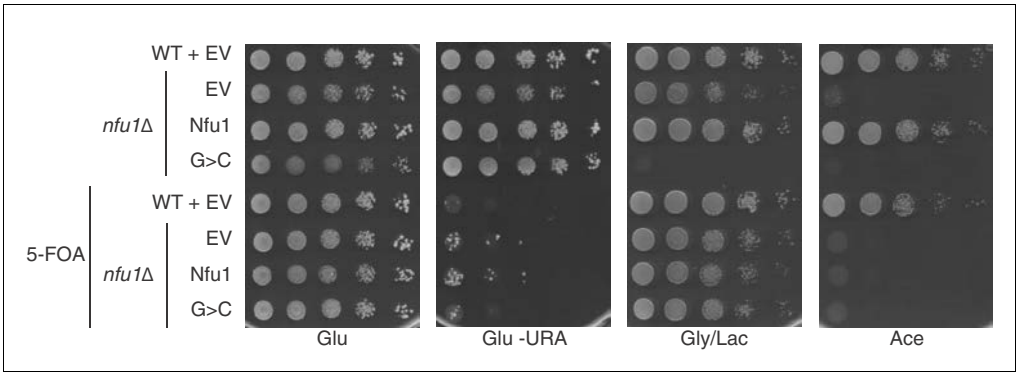

Figure 3—figure supplement 1. Yeast growth tests evaluating respiratory growth (Gly/Lac) of *nfu1*Δ + G>C cells following treatment with 5'-Fluoroorotic acid (5-FOA) to show cells have not lost their mitochondrial DNA (rho$^-$). 5-FOA was used to induce shedding of the pRS416 vector. Glu-URA is SC media with 2% glucose lacking Uracil to show the successful loss of the pRS416 vector.
DOI: 10.7554/eLife.15991.006

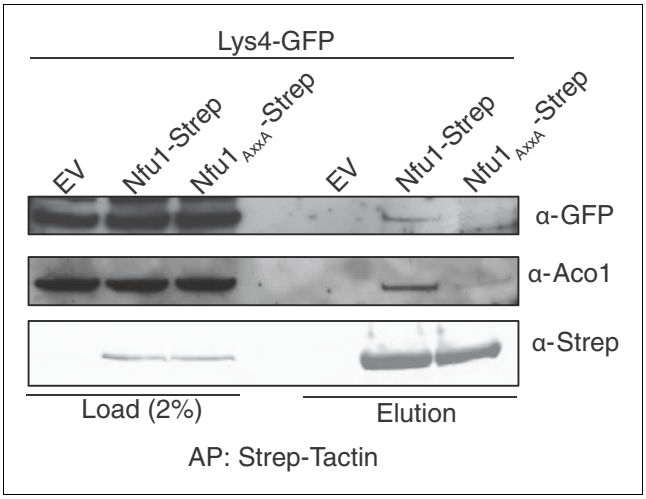

Figure 3—figure supplement 2. Affinity purification using Strep-Tactin to immobilize Strep tagged Nfu1 and the Nfu1 AxxA variant expressed ectopically in the BY4743 background with a single copy of Lys4 chromosomally tagged with GFP.
DOI: 10.7554/eLife.15991.007

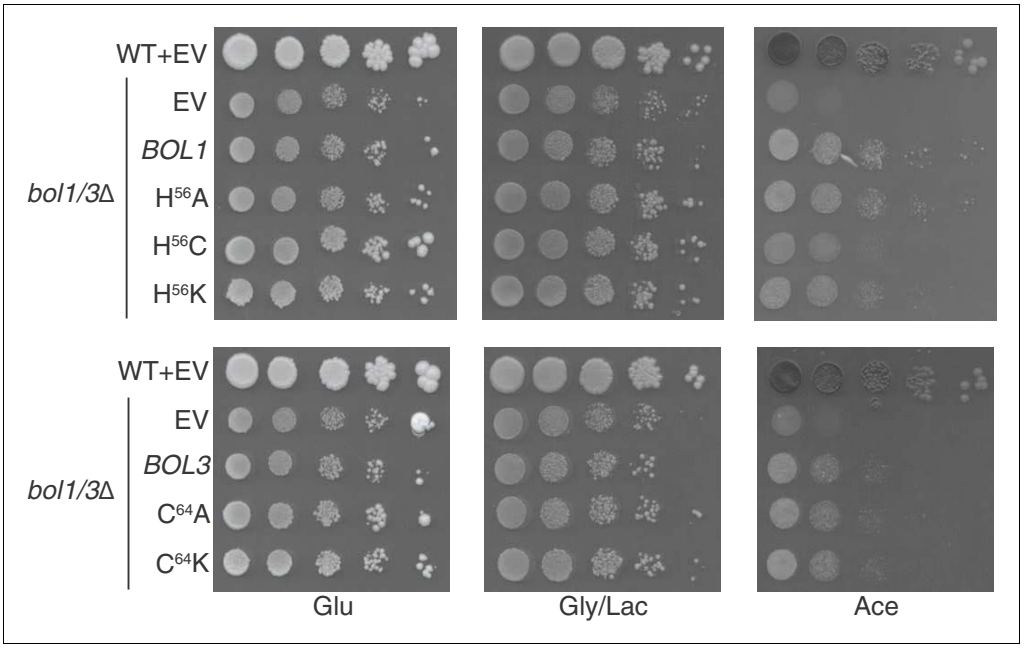

Figure 4—figure supplement 1. Yeast growth tests evaluating the viability of cells expressing mitochondrial Bol1 and Bol3 N-terminal ligands mutated to lysine in the *bol1/3*Δ background.
DOI: 10.7554/eLife.15991.009

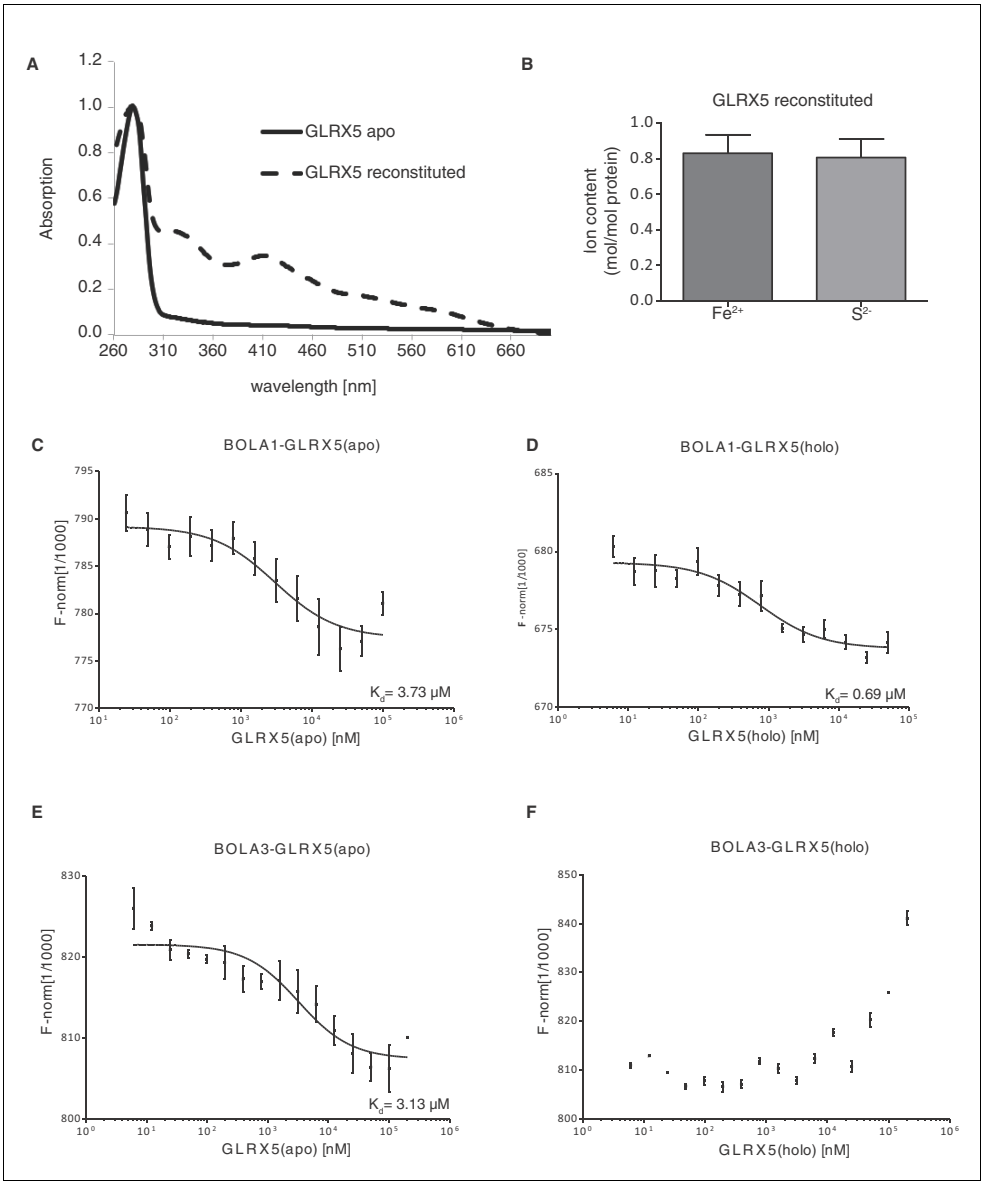

Figure 5—figure supplement 1. Interaction studies of human BOLA proteins with GLRX5. (**A**) UV–visible absorption spectrum of apo-GLRX5 (black line) and chemically reconstituted GLRX5 (dashed line). Reconstituted human GLRX5 (100 µM) showed absorption bands at 320 nm and 425 nm besides

Figure 5—figure supplement 1 continued on next page

Figure 5 continued

Strep-tagged protein divided by the total number of spectral counts for that protein identified from all seven samples. Strep-tagged proteins were expressed from low-copy plasmids in corresponding single deletion mutants. Samples were Strep-affinity purified as in ***Figure 3***. Bol1m is the H93C variant. Bol3m is the $H^{101}C$ variant. Nfu1m is the G/T>H variant. WT is wild-type BY4741 expressing an empty vector. All were fused with a C-terminal Strep-tag. WT is BY4741 wild type harboring a low-copy empty plasmid. (**C**) Human GLRX5 or NFU1 were used in apo- and holo- form and mixed at increasing concentrations with 200 nM fluorescently labelled BOLA1 or BOLA3. Microscale thermophoresis were performed and dissociation constants (K_d) were determined. Error bars indicate the SD (n=3). (**D**) Strep-tag affinity purification of Nfu1-Strep in the presence of ectopically expressed Ilv3-FLAG. (**E**) Affinity purification using Strep-Tactin agarose beads to purify Nfu1-Strep from an *nfu1*Δ background expressing either WT Aco1 or Aco1 AxxA mutant.

DOI: 10.7554/eLife.15991.010

The following source data is available for figure 5:

Source data 1. (Table 1) Spectral counts, unique peptides, and coverage of mitochondrial Fe-S client proteins, bait proteins, and Fe-S assembly machinery identified by MS proteomics.

DOI: 10.7554/eLife.15991.011

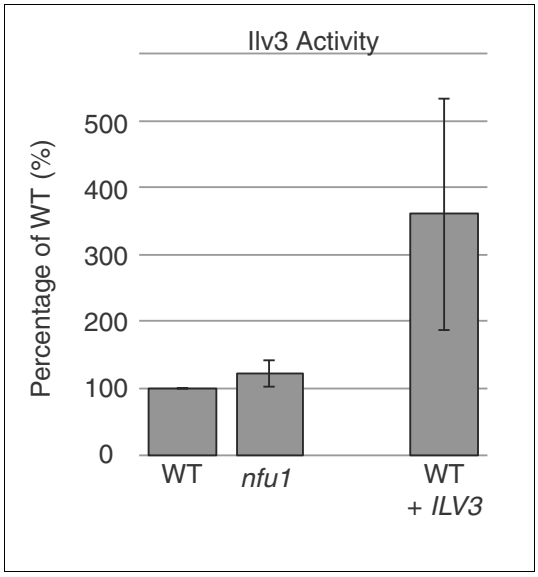

Figure 5—figure supplement 2. Ilv3 activity assay using wild-type and *nfu1*Δ purified mitochondria along with wild-type overexpressing Ilv3 as a control.
DOI: 10.7554/eLife.15991.013

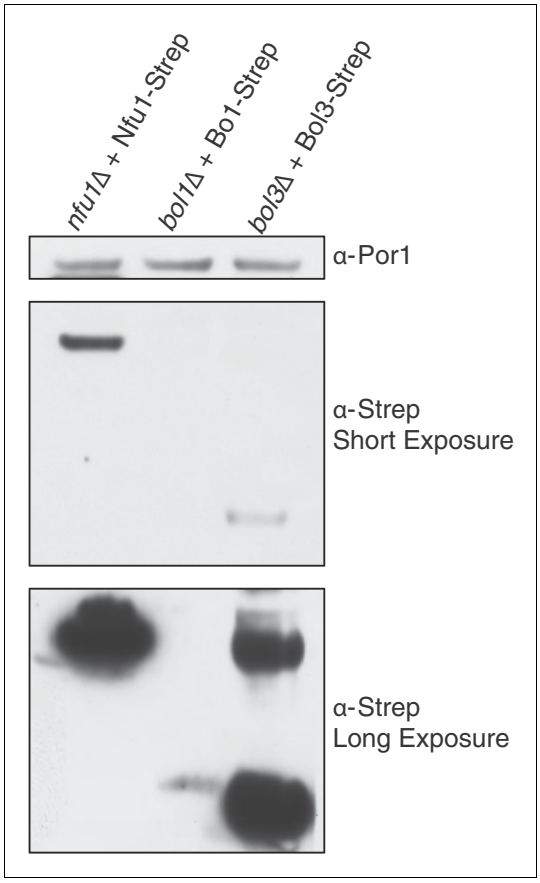

Figure 6—figure supplement 1. SDS-PAGE followed by immunoblotting to evaluate the different steady state levels of Nfu1-Strep, Bol1-Strep, and Bol3-Strep while being expressed under the same heterologous *MET25* promoter and *CYC1* terminator.
DOI: 10.7554/eLife.15991.015

Table 1

	Bait->	Bol1			Bol1 Mutant			Bol3			Bol3 Mutant			Nfu1			Nfu1 Mutant			WT		
	Target	Spectral Counts	Unique peptides	Coverage (%)	Spectral Counts	Unique peptides	Coverage (%)	Spectral Counts	Unique peptides	Coverage (%)	Spectral Counts	Unique peptides	Coverage (%)	Spectral Counts	Unique peptides	Coverage (%)	Spectral Counts	Unique peptides	Coverage (%)	Spectral Counts	Unique peptides	Coverage (%)
Fe-S Clients	**Sdh2**	0	0	0.0%	0	0	0.0%	13	10	27.8%	10	7	27.8%	7	6	17.7%	11	8	25.6%	0	0	0.0%
	Lip5	0	0	0.0%	0	0	0.0%	3	3	9.9%	3	3	12.6%	9	8	26.6%	15	9	31.9%	0	0	0.0%
	Bio2	0	0	0.0%	0	0	0.0%	2	2	7.5%	8	6	16.0%	4	4	13.3%	12	7	20.5%	0	0	0.0%
	Aco1	7	7	10.7%	3	3	5.8%	21	16	28.3%	48	29	35.0%	48	27	32.1%	88	35	29.6%	2	2	4.1%
	Lys4	0	0	0.0%	0	0	0.0%	2	2	4.3%	6	6	13.4%	0	0	0.0%	12	6	10.2%	0	0	0.0%
	Aco2	0	0	0.0%	0	0	0.0%	0	0	0.0%	2	2	3.3%	3	3	4.7%	14	11	19.3%	0	0	0.0%
	Ilv3	5	5	13.7%	0	0	0.0%	19	15	31.8%	55	33	48.2%	10	9	25.8%	33	20	30.4%	0	0	0.0%
	Rip1	0	0	0.0%	0	0	0.0%	4	4	18.4%	0	0	0.0%	0	0	0.0%	0	0	0.0%	0	0	0.0%

	Bait >	Bol1			Bol1 Mutant			Bol3			Bol3 Mutant			Nfu1			Nfu1 Mutant			WT		
	Target	Spectral Counts	Unique peptides	Coverage (%)	Spectral Counts	Unique peptides	Coverage (%)	Spectral Counts	Unique peptides	Coverage (%)	Spectral Counts	Unique peptides	Coverage (%)	Spectral Counts	Unique peptides	Coverage (%)	Spectral Counts	Unique peptides	Coverage (%)	Spectral Counts	Unique peptides	Coverage (%)
Bait	**Bol1**	30	13	82.7%	34	10	53.6%	0	0	0.0%	0	0	0.0%	0	0	0.0%	0	0	0.0%	0	0	0.0%
	Bol3	0	0	0.0%	0	0	0.0%	53	17	58.5%	36	10	44.1%	0	0	0.0%	0	0	0.0%	0	0	0.0%
	Nfu1	0	0	0.0%	0	0	0.0%	0	0	0.0%	4	4	14.5%	213	22	60.5%	152	20	50.0%	0	0	0.0%

	Bait >	Bol1			Bol1 Mutant			Bol3			Bol3 Mutant			Nfu1			Nfu1 Mutant			WT		
	Target	Spectral Counts	Unique peptides	Coverage (%)	Spectral Counts	Unique peptides	Coverage (%)	Spectral Counts	Unique peptides	Coverage (%)	Spectral Counts	Unique peptides	Coverage (%)	Spectral Counts	Unique peptides	Coverage (%)	Spectral Counts	Unique peptides	Coverage (%)	Spectral Counts	Unique peptides	Coverage (%)
Fe-S Machinery	**Grx5**	16	10	52.0%	2	2	18.0%	7	4	30.7%	6	5	30.7%	3	3	28.0%	0	0	0.0%	0	0	0.0%
	Isa2	0	0	0.0%	0	0	0.0%	0	0	0.0%	3	2	20.0%	0	0	0.0%	3	3	26.5%	0	0	0.0%
	Nfs1	0	0	0.0%	2	2	5.0%	2	2	5.8%	4	4	14.1%	0	0	0.0%	3	3	10.5%	0	0	0.0%

Table 2

	Bait >	Bol1			Bol1 Mutant			Bol3			Bol3 Mutant			Nfu1			Nfu1 Mutant			WT		
Target	Replicate	Spectral Counts	Unique peptides	Coverage (%)	Spectral Counts	Unique peptides	Coverage (%)	Spectral Counts	Unique peptides	Coverage (%)	Spectral Counts	Unique peptides	Coverage (%)	Spectral Counts	Unique peptides	Coverage (%)	Spectral Counts	Unique peptides	Coverage (%)	Spectral Counts	Unique peptides	Coverage (%)
Grx5	1	16	10	52.0%	2	2	18.0%	7	4	30.7%	6	5	30.7%	3	3	28.0%	0	0	0.0%	0	0	0.0%
	2	28	10	59.3%	31	9	52.0%	1	1	10.7%	7	6	42.7%	0	0	0.0%	0	0	0.0%	0	0	0.0%
Aco1	1	7	7	10.7%	3	3	5.8%	21	16	28.3%	48	29	35.0%	48	27	32.1%	88	35	29.6%	2	2	4.1%
	2	2	2	3.5%	13	6	11.1%	0	0	0.0%	15	8	16.4%	30	8	9.0%	31	11	16.8%	0	0	0.0%
Lip5	1	0	0	0.0%	0	0	0.0%	3	3	9.9%	3	3	12.6%	9	8	26.6%	15	9	31.9%	0	0	0.0%
	2	0	0	0.0%	0	0	0.0%	0	0	0.0%	0	0	0.0%	0	0	0.0%	3	2	12.6%	0	0	0.0%
Prx1	1	18	10	38.3%	18	10	32.6%	10	6	20.7%	9	6	20.7%	10	7	28.0%	7	5	19.9%	0	0	0.0%
	2	16	7	36.8%	23	9	31.8%	0	0	0.0%	2	2	11.1%	3	1	6.1%	0	0	0.0%	0	0	0.0%

CHAPTER 4

IDENTIFICATION OF A NFU1 RECOGNITION MOTIF FOR [4Fe-4S] CLIENT PROTEINS

4.1 Introduction

Biology has evolved intricate pathways to synthesize the redox activate cofactors, iron-sulfur (Fe/S) clusters. Following the synthesis, dedicated systems have also arisen to safely transfer preformed Fe/S clusters from the assembly systems to client proteins, requiring these cofactors for their function within the cell. These client proteins are found throughout the cell, in the nucleus identifying DNA damage, in the cytosol assembling ribosomes and participating in the biosynthesis of various nucleotides, and in the mitochondria functioning in the TCA cycle, OXPHOS respiratory complexes, and various cofactor biogenesis pathways. Within the mitochondria, clients use three unique species of iron-sulfur cluster, [2Fe-2S], [3Fe-4S], and [4Fe-4S] clusters.

The biogenesis of all cellular Fe/S clusters begins with the early steps of the mitochondrial iron-sulfur cluster biogenesis pathway (ISC), which generates a [2Fe-2S] cluster on the scaffold protein Isu1 (Gerber et al., 2003; Gerber et al., 2004; Muhlenhoff et al., 2003). This scaffold protein receives sulfane from the cysteine desulfurase protein Nfs1, reducing power from the [2Fe-2S] client protein ferredoxin to form sulfide anions, and ferrous iron from an undefined source (Kispal et al., 1999; Lange et al., 2000; Pandey et al., 2012; Webert et al., 2014). The initial preformed cluster is removed from the scaffold and transferred to the glutaredoxin protein, Grx5, by the Hsp70 chaperone, Ssq1, and the DnaJ protein, Jac1 (Kim et al., 2012b; Majewska et al., 2013; Uzarska et al., 2013). From Grx5, [2Fe-2S] clusters can be transferred to client proteins or to the [4Fe-4S] cluster biosynthetic ISA complex, on which two [2Fe-2S] clusters are condensed into a single [4Fe-4S] cluster (Banci et al., 2014; Brancaccio et al., 2014). Nfu1 subsequently removes the [4Fe-4S] cluster from the ISA complex and transfers it to client proteins with

the help of the BolA family member, Bol3 (Melber et al., 2016). Additionally, the Grx5 cluster plays a role in the export of a substrate required for the formation of Fe/S clusters in the cytosol (Rodriguez-Manzaneque et al., 2002).

Client proteins coordinate these various clusters primarily with four (sometimes fewer) cysteinyl or histidyl ligands. These coordinating environments are so similar that it has been observed that some iron centers bind the wrong cluster (Collins and Zhou, 2011). If the ability for a client to bind a cluster does not restrict the client from having the incorrect Fe/S cluster from associating, how do the various Fe/S cluster transfer systems identify the proper client protein? We recently reported that Nfu1 acts as the transfer protein for mitochondrial [4Fe-4S] clusters by transferring the cluster from the ISA complex to client proteins (Melber et al., 2016). In that study, we demonstrated that removing the ability of the client protein Aco1 to bind a [4Fe-4S] cluster had no bearing on the ability of Nfu1 to recognize the client and associate with the client. Here we sought to establish a common feature that Nfu1 utilizes to recognize all of the mitochondrial [4Fe-4S] cluster client proteins.

4.2 Results

4.2.1 Identification of a [4Fe-4S] cluster recognition motif

We previously reported that mutation of the Fe/S cluster binding cysteine ligands on yeast Aco1 did not affect the interaction with the late stage [4Fe-4S] cluster transfer protein Nfu1 (Melber et al., 2016). Given this, we postulated that a common interaction motif existed that was important for the Fe/S cluster transfer protein Nfu1 to identify [4Fe-4S] cluster clients. To address this prediction, we sought to identify a primary

sequence motif by assuming a motif would be conserved between [4Fe-4S] cluster client proteins and between species. Based on this assumption, we assembled a list of the known [4Fe-4S] cluster mitochondrial proteins from yeast (*S.c.*), fruit fly (*D.m.*), and human (*H.s.*), which have been identified in yeast studies as dependent on Nfu1 for cluster transfer. In the absence of higher a eukaryotic homologue, the *S. pombe* (*S.p.*) homologue was used to increase the number of sequences compared. This list included Sdh2, the Fe/S containing subunit of the respiratory complex II, succinate dehydrogenase, lipoate synthase, and mitochondrial aconitase from *S.c., D.m.,* and *H.s.*. Additionally, biotin synthase, Aco2 and Lys4, both hydratases in lysine biosynthesis from *S.c.* and *S.p.* were used. Since our initial studies demonstrating the interaction of Nfu1 with [4Fe-4S] cluster client proteins were performed in *S. cerevisiae* that lacks respiratory Complex I, the CI subunits containing [4Fe-4S] clusters were not included in our motif search. Using the web based motif search (http://motifsearch.com), a candidate 12-residue motif was identified, TIMNMGRECGAG (Dinh et al., 2012). It is worth noting that when mitochondrial [2Fe-2S] cluster client proteins are included in the list of [4Fe-4S] cluster client proteins in the motif search, this motif was still identified in [4Fe-4S] clients, but not in any [2Fe-2S] client proteins. Within the candidate 12-residue motif, a set of five residues were most strongly conserved TIMNM (Figure 4.1A). Moving forward, we centered our analysis on the 5-mer starting with an invariant threonine, followed by a isoluecine or valine, followed by three residues that generally are methionine or cysteine, asparagine, and methionine or cysteine.

Further analysis of this potential motif utilized the 12 flanking residues upstream and downstream of the 5-mer, resulting in a 29-residue segment, which we analyzed as

the potential recognition motif. We compared the sequence similarity of the 29-residue segment between yeast and human, and fly and human clients, to the sequence similarity of the entire proteins without the inclusion of mitochondrial targeting sequences (MTS) (Figure 4.1B). This suggests that the motif was a selectively conserved region of each client protein through evolution.

No consistent primary sequence spacing appears to exist between Fe/S cluster ligands and the candidate motif. In the case of Sdh2, the motif is juxtaposed to the [4Fe-4S] cluster ligands with the closest ligand just four residues downstream of the motif (Figure 4.1C and 4.1D). In contrast, the Aco1 motif is over 100 residues upstream of the first ligand. Despite the distance variation between the motif and Fe/S ligands in the primary sequence of aconitase, the motif lies as close as 5.4 angstroms away from the cluster in the cluster bound tertiary structure of aconitase (Figure 4.1E). These observations led us to test the role of the TIMNM motif for Nfu1-mediated transfer of [4Fe-4S] clusters to mitochondrial client proteins.

4.2.2 Heterologous protein can bind Nfu1 with the addition of the TIMNM motif

To test the sufficiency of this potential motif to direct Nfu1 to the correct [4Fe-4S] clients, we appended segments of the Aco1 candidate motif to the C-terminal end of a soluble of Rip1 (the transmembrane domain, residues 33-85, is deleted), Rip1 a [2Fe-2S] cluster client protein that we have demonstrated previously does not interact with Nfu1 (Melber et al., 2016). The chimeras were generated with two glycine linkers on either side of the motif with a single Myc tag appended to the C-terminus downstream of the second glycine linker (Figure 4.2A). A series of chimeras were generated by cloning 13

residue segments from Aco1 surrounding the central five amino acid motif. An additional chimera using C-terminal 13-residues of Aco1 was used as a negative control along with a construct containing only sRip1-Myc (No Motif, NM) and a construct with just TICNM (5-mer) residues.

Expression of the chimeras resulted in mitochondrial localization of each protein, although steady-state stability of the chimeras varied significantly (Figure 4.2B). This may be expected considering the long unstructured segments appended to the C-terminus of the sRip1. The chimeras were expressed in *nfu1*Δ cells harboring Nfu1-Strep enabling Strep-tactin affinity purification of Nfu1. Despite the various stabilities, two of the eight constructs co-purified with Nfu1-Strep during purification (Figure 4.2B). The first construct purified was the 12T chimera that contained only the invariant threonine of the motif along with the 12-residues upstream. The other chimera purified by Nfu1-Strep was the M8 chimera that included the entire 5-residue motif along with the 8-residues downstream. This suggests the importance of the TIMNM motif, but also reflects the importance of the residues flanking the central 5-mer both up and downstream.

4.2.3 Aconitase function diminishes with mutations to the TIMNM motif

Since appending the Aco1 candidate motif to a heterologous protein was sufficient to produce an interaction with Nfu1, we sought to investigate if mutations to the motif would compromise Aco1 function and interaction with Nfu1. The motif in Aco1 is conserved through evolution from yeast to human and in the related mitochondrial [4Fe-4S] hydrotases Aco2 and Lys that function in lysine biosynthesis (Fazius et al., 2012) (Figure 4.3A). The motifs for each of these three clients reside

internally in the tertiary folds of the hydrolases, so alanine substitutions were engineered in attempt to minimize any structural changes in the proteins. A series of mutations generated to an ectopically expressed Aco1-Flag, these include: TI>AA, N>A, TIN>AAA, and CNM>ANA (Figure 4.3B). Aconitase is an excellent molecule with which to preform these experiments, since the protein is stable without its [4Fe-4S] cluster (Robbins and Stout, 1989).

Cells devoid of their endogenous Aco1 (*aco1*Δ) were transformed with either wild-type or the motif variants, and mitochondria were purified from these cells. Quantitation of the aconitase activity in mitochondria isolated from these cultures revealed that each Aco1 variant exhibited an attenuation of enzymatic activity. The TI>AA, N>A, and TIN>AAA variants showed near complete loss of activity, and the CNM>ANA variant retained limited activity relative to the wild-type enzyme (Figure 4.3C). This suggests the necessity of the TICNM motif of aconitase for function, albeit this does not mean that these amino acids are necessarily important for Nfu1 mediated cluster transfer.

To examine if the defect in aconitase activity was due to a loss of interaction with Nfu1, the Aco1-Flag variants were expressed in *nfu1*Δ cells harboring the Nfu1-Strep chimera. Mitochondria purified from these cells were used for Strep-Tactin affinity purification of Nfu1-Strep. As expected, the wild-type Aco1-Flag co-purified with Nfu1-Strep, and all of the Aco1 variants co-purified to a lesser extent than the wild-type construct (Figure 4.3D). These data, along with the experiments in Figure 2B, show a necessity and sufficiency for the TICNM motif of aconitase to facilitate interaction with Nfu1 for proper cluster transfer.

4.2.4 Sdh2 stability is reduced by mutations in the TIMNM motif

We also tested the necessity of the TIMNM motif for the function of Sdh2. Sdh2 is the Fe/S containing subunit of respiratory complex II, succinate dehydrogenase (SDH). It contains three unique clusters, a [3Fe-4Fe], a [4Fe-4S], and a [2Fe-2S] cluster, that are all required to transfer the electron released from the catalytic subunit, Sdh1, to the ubiquinone binding site at the matrix side surface of the inner mitochondrial membrane. To test the importance of the TIMNC motif for Sdh2 function, three different mutants, TI>AA, MNC>ANA, and N>A, were generated to an exogenous Sdh2 protein with six repeated histidine residues and two c-myc tags appended to the C-terminus (Figure 4.4A).

SDH function is required for yeast to grow on nonfermentable media, so we first tested the ability of these mutants to grow on media with glycerol/lactate (G/L) or acetate as the carbon source. The MNC>ANA mutant was unable to grow on media with either nonfermentable carbon source. The TI>AA mutant struggled to survive on acetate containing media, but grew similar to cells containing a wild-type copy of Sdh2 on G/L. Interestingly, when the superoxide generator, paraquat is added to the G/L containing media, TI>AA fails to thrive (Figure 4.4B). The ability of yeast to grow on G/L, but not with the addition of paraquat or with acetate as the carbon source, is very similar to the growth phenotype of yeast lacking Nfu1 (Melber et al., 2016). This suggests the TI>AA mutant is not interacting with Nfu1, and Sdh2 maturation is being disrupted. Unfortunately, the MNC>ANA mutant's stability is likely compromised beyond just the loss of interaction with Nfu1 and is not informative for these studies.

It is known that the structural stability of Sdh2 is compromised when any one of the three clusters in not successfully inserted into the protein (Na et al., 2014). This can

easily be observed by SDS-PAGE western blot analysis. Each of the three mutants displayed reduced protein levels compared to the wild-type protein (Figure 4.4C). Notably, the MNC>ANA was completely destabilized, consistent with the suggestion from the growth assay that the mutant is more severely compromised than just losing interaction with Nfu1. In order to more rigorously test the function of SDH, activity was measured using an activity assay that probes the ability of mitochondria to reduce ubiquinone to ubiquinol, which requires successful electron transfer through the Fe/S cofactors of Sdh2. Not surprisingly, the TI>AA and MNC>ANA mutants saw significant reductions in SDH activity. Interestingly, the N>A mutant's activity was about 30%of wild-type (Figure 4.4D). It is known that yeast does not exhibit a growth defect until the activity of SDH is comprised beyond roughly 25% of wild-type.

Lastly, we evaluated the interaction of the TI>AA and N>A mutants with Nfu1. The MNC>ANA mutant was not evaluated since there was no detectable steady state protein. As before with the Aco1 motif mutants, we transformed *nfu1*Δ + Nfu1-Strep cells with the Sdh2 mutants and purified mitochondria. The purified mitochondria were lysed and incubated with Strep-Tactin beads to purify Nfu1-Strep. The elutes were analyzed with SDS-PAGE western blots to evaluate the amount of mutant Sdh2 that co-purified by probing with Sdh2 antibody, since a 6xHis/2xMyc provides a significant size shift to distinguish the exogenous mutant Sdh2 from the wild-type endogenous Sdh2. Both mutants saw a significant loss of co-purification with Nfu1-Strep (Figure 4.4E). These data show the importance of the Sdh2 motif TIMNC for the function through the interaction with Nfu1 during the maturation process of the SDH complex.

4.3 Discussion

The role of a recognition motif for [4Fe-4S] cluster transfer is likely important for Nfu1 to properly identify clients of only [4Fe-4S] clusters and to prevent transfer to inappropriate client proteins. However, major questions remain around the Nfu1 client interaction. The central five amino acids, TIMNM, were initially found computationally; however, during the chimera experiments appending the Aco1 motif to sRip1, we observed that amino acid sequences on the fringe of this motif had a strong propensity to bind Nfu1. Given that the complete primary sequence of the motif is still unresolved, it is not surprising that we cannot predict how the motif is structured. We do get a hint from the holo-protein structures, since all of the motifs have a helical fold to them (Figure 4.1D and 4.1E). Given the helical propensity, we projected the sequences on a helical wheel, which revealed a nonpolar face on about a third of the helix, flanked on each side of the face by one or two polar residues, normally, a threonine or serine. This might be misleading if the entire motif is not folded as a helix in the holo-protein structures. Structural studies will be needed to determine how Nfu1 binds the motif. These studies should define the complete length of the motif and identify the most important residues of the motif.

Additional questions exist about the interplay of the client motif with holo- and an apo-Nfu1 would also be answered with structural studies. It will be interesting to discern whether the motif can change the conformer of the stable Nfu1 cluster loaded dimer to produce release and transfer. Furthermore, the highly conserved asparagine is particularly interesting, since asparagine can act as a ligand to a cluster and thus may disrupt the existing ligand environment of the Nfu1 dimer to induce release (Berkovitch et al., 2004).

All of these questions about how the motif and Nfu1 interacts are currently being evaluated by collaborative NMR studies.

Other Fe/S cluster recognition motifs have been suggested for the [2Fe-2S] cluster clients in the mitochondria, with the presence of LYR motifs on assembly factors Sdh2 and Rip1 (Maio and Rouault, 2016). However, this motif does not exist in other yeast mitochondrial [2Fe-2S] cluster client proteins, like ferredoxin and biotin synthase, Bio2. We performed the same motif search approach on mitochondrial [2Fe-2S] client proteins as we did to identify the TIMNM motif of [4Fe-4S] client proteins, but did not identify any potential motifs that were inclusive of all [2Fe-2S] clients.

We have not explored the cytosolic Fe/S centers for potential delivery motifs. The cytosolic Fe/S assembly (CIA) pathway ends with the CIA targeting complex of MMS19, Cia1, and Cia2 performing transfer to client proteins (Gari et al., 2012; Stehling et al., 2012; van Wietmarschen et al., 2012). Clients interact with this system either directly, or in the case of the ribosome assembly factor Ril1, interaction is mediated through the adaptor proteins Lto1 and Yae1 that coordinate this interaction by a c-terminal tryptophan (Paul et al., 2015). Some groups have taken an opposite approach to understanding client interaction with transfer systems in the CIA by defining that importance of the c-terminus of MMS19 for most client protein binding (Odermatt and Gari, 2017). Similar approaches maybe necessary to define how Nfu1 recognizes the TIMNM motif of clients.

4.4 Materials and methods

W303 strains were used for all of the experiments. Deletion strains of *NFU1* and *SDH2* and the corresponding tagged expression constructs were all previously described (Melber et al., 2016; Na et al., 2014). John D Philips and Betty Liebold generously provided the deletion strain of *ACO1*, and Jerry Kaplan provided the Aco1-Flag construct. Chimeric sRip constructs were made using homologous recombination in yeast (Ma et al., 1987). Mutations were made using Phusion DNA Polymerase from Thermo Fischer Scientific.

Strep-Tactin affinity purifications and enzymatic activity assays of succinate dehydrogenase (SDH) and aconitase were performed using purified mitochondrial as described previously (Melber et al., 2016; Na et al., 2014). Mitochondrial were purified from yeast using the differential centrifugation method of Glick and Pon (Glick and Pon, 1995). Proteins were analyzed by SDS-PAGE and immunoblotting using standard procedures. The primary antibodies to yeast Sdh1 and Sdh2 were previously described (Kim et al., 2012a). The commercial primary antibodies used were Anti-Por1, Anti-Strep, Anti Myc, and Anti-Flag from Invitrogen, Qiagen, Santa Cruz Biotechnology, and Roche, respectively.

4.5 References

Banci, L., Brancaccio, D., Ciofi-Baffoni, S., Del Conte, R., Gadepalli, R., Mikolajczyk, M., Neri, S., Piccioli, M., and Winkelmann, J. (2014). [2Fe-2S] cluster transfer in iron–sulfur protein biogenesis. Proceedings of the National Academy of Sciences *111*, 6203-6208.

Berkovitch, F., Nicolet, Y., Wan, J.T., Jarrett, J.T., and Drennan, C.L. (2004). Crystal structure of biotin synthase, an S-adenosylmethionine-dependent radical enzyme. Science *303*, 76-79.

Brancaccio, D., Gallo, A., Mikolajczyk, M., Zovo, K., Palumaa, P., Novellino, E., Piccioli, M., Ciofi-Baffoni, S., and Banci, L. (2014). Formation of [4Fe-4S] clusters in the mitochondrial iron-sulfur cluster assembly machinery. J Am Chem Soc *136*, 16240-16250.

Collins, D.J., and Zhou, H.-C. (2011). Iron–Sulfur Models of Protein Active Sites. In Encyclopedia of Inorganic and Bioinorganic Chemistry (John Wiley & Sons, Ltd).

Dinh, H., Rajasekaran, S., and Davila, J. (2012). qPMS7: A Fast Algorithm for Finding (ℓ, d)-Motifs in DNA and Protein Sequences. PLOS ONE *7*, e41425.

Fazius, F., Shelest, E., Gebhardt, P., and Brock, M. (2012). The fungal α-aminoadipate pathway for lysine biosynthesis requires two enzymes of the aconitase family for the isomerization of homocitrate to homoisocitrate. Molecular Microbiology *86*, 1508-1530.

Gari, K., León Ortiz, A.M., Borel, V., Flynn, H., Skehel, J.M., and Boulton, S.J. (2012). MMS19 links cytoplasmic iron-sulfur cluster assembly to DNA metabolism. Science (New York, NY) *337*, 243-245.

Gerber, J., Muhlenhoff, U., and Lill, R. (2003). An interaction between frataxin and Isu1/Nfs1 that is crucial for Fe/S cluster synthesis on Isu1. EMBO Rep *4*, 906-911.

Gerber, J., Neumann, K., Prohl, C., Mühlenhoff, U., and Lill, R. (2004). The yeast scaffold proteins Isu1p and Isu2p are required inside mitochondria for maturation of cytosolic Fe/S proteins. Mol Cell Biol *24*, 4848-4857.

Glick, B.S., and Pon, L.A. (1995). Isolation of highly purified mitochondria from Saccharomyces cerevisiae. Methods Enzymol *260*, 213-223.

Kim, H.J., Jeong, M.Y., Na, U., and Winge, D.R. (2012a). Flavinylation and assembly of succinate dehydrogenase are dependent on the C-terminal tail of the flavoprotein subunit. J Biol Chem *287*, 40670-40679.

Kim, J.H., Tonelli, M., Frederick, R.O., Chow, D.C., and Markley, J.L. (2012b). Specialized Hsp70 chaperone (HscA) binds preferentially to the disordered form, whereas J-protein (HscB) binds preferentially to the structured form of the iron-sulfur cluster scaffold protein (IscU). J Biol Chem *287*, 31406-31413.

Kispal, G., Csere, P., Prohl, C., and Lill, R. (1999). The mitochondrial proteins Atm1p and Nfs1p are essential for biogenesis of cytosolic Fe/S proteins. EMBO J *18*, 3981-3989.

Lange, H., Kaut, A., Kispal, G., and Lill, R. (2000). A mitochondrial ferredoxin is essential for biogenesis of cellular iron-sulfur proteins. Proc Natl Acad Sci USA *97*, 1050-1055.

Ma, H., Kunes, S., Schatz, P.J., and Botstein, D. (1987). Plasmid construction by homologous recombination in yeast. Gene *58*, 201-216.

Maio, N., and Rouault, T.A. (2016). Mammalian Fe-S proteins: definition of a consensus motif recognized by the co-chaperone HSC20. Metallomics *8*, 1032-1046.

Majewska, J., Ciesielski, S.J., Schilke, B., Kominek, J., Blenska, A., Delewski, W., Song, J.Y., Marszalek, J., Craig, E.A., and Dutkiewicz, R. (2013). Binding of the chaperone Jac1 protein and cysteine desulfurase Nfs1 to the iron-sulfur cluster scaffold Isu protein is mutually exclusive. J Biol Chem *288*, 29134-29142.

Melber, A., Na, U., Vashisht, A., Weiler, B.D., Lill, R., Wohlschlegel, J.A., and Winge, D.R. (2016). Role of Nfu1 and Bol3 in iron-sulfur cluster transfer to mitochondrial clients. eLife *5*, e15991.

Muhlenhoff, U., Gerber, J., Richhardt, N., and Lill, R. (2003). Components involved in assembly and dislocation of iron-sulfur clusters on the scaffold protein Isu1p. EMBO J *22*, 4815-4825.

Na, U., Yu, W., Cox, J., Bricker, D.K., Brockmann, K., Rutter, J., Thummel, C.S., and Winge, D.R. (2014). The LYR factors SDHAF1 and SDHAF3 mediate maturation of the iron-sulfur subunit of succinate dehydrogenase. Cell Metab *20*, 253-266.

Odermatt, D.C., and Gari, K. (2017). The CIA Targeting Complex Is Highly Regulated and Provides Two Distinct Binding Sites for Client Iron-Sulfur Proteins. Cell Rep *18*, 1434-1443.

Pandey, A., Yoon, H., Lyver, E.R., Dancis, A., and Pain, D. (2012). Identification of a Nfs1p-bound persulfide intermediate in Fe-S cluster synthesis by intact mitochondria. Mitochondrion *12*, 539-549.

Paul, V.D., Muhlenhoff, U., Stumpfig, M., Seebacher, J., Kugler, K.G., Renicke, C., Taxis, C., Gavin, A.C., Pierik, A.J., and Lill, R. (2015). The deca-GX3 proteins Yae1-Lto1 function as adaptors recruiting the ABC protein Rli1 for iron-sulfur cluster insertion. Elife *4*, e08231.

Robbins, A.H., and Stout, C.D. (1989). Structure of activated aconitase: formation of the [4Fe-4S] cluster in the crystal. Proc Natl Acad Sci U S A *86*, 3639-3643.

Rodriguez-Manzaneque, M.T., Tamarit, J., Belli, G., Ros, J., and Herrero, E. (2002). Grx5 is a mitochondrial glutaredoxin required for the activity of iron/sulfur enzymes. Mol Biol Cell *13*, 1109-1121.

Stehling, O., Vashisht, A.A., Mascarenhas, J., Jonsson, Z.O., Sharma, T., Netz, D.J.A., Pierik, A.J., Wohlschlegel, J.A., and Lill, R. (2012). MMS19 assembles iron-sulfur proteins required for DNA metabolism and genomic integrity. Science (New York, NY)

337, 195-199.

Uzarska, M.A., Dutkiewicz, R., Freibert, S.-A., Lill, R., and Mühlenhoff, U. (2013). The mitochondrial Hsp70 chaperone Ssq1 facilitates Fe/S cluster transfer from Isu1 to Grx5 by complex formation. Mol Biol Cell.

van Wietmarschen, N., Moradian, A., Morin, G.B., Lansdorp, P.M., and Uringa, E.-J. (2012). The mammalian proteins MMS19, MIP18, and ANT2 are involved in cytoplasmic iron-sulfur cluster protein assembly. J Biol Chem *287*, 43351-43358.

Webert, H., Freibert, S.A., Gallo, A., Heidenreich, T., Linne, U., Amlacher, S., Hurt, E., Muhlenhoff, U., Banci, L., and Lill, R. (2014). Functional reconstitution of mitochondrial Fe/S cluster synthesis on Isu1 reveals the involvement of ferredoxin. Nat Commun *5*, 5013.

Figure 4.1 Computational identification of the [4Fe-4S] client recognition motif. A) LOGO plot of the TIMNM 5-mer flanked on each side by 12-residues. This was plotted using the motifs of Sdh2, aconitase, and lipoate synthase from *S.c., D.m.* and *H.s.*, Aco2 and Lys4 from *S.c.* and *S.p.* B) Protein similarities without the MTS or the 29 amino acid region around the TIMNM motif for Aconitase, Sdh2/B, and LIAS. C) Protein alignment from the species used in A, in green, are the common residues to the TIMNM motif and in red are [4Fe-4S] cluster ligands. D) Structure of holo-SDH complex zoomed in on the three Fe/S clusters (yellow is sulfur/orange is iron), the motif is in red with Sdh2 in blue and Sdh1 in green. PDB ID: 1Z0Y, Porcine Heart. E) Structure of holo-aconitase zoomed in on the [4Fe-4S] cluster and the motif in red. PDB ID: 1ACO, Bos Taurus.

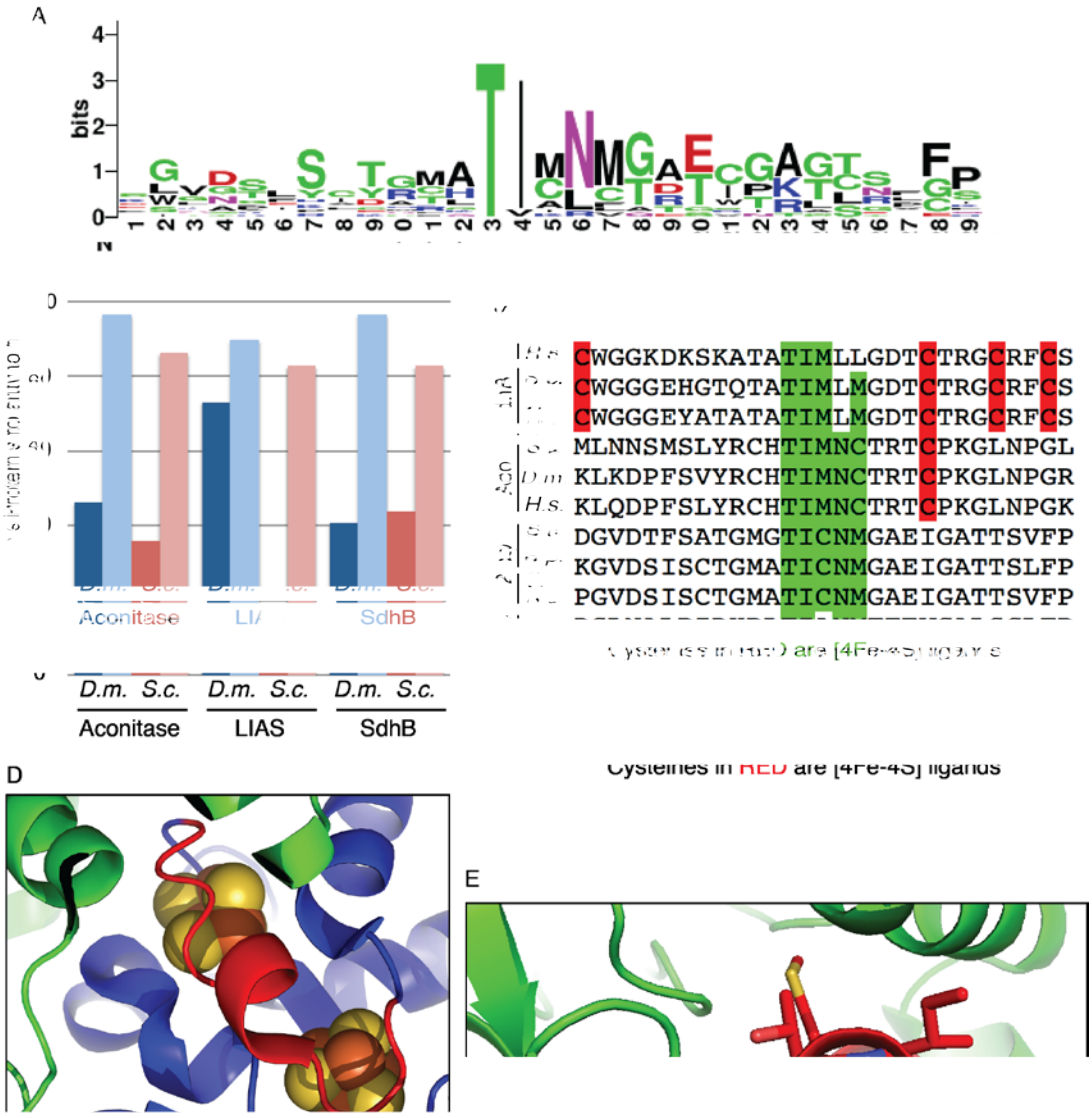
A
bits
D.m. S.c. D.m. S.c. D.m. S.c.
Aconitase
LIAS
SdhB
CWGGKDKSKATATIMLLGDTCTRGCRFCS
CWGGGEHGTQTATIMLMGDTCTRGCRFCS
CWGGGEYATATATIMLMGDTCTRGCRFCS
MLNNSMSLYRCHTIMNCTRTCPKGLNPGL
KLKDPFSVYRCHTIMNCTRTCPKGLNPGR
KLQDPFSLYRCHTIMNCTRTCPKGLNPGK
DGVDTFSATGMGTICNMGAEIGATTSVFP
KGVDSISCTGMATICNMGAEIGATTSLFP
PGVDSISCTGMATICNMGAEIGATTSVFP
D
E

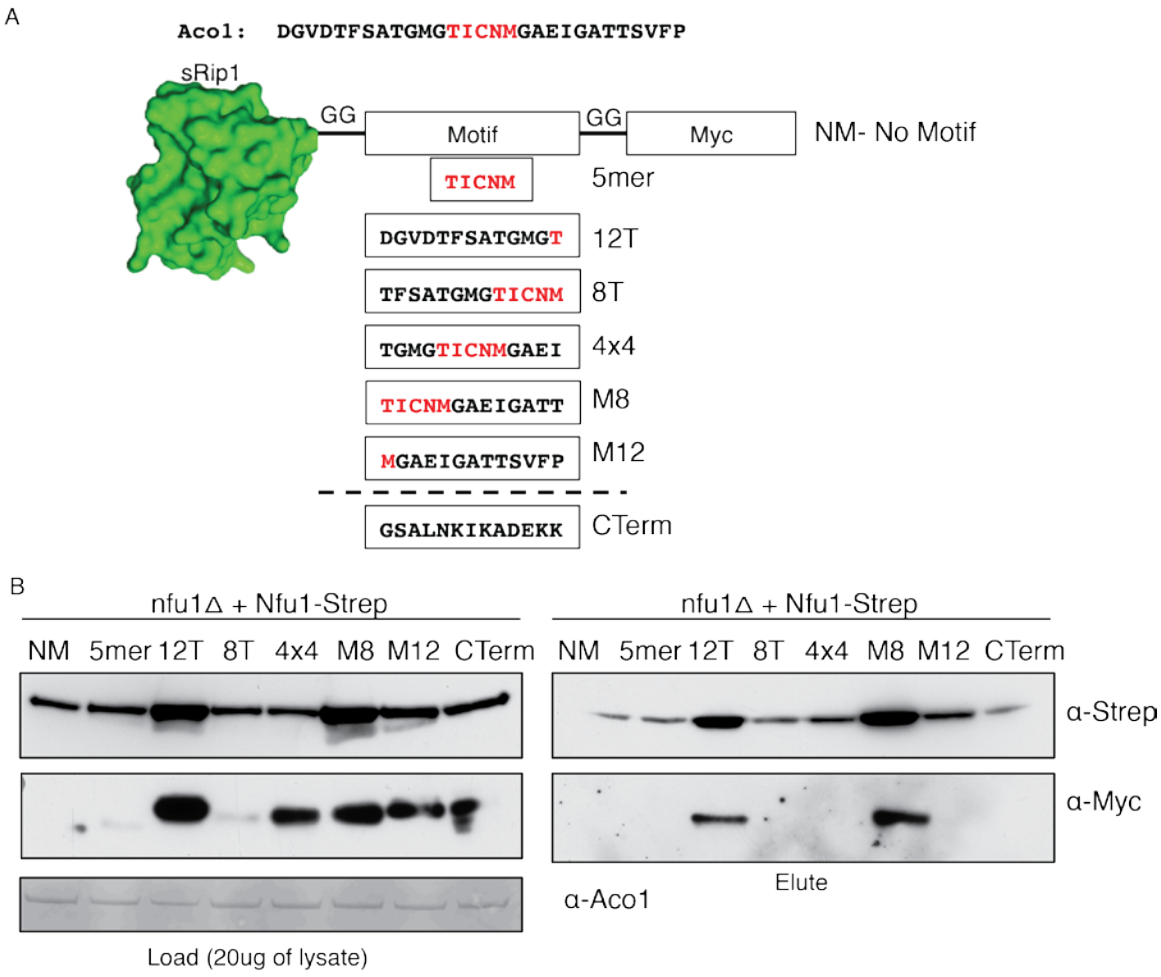

Figure 4.2 TIMNM motif creates interaction of Nfu1 with heterologous protein.
A) Construct design using the sRip1 protein (Rip1, Reiske Fe/S protein from complex III with the transmembrane domain removed) with 13-residue segments around the TICNM motif of yeast aconitase, Aco1, attached to the c-terminus along with a c-Myc tag. B) Western blot analysis of a Strep-Tactin affinity purification of the sRip1-TICMM constructs co-expressed with Nfu1-Strep in *nfu1*Δ cells.

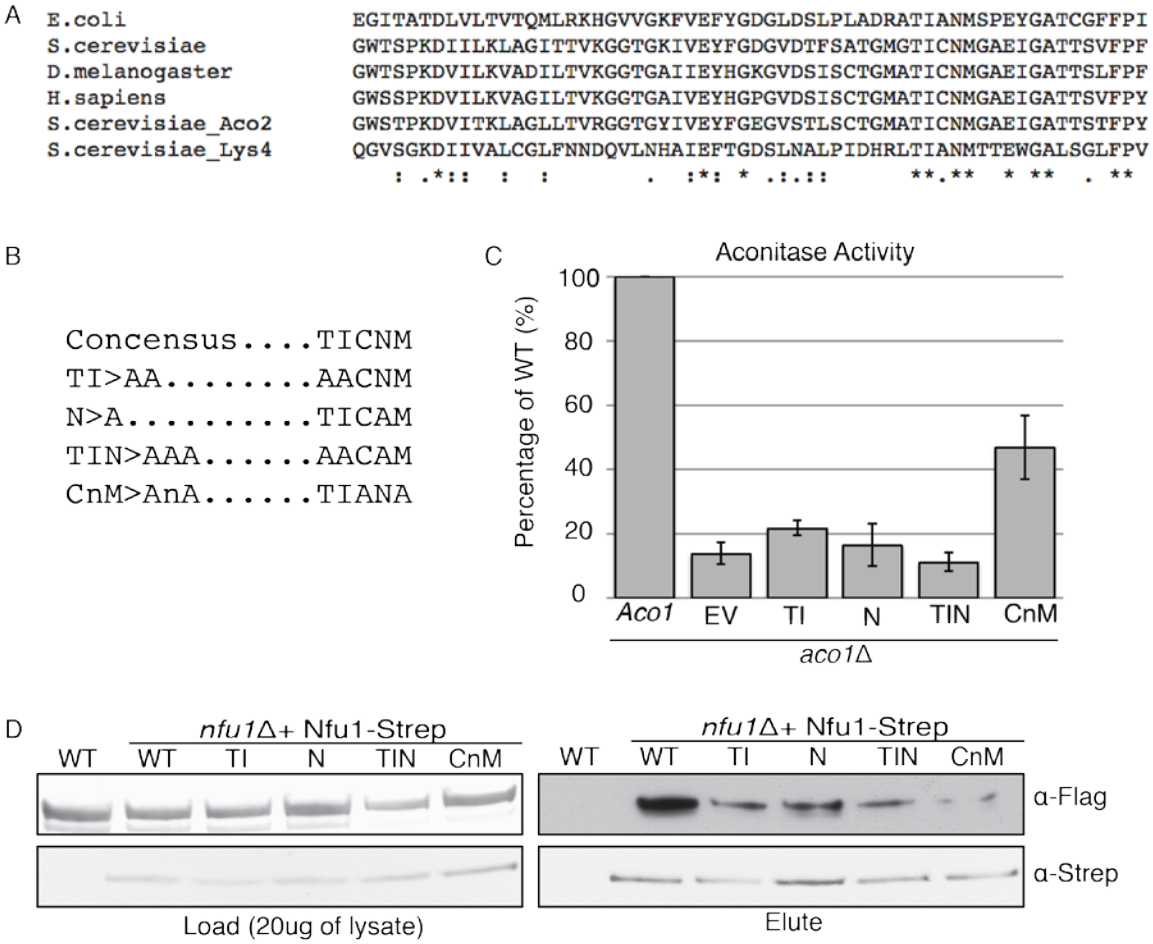

Figure 4.3 Mutation of the Aco1 TICNM motif compromises protein function and Nfu1 interaction. A) Clustal omega alignment of aconitase protein from *E. coli, S.c., D.m.,* and *H.s.,* along with the *S.c.* sequences of the lysine biosynthesis enzymes, Aco2 and Lys4. B) The mutations made to yeast Aco1. C) Aconitase enzymatic activities of mitochondria purified from *aco1*Δ cells express the Aco1-Flag as wild-type (WT) or with the TICNM mutations or an empty vector (EV). D) Strep-Tactin affinity purification of Nfu1-Strep in *nfu1*Δ cells coexpressing the Aco1-Flag TICNM mutants.

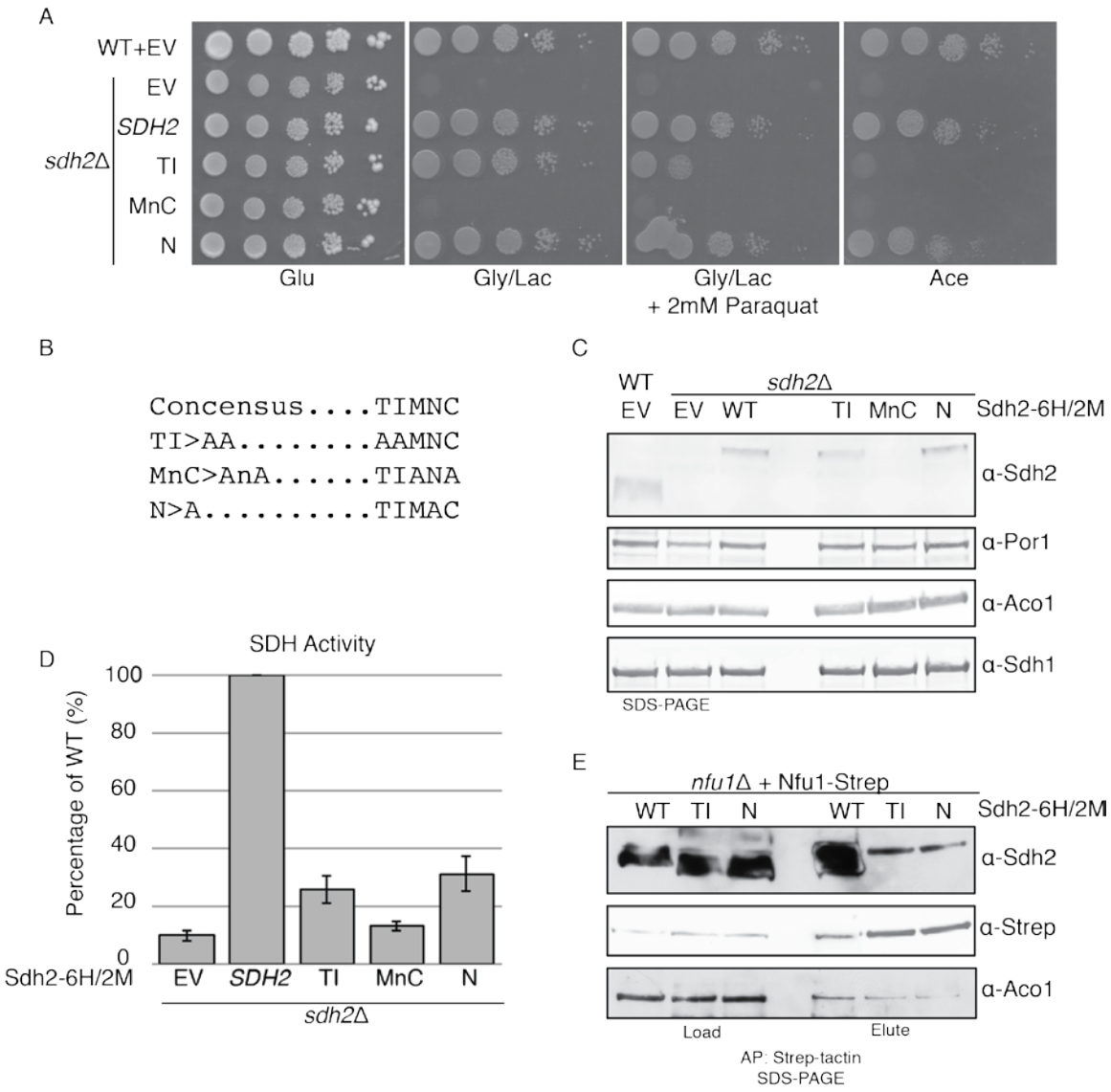

Figure 4.4 Sdh2 TIMNC motif mutants have decreased stability, function, and interaction with Nfu1. A) Growth assay drop test on *sdh2*Δ cells expressing Sdh2-6xHIS-2xMyc (6H/2M) with various TIMNC motif mutants. B) List of the various TIMNC motif mutations made to Sdh2-6H/2M. C) SDS-PAGE, western blot analysis of *sdh2*Δ cells expressing Sdh2-6xHIS-2xMyc (6H/2M) with various TIMNC motif mutants to evaluate the steady-state protein stability of the mutants. D) SDH complex activity by measurements of the TIMNC mutants expressed in *sdh2*Δ cells. E) Strep-Tactin affinity purification of Nfu1-Strep co-expressed with the Sdh2 TIMNC mutants in *nfu1*Δ cells.

CHAPTER 5

CONCLUSION

Redox-active cofactors are essential to facilitate many cellular processes; as such, the successful transfer of these molecules from the *de novo* assembly pathways to client proteins is vitally important to the health of the organism. Transfer systems exist as the final step of all of the Fe/S cluster biogenesis pathways in biology. The bacterial biogenesis pathways, ISC, SUF, and NIF, all have independently developed transfer systems (Roche et al., 2013). The NIF pathway's transfer unit is the NifU domain that was appended directly to the scaffolding domain for cluster biosynthesis. In eukaryotes, the same NifU domain is the C-terminal domain of the Nfu1. This dissertation is focused on the characterization of the Nfu1 and Bol3 mediated [4Fe-4S] cluster transfer in the mitochondria. In the process, these studies also revealed a novel component of [2Fe-2S] transfer in the mitochondria with the identification of the glutaredoxin, Grx5, binding partner Bol1.

Cofactor transfer is an important challenge for the OXPHOS respiratory complexes, which have intricate assembly processes to properly integrate a plethora of subunits and cofactors. Complex I, NADH:ubiquinone oxidoreductase contains 44 subunits and eight Fe/S cofactors. Complex II, succinate dehydrogenase (SDH), contains only four subunits, but coordinates a flavin, three different Fe/S clusters, and a heme. Complex III, cytochrome bc_1, is a dimeric complex with each monomer containing eleven subunits with two heme cofactors and a [2Fe-2S] cluster. Complex IV, cytochrome oxidase, does not contain any Fe/S clusters but instead uses a dinuclear copper, a heme, and a heterobimetalic heme-copper center in the fourteen subunits. Most of the redox cofactors act to transfer electrons through the complex. Complexes I, III, and IV form a larger supercomplex known as the respirasome containing the dimeric complex III and a

single complex I and IV. The function and potential regulatory mechanisms of these complexes is defined in greater detail in Chapter 2. The intrinsic complexity of these complexes creates a challenge for the cell to coordinate the proper assembly of subunits with their respective cofactors. We sought to better understand the assembly process of SDH by identifying how it received Fe/S clusters. This led to the identification of Nfu1 as an interacting partner of an assembly intermediate of SDH and the subsequent characterization of Nfu1 as the [4Fe-4S] cluster transfer protein for the mitochondria.

In Chapter 3, we describe in molecular detail the [4Fe-4S] cluster transfer process in eukaryotic mitochondria. The trimeric ISA complex facilitates the formation of [4Fe-4S] clusters. The subunits Isa1 and Isa2 each receive an individual [2Fe-2S] cluster from the mitochondrial [2Fe-2S] cluster transfer protein, Grx5 (Banci et al., 2014). Isa1 and Isa2 condense their [2Fe-2S] clusters into a single [4Fe-4S] cluster with the help of Iba57, the third component of the trimer (Brancaccio et al., 2014). We demonstrated the interaction of Nfu1 with these subunits and with all of the mitochondrial [4Fe-4S] client proteins known in yeast.

These studies were also motivated by the identification of several patient mutations in the NFU1 coding sequence. These patients were described to have defects in multiple mitochondria enzymes including in the OXPHOS respiratory complexes and enzymes requiring lipoic acid (Cameron et al., 2011; Navarro-Sastre et al., 2011). Eventually, these patients were classified in a broader group with Multiple Mitochondrial Dysfunctions Syndrome (MMDS). When we started our studies, only a few mutations were defined as causative for MMDS and most were frameshift mutants or splicing defects that caused significant reduction in overall Nfu1 protein levels. At the time, the

only coding point mutant of MMDS that did not result in a loss of protein was a glycine mutated to a cysteine just two residues upstream of the CxxC motif, this mutation is Gly208C. Given the juxtaposition to the CxxC motif and the protein stability, we made the same mutation in yeast (Gly194C). This ended up being a fruitful mutation from the discovery standpoint as it was a dominant negative mutant that stalled the Nfu1 interaction with client proteins.

At the same time these initial Nfu1 patients were characterized, some patients that presented similarly were determined to have causative mutations in the BOLA3 gene (Cameron et al., 2011). Given the similar presentation of patients with mutations in NFU1 and BOLA3, we pursed studies of the yeast mitochondrial BolA proteins, Bol1 and Bol3. In the interaction studies that determined Nfu1 interacted with [4Fe-4S] client proteins, it was determined that Bol3 also interacted with the same [4Fe-4S] client proteins. This suggested that Nfu1 and Bol3 could function in a synergistic fashion. Follow-up genetic studies further elaborated that Bol3 functioned through Nfu1; however, the mechanistic function of Bol3 has remained elusive. The initial identification of BolA3 in patients with a Fe/S cluster biogenesis defect came with the suggestion that it functioned with the glutaredoxin Grx5. Grx5 is thought to be the protein responsible for the transfer of [2Fe-2S] clusters. Glutaredoxins and BolA proteins have been described to form a heterodimer bridged by a [2Fe-2S] cluster that performs cluster transfer in the cytosol and in bacteria (Johansson et al., 2011). As we redefined Bol3 as a functional partner of Nfu1, we found that Grx5 interacted the other mitochondria BolA protein Bol1.

During the course of our studies, more MMDS patients were identified with novel

mutations in Nfu1 and BolA3, along with mutations in the ISA complex subunits Isa2 and Iba57 (Ahting et al., 2015; Ajit Bolar et al., 2013; Al-Hassnan et al., 2015; Lossos et al., 2015; Torraco et al., 2017). Many of the newly identified causative mutations were point mutations that did not completely abrogate protein stability. One of these mutations was to the CxxC motif responsible for binding the [4Fe-4S] cluster from the ISA complex. Other novel patient mutations to NFU1 are changes to the amino acids conserved throughout eukaryotes, but do not have defined roles in the protein function of Nfu1. These mutations could be potential hints to binding interfaces on Nfu1 and should be utilized in future studies. As we preformed the molecular studies in yeast that linked Nfu1 and Bol3 with [4Fe-4S] cluster biogenesis, the identification of patients with similar presentations caused by mutations in genes coding for ISA complex components added an independent layer of confidence in our results.

The need for dedicated Fe/S cluster transfer systems is for the protection of the performed cluster from endogenous oxidants as it moves from the scaffold proteins to client proteins. Fe/S clusters' redox active nature that allows them to accept or donate an extra electron also makes them very susceptible to oxidative damage that destroys the cluster and releases free iron(II). Unbound iron(II) can act in a feed forward mechanism through Fenton chemistry that oxidizes hydrogen peroxide to superoxide anions (Imlay, 2006). Those superoxide anions can then react with other Fe/S clusters and propagate oxidative damage (Gomez et al., 2014). The importance of transfer proteins to protect the performed clusters is evident by experiments in Chapter 3 that showed cells grown in anaerobic conditions do not need the transfer protein Nfu1. This is further illustrated by the lack of the BolA transfer proteins in anaerobic bacteria (Willems et al., 2013).

The other significance of the transfer systems for preformed clusters from the scaffolding proteins is for proper cofactor delivery. The ligand coordination environments of many [2Fe-2S], [3Fe-4S], and [4Fe-4S] clusters are very similar (Collins and Zhou, 2011). In several cases when the biosynthetic pathway for one cluster is blocked, clients have still been able to bind other iron cofactors. These clients bound to incorrect cofactors do not retain activity, so these events are not beneficial for the organism. To avoid this problem, transfer proteins must recognize intrinsic characteristics of the clients independent of protein's ability to bind the cofactor.

In the cytosol, the cytosolic iron sulfur cluster assembly (CIA) assembles [4Fe-4S] clusters with the use of a sulfide containing substrate from the mitochondrial ISC pathway and transfers the performed clusters to clients the through CIA targeting complex consisting of Mms19, Cia1, and Cia2 (Gari et al., 2012; Stehling et al., 2012). In some cases, client proteins receive clusters through direct interaction with the targeting complex, and in other cases, adapter proteins are necessary to mediate client interaction with the targeting complex. A single C-terminal tryptophan on the adapter proteins Yae1 and Lto1 has been identified to be important for their binding to the CIA targeting complex (Paul et al., 2015). The authors went on to indicate that a C-terminal tryptophan is important for many clients' direct association to the targeting complex.

The nature of a [2Fe-2S] recognition motif in any system has not yet to been resolved. Several [2Fe-2S] cluster proteins in the mitochondria have LYR (leucine, tyrosine, arginine) proteins that act as assembly factors (SDH and Cytochrome bc_1) and have led some to suggest that this acts as a [2Fe-2S] cluster recognition motif (Maio and Rouault, 2016). This is unlikely since several LYR proteins assemble complexes that do

not bind [2Fe-2S] clusters (ATP synthase) and not all [2Fe-2S] clients in the mitochondria have a known LYR motif or interacting LYR protein (ferredoxin and biotin synthase). In Chapter 4, we revealed the mitochondrial [4Fe-4S] cluster transfer protein Nfu1 recognizes clients by a TIMNM motif that was identified due to its conservation between all [4Fe-4S] clients in the mitochondria throughout eukaryotes. Currently, NMR studies are evaluating the motif-Nfu1 interaction to characterize the Nfu1 binding interface that recognizes the motif and to define any potential structural changes that are induced by the motif binding to Nfu1. These structural changes may be indicative of a mechanism for [4Fe-4S] cluster release from Nfu1 during transfer.

The completion of this dissertation has revealed the function of the Nfu1 as the mitochondrial [4Fe-4S] cluster transfer protein and Bol3 as an adapter protein that assists in this process. Additionally, these studies identified Bol1 as an interacting partner with Grx5 the [2Fe-2S] cluster transfer protein. Studies to integrate our known SDH assembly factors like Sdh6 and Sdh7, Sdh2 (the Fe/S containing subunit) specific assembly factors, with Fe/S cluster transfer systems are underway. Nfu1 has not been studied in the context of complex I cofactor delivery since the Nfu1 studies were done in yeast, where complex I is not present. One of complex I's known assembly factors is Ind1 that has been implicated in the insertion of Fe/S clusters. Whether any interplay of this assembly factor with Nfu1 exists to facilitate Fe/S transfer has not yet been studied. Additional studies have been spurred from this work surrounding the mitochondrial the BolA proteins. Collaborators are currently pursuing deeper mechanistic studies seeking to understand the function the BolA proteins. Bol1 was shown to function with Grx5 in Fe/S cluster biogenesis and Bol3 with Nfu1 in [4Fe-4S] cluster transfer, but the mechanistic function

is still an enigma.

5.1 References

Ahting, U., Mayr, J.A., Vanlander, A.V., Hardy, S.A., Santra, S., Makowski, C., Alston, C.L., Zimmermann, F.A., Abela, L., Plecko, B.*, et al.* (2015). Clinical, biochemical, and genetic spectrum of seven patients with NFU1 deficiency. Front Genet *6*, 123.

Ajit Bolar, N., Vanlander, A.V., Wilbrecht, C., Van der Aa, N., Smet, J., De Paepe, B., Vandeweyer, G., Kooy, F., Eyskens, F., De Latter, E.*, et al.* (2013). Mutation of the iron-sulfur cluster assembly gene IBA57 causes severe myopathy and encephalopathy. Hum Mol Genet *22*, 2590-2602.

Al-Hassnan, Z.N., Al-Dosary, M., Alfadhel, M., Faqeih, E.A., Alsagob, M., Kenana, R., Almass, R., Al-Harazi, O.S., Al-Hindi, H., Malibari, O.I.*, et al.* (2015). ISCA2 mutation causes infantile neurodegenerative mitochondrial disorder. J Med Genet *52*, 186-194.

Banci, L., Brancaccio, D., Ciofi-Baffoni, S., Del Conte, R., Gadepalli, R., Mikolajczyk, M., Neri, S., Piccioli, M., and Winkelmann, J. (2014). [2Fe-2S] cluster transfer in iron–sulfur protein biogenesis. Proceedings of the National Academy of Sciences *111*, 6203-6208.

Brancaccio, D., Gallo, A., Mikolajczyk, M., Zovo, K., Palumaa, P., Novellino, E., Piccioli, M., Ciofi-Baffoni, S., and Banci, L. (2014). Formation of [4Fe-4S] clusters in the mitochondrial iron-sulfur cluster assembly machinery. J Am Chem Soc *136*, 16240-16250.

Cameron, J.M., Janer, A., Levandovskiy, V., Mackay, N., Rouault, T.A., Tong, W.-H., Ogilvie, I., Shoubridge, E.A., and Robinson, B.H. (2011). Mutations in iron-sulfur cluster scaffold genes NFU1 and BOLA3 cause a fatal deficiency of multiple respiratory chain and 2-oxoacid dehydrogenase enzymes. Am J Hum Genet *89*, 486-495.

Collins, D.J., and Zhou, H.-C. (2011). Iron–Sulfur Models of Protein Active Sites. In Encyclopedia of Inorganic and Bioinorganic Chemistry (John Wiley & Sons, Ltd).

Gari, K., León Ortiz, A.M., Borel, V., Flynn, H., Skehel, J.M., and Boulton, S.J. (2012). MMS19 links cytoplasmic iron-sulfur cluster assembly to DNA metabolism. Science (New York, NY) *337*, 243-245.

Gomez, M., Perez-Gallardo, R.V., Sanchez, L.A., Diaz-Perez, A.L., Cortes-Rojo, C., Meza Carmen, V., Saavedra-Molina, A., Lara-Romero, J., Jimenez-Sandoval, S., Rodriguez, F.*, et al.* (2014). Malfunctioning of the iron-sulfur cluster assembly machinery in Saccharomyces cerevisiae produces oxidative stress via an iron-dependent mechanism, causing dysfunction in respiratory complexes. PLoS One *9*, e111585.

Imlay, J.A. (2006). Iron-sulphur clusters and the problem with oxygen. Mol Microbiol *59*, 1073-1082.

Johansson, C., Roos, A.K., Montano, S.J., Sengupta, R., Filippakopoulos, P., Guo, K., von Delft, F., Holmgren, A., Oppermann, U., and Kavanagh, K.L. (2011). The crystal structure of human GLRX5: iron-sulfur cluster co-ordination, tetrameric assembly and monomer activity. Biochem J *433*, 303-311.

Lossos, A., Stumpfig, C., Stevanin, G., Gaussen, M., Zimmerman, B.E., Mundwiller, E., Asulin, M., Chamma, L., Sheffer, R., Misk, A.*, et al.* (2015). Fe/S protein assembly gene IBA57 mutation causes hereditary spastic paraplegia. Neurology *84*, 659-667.

Maio, N., and Rouault, T.A. (2016). Mammalian Fe-S proteins: definition of a consensus motif recognized by the co-chaperone HSC20. Metallomics *8*, 1032-1046.

Navarro-Sastre, A., Tort, F., Stehling, O., Uzarska, M.A., Arranz, J.A., Del Toro, M., Labayru, M.T., Landa, J., Font, A., Garcia-Villoria, J.*, et al.* (2011). A fatal mitochondrial disease is associated with defective NFU1 function in the maturation of a subset of mitochondrial Fe-S proteins. Am J Hum Genet *89*, 656-667.

Paul, V.D., Muhlenhoff, U., Stumpfig, M., Seebacher, J., Kugler, K.G., Renicke, C., Taxis, C., Gavin, A.C., Pierik, A.J., and Lill, R. (2015). The deca-GX3 proteins Yae1-Lto1 function as adaptors recruiting the ABC protein Rli1 for iron-sulfur cluster insertion. Elife *4*, e08231.

Roche, B., Aussel, L., Ezraty, B., Mandin, P., Py, B., and Barras, F. (2013). Iron/sulfur proteins biogenesis in prokaryotes: formation, regulation and diversity. Biochim Biophys Acta *1827*, 455-469.

Stehling, O., Vashisht, A.A., Mascarenhas, J., Jonsson, Z.O., Sharma, T., Netz, D.J.A., Pierik, A.J., Wohlschlegel, J.A., and Lill, R. (2012). MMS19 assembles iron-sulfur proteins required for DNA metabolism and genomic integrity. Science (New York, NY) *337*, 195-199.

Torraco, A., Ardissone, A., Invernizzi, F., Rizza, T., Fiermonte, G., Niceta, M., Zanetti, N., Martinelli, D., Vozza, A., Verrigni, D.*, et al.* (2017). Novel mutations in IBA57 are associated with leukodystrophy and variable clinical phenotypes. J Neurol *264*, 102-111.

Willems, P., Wanschers, B.F., Esseling, J., Szklarczyk, R., Kudla, U., Duarte, I., Forkink, M., Nooteboom, M., Swarts, H., Gloerich, J.*, et al.* (2013). BOLA1 is an aerobic protein that prevents mitochondrial morphology changes induced by glutathione depletion. Antioxid Redox Signal *18*, 129-138.